UNIVERSITÀ DEGLI STUDI DI NAPOLI

PARTHENOPE

University of Study of Naples "Parthenope"

Department of Science and Technology

PhD Program in Environmental Phenomena and Risks

XXXVIII Cycle

Oceanographic and weather forcing on PAH transport. The case study of mussel farming in the Gulf of Pozzuoli (Southern Tyrrhenian Sea)

Academic Year 2024/2025

Author:

Laura Fortunato

Supervisor:

Prof. Yuri Cotroneo

PhD Program Coordinator:

Prof. Antonio Occhiuzzi

TABLE OF CONTENTS

Preface

This thesis is submitted in partial fulfillment of the requirements for the PhD degree. The PhD studies were carried out at the University of Naples Parthenope, at the Department of Science and Technology (DIST), under the supervision of Associate Professor Yuri Cotroneo. The research was conducted from November 2022 to October 2025.

During my PhD studies, I spent six months abroad at Instituto Mediterráneo de Estudios Avanzados (IMEDEA) under the supervision of Dr. Ananda Pascual and Dr. Vincent Combes.

This PhD research was funded by the PNRR (Piano Nazionale di Ripresa e Resilienza), Mission 4 – Education and Research, Component 1, Investment 3.4 "Potenziamento dell'offerta dei servizi di istruzione: dagli asili nido all'Università" and Investment 4.1 "Didattica e competenze universitarie avanzate" and "Estensione del numero di dottorati di ricerca e dottorati innovativi per la pubblica amministrazione e il patrimonio culturale". The doctoral scholarship was awarded pursuant to Ministerial Decree (DM) No. 351/2022 CUP: I61I22000080007 and is financed by the European Union – NextGenerationEU.

The grant supported all aspects of the doctoral research, including fieldwork, research activities, and international collaboration.

Finanziato dall'Unione europea NextGenerationEU

Ministero dell'Università e della Ricerca

Italiadomani PIANO NAZIONALE DI RIPRESA E RESILIENZA

Abstract

This thesis investigates the oceanographic and meteorological mechanisms driving recurrent exceedances of polycyclic aromatic hydrocarbons (PAHs) in mussels farmed at Lucrino, within the Gulf of Pozzuoli (Southern Italy). Despite long-term monitoring, the processes responsible for contaminant transport and accumulation remained poorly understood.

Two complementary experimental frameworks were designed to address this issue. A local model-based approach for the year 2016 integrating chemical monitoring, high-frequency physical and dynamical observations along the water column, oceanographic model outputs, and Lagrangian simulations to analyse the contamination episodes. The results revealed that PAH exceedances occur predominantly during late autumn and winter, under persistent southerly winds associated with enhanced wave energy (Wave height > 1.2 m; Wave period > 8 s). This setting induces sediment resuspension and northwestward nearshore advection from the Bagnoli brownfield toward Lucrino farm.

An alternative and complementary regional altimetry-based approach used geostrophic velocities, wind datasets, and particle tracking to evaluate basin-scale contamination dynamics for the 2024 contamination events. The analyses identified wind-driven advection of nautical-fuel residues as a possible source of surface contamination, highlighting the combined role of maritime traffic emissions and large-scale circulation.

The integration of both approaches provides a comprehensive multi-scale framework linking local sediment dynamics to regional atmospheric and oceanic forcing. The results demonstrate that PAH contamination at Lucrino might arise from two processes that could interact, namely sediment resuspension and wind-driven surface advection — both modulated by seasonal meteorological patterns.

The two hypotheses regarding contamination sources, which account for multi-scale processes, form the basis for a forecast-oriented risk management strategy that

integrates real-time meteorological data, hydrodynamic models, and satellite observations.

Beyond the Gulf of Pozzuoli, the methodology is transferable to other semi-enclosed or industrially impacted coastal systems, supporting operational monitoring, pollution mitigation, and sustainable aquaculture management.

Chapter I

1. INTRODUCTION

Coastal marine environments represent dynamic interfaces where natural processes and anthropogenic activities interact, generating complex physical–biogeochemical feedback that influences water quality, sediment dynamics, and ecosystem health. In semi-enclosed basins such as the Gulf of Pozzuoli (southern Tyrrhenian Sea, Italy), limited water exchange combined with intense human pressure enhances the vulnerability of coastal ecosystems to contamination and eutrophication. Over the past decades, increasing attention has been directed toward the persistence of anthropogenic contaminants, such as polycyclic aromatic hydrocarbons (PAHs), in these environments due to their toxicity, persistence, and potential for bioaccumulation in marine organisms.

The Gulf of Pozzuoli, located in the northwestern sector of the Gulf of Naples, provides a representative case study of the challenges faced by post-industrial coastal systems. Historically influenced by the Bagnoli industrial complex—one of Italy's major steel and chemical production centres active from the mid-19th to the late 20th century—the area has experienced progressive environmental degradation. Sediments continue to serve as secondary sources of contamination even decades after industrial closure. At the same time, the Gulf of Pozzuoli supports economically and socially important aquaculture activities, particularly the farming of *Mytilus galloprovincialis*. Mussels serve both as a vital economic resource and as sensitive bioindicators of environmental quality. Recurrent exceedances of regulatory PAH limits have been documented at the Lucrino farm, raising significant public health and management concerns.

Understanding the mechanisms behind these contamination events requires an integrated assessment of hydrodynamic, meteorological, and chemical processes, examined across multiple spatial and temporal scales. Previous studies (Esposito et al. 2017) have shown pronounced seasonal variability in PAH concentrations, with peaks during late autumn and winter. These periods coincide with enhanced wind and wave forcing from the southern quadrants, suggesting a linkage between meteo-oceanographic conditions and the contamination episodes. However, the relative contributions of local sources, such as sediment resuspension from the Bagnoli brownfield, versus regional sources, including maritime traffic emissions and basin-scale transport, remain poorly demonstrated.

This doctoral research addresses this gap by combining high-resolution local observations with regional satellite-driven analyses to clarify the mechanistic pathways governing PAH transport toward the Lucrino mussel farm. Two complementary experimental modelling frameworks were developed. The first, a local model-based approach, integrates in situ oceanographic observations, hydrodynamic model outputs, and Lagrangian forward simulations to investigate dynamics linked to the contamination events in 2016. The second, a regional altimetry-based approach, integrates SWOT (Surface Water and Ocean Topography mission)-enhanced geostrophic velocities, ERA5 (European Centre for Medium-Range Weather Forecasts Reanalysis version 5) winds, local meteorological data, and Lagrangian forward simulations to explore basin-scale PAH dispersion associated with maritime emissions and wind-driven transport.

Together, these approaches provide a multi-scale understanding of the physical drivers and temporal recurrence of PAH exceedances in mussels, offering both scientific insights and practical guidance for environmental management. The specific objectives of this thesis are to: (i) characterize the hydrodynamic and meteorological conditions preceding PAH contamination events in the Gulf of Pozzuoli; (ii) identify and compare the dominant source–transport pathways of PAHs affecting the Lucrino mussel farm, distinguishing between sediment-derived and fuel-derived inputs; (iii) quantify the role of wave-induced resuspension and wind-driven advection in influencing contaminant mobilization and coastal convergence; (iv) evaluate the complementarity and limitations of local versus regional modelling frameworks in resolving nearshore pollution dynamics; and (v) propose operational strategies for contamination risk forecasting, monitoring optimization, and long-term mitigation.

By integrating multi-source observations, advanced numerical modelling, and chemical evidence, this thesis contributes to a mechanistic and predictive understanding of contaminant dynamics in semi-enclosed coastal systems. Beyond its local relevance, the methodological framework developed here offers a transferable tool for diagnosing contamination risks in other Mediterranean and global coastal environments affected by both legacy industrial and contemporary maritime pollution sources. Ultimately, this research provides the scientific basis for developing early-warning systems and evidence-based management strategies to ensure the sustainable use of coastal resources and the protection of marine environmental quality.

Chapter II

2. OCEANOGRAPHIC AND ENVIRONMENTAL CONTEXT OF THE STUDY AREA

2.1 Oceanographic Setting: From the Tyrrhenian Sea to the Gulf of Pozzuoli

2.1.1 General circulation in the Tyrrhenian Sea

A detailed knowledge of the large-scale circulation of the Tyrrhenian Sea (TYS, hereafter) is necessary for the correct description of the oceanographic features and for the management of the socio-economic activities that take place along its coastal areas, including the Gulf of Naples (GoN, hereafter) and the Gulf of Pozzuoli (GoP, hereafter). Ocean circulation directly influences planning in marine resource exploitation—including mussel farming—and its characterization at different spatial and temporal scales can help, prevent, and possibly mitigate the environmental and health-related risks.

The TYS is a semi-enclosed basin of the western Mediterranean Sea, bordered by the Italian Peninsula to the east, the islands of Sardinia and Corsica to the west and northwest, and Sicily to the south (Fig. 1). Covering about 231,000 km² and reaching a maximum depth of 3,785 m in its central plain (Marani et al., 1993), it is considered the most isolated basin in the western Mediterranean due to its geographical position (Krivosheya and Ovchinnikov, 1973). Despite its geographically confined position, the TYS plays a direct role in the overall thermohaline circulation of the Mediterranean Sea (Hopkins, 1988; Astraldi and Gasparini, 1994), contributing to the formation and redistribution of dense water masses whose properties have shown significant variability in recent decades (Millot et al., 2006; Fusco et al., 2008). The basin's bathymetry is complex, with a deep central plain surrounded by steep continental slopes and several prominent seamounts and ridges, including the Vavilov and Marsili seamounts, which significantly influence local circulation and mixing processes (Aulicino et al., 2016; Iacono et al., 2013).

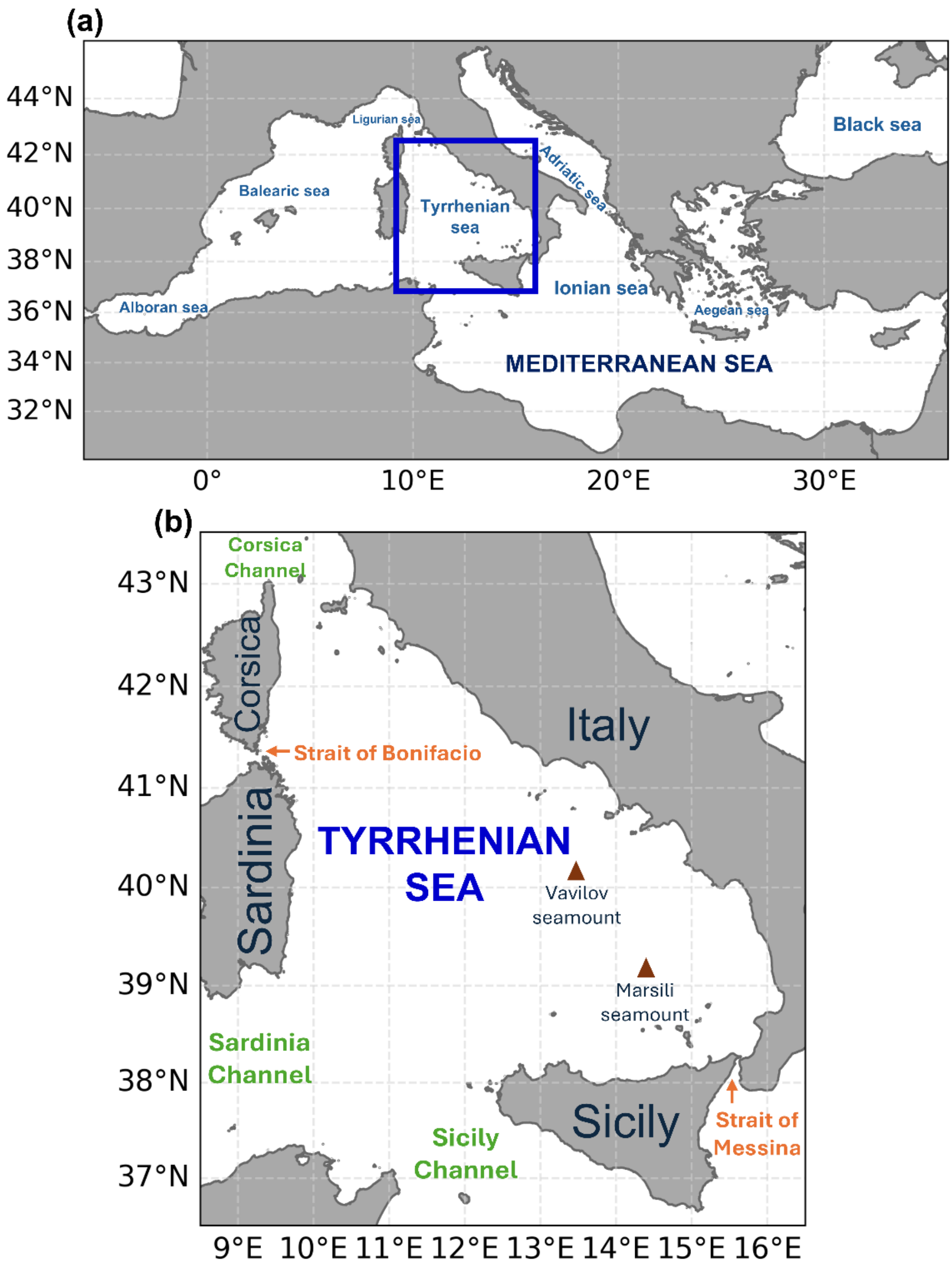

Figure 1. a) Map of the Mediterranean Sea, highlighting the study region; b) Map of the Tyrrhenian Sea, highlighting its main topographic features, including straits, channels, and seamounts.

The general circulation of the TYS is closely linked to the basin's morphology and bathymetry (Iacono et al., 2013). It is influenced by three main openings: the Corsica Channel (north), the Sardinia Channel (southwest), and the Strait of Sicily (south). Additionally, smaller but significant straits, such as the Strait of Bonifacio (between Corsica and Sardinia) and the Strait of Messina (between Sicily and Italy mainland), play important roles in shaping regional circulation patterns.

Circulation within the TYS results from the interaction of different water masses and forcing mechanisms (Fig. 2). Several water masses occupy the basin from the surface to the deep layers. In the upper 100–200 m, a flow of modified Atlantic Water (mAW), characterized by a subsurface salinity minimum ($S < 37.4$), enters the basin primarily along the northern coast of Sicily (Astraldi et al., 2002; Poulain and Zambianchi, 2007). At intermediate depths, the salty ($S > 38.5$) Levantine Intermediate Water (LIW) enters from the eastern Mediterranean through the Strait of Sicily and undergoes transformation and mixing within the basin (Millot, 1987; Astraldi et al., 1996). The deepest layers are filled with Western Mediterranean Deep Water (WMDW), characterized by lower potential temperature ($\theta < 13°C$) and salinity ($S < 38.5$), which enters through the deep passages between Sardinia and Sicily. Mixing between LIW and WMDW below 1000 m forms a distinct water mass known as Tyrrhenian Deep Water (Hopkins, 1988; Millot, 1999; Budillon et al., 2009). The interaction of these water masses with basin morphology, wind forcing, and buoyancy fluxes produces a circulation pattern that undergoes marked seasonal changes (Iacono et al., 2013; Millot 1999).

During winter and spring, the surface and intermediate layers have similar circulation patterns (Astraldi and Gasparini, 1994). A flux enters TYS from the south along the Sicilian coast, while a part of this flux recirculates next to the southern opening, the remaining flux proceeds northward along the Italian coastline until reaching the Corsica Channel. A part of this current, primarily composed of mAW, flows into the Ligurian Sea. The remaining mAW, depleted by the Ligurian outflow, migrates southward and becomes entrained in a cyclonic gyre off the Bonifacio Strait. In contrast, the LIW moves in proximity to Sardinia Channel and exits through the southern opening . In the winter and spring period at the surface (Iacono et al., 2013; Rinaldi et al., 2010) TYS western portion is dominated by a wind-induced dipole off the Bonifacio strait and by a cyclonic circulation further south at a larger scale (flowing along Campania coasts).

In summer, increasing stratification isolates the basin from surrounding Mediterranean waters through strong thermohaline fronts (Bonaduce et al., 2021; Fusco et al., 2003). The large-scale cyclonic cell weakens, and both mAW and LIW tend to recirculate within the basin, with minimal outflow through the Corsica Channel. Circulation becomes more fragmented, with mesoscale eddies and coastal jets persisting for longer periods but exhibiting reduced kinetic energy. Additional eddies often emerge in the eastern Tyrrhenian Sea, enhanced by the stratified conditions and weaker basin-scale flow (Budillon et al., 2009). By autumn, the TYS enters a transitional phase. Summer stratification persists in the upper layers but increasing wind activity and shifting buoyancy fluxes enhance vertical mixing. This gradual weakening of the summer structure re-intensifies the cyclonic circulation, progressively re-establishing the winter–spring configuration.

Below the surface, the Tyrrhenian Sea exhibits a stepped vertical structure, often referred to as thermohaline “staircases”, resulting from the superposition of distinct water masses of different origin and properties. These layers reflect the coexistence of mAW in the upper 100 m, Tyrrhenian Intermediate Water at intermediate depths, and the saltier Levantine Intermediate Water below (Millot, 1999; Sparnocchia et al., 1999; Zodiatis and Gasparini, 1996). The staircases are associated with double-diffusive convection processes that generate alternating well-mixed layers and sharp interfaces, which can persist over long timescales and significantly influence vertical mixing and heat–salt fluxes within the basin (Durante et al., 2019; Durante et al., 2021). Recent observations indicate that such thermohaline staircases are a permanent and dynamically active feature of the Tyrrhenian interior (Durante et al., 2021).

One of the most notable characteristics of the Tyrrhenian circulation is the pronounced seasonal variability of the coastal current. This dynamic plays a crucial role in coastal ecosystems and human activities, such as mussel farming, especially in the GoN. Given that the GoN is an inlet of the TYS, its surface circulation is partially influenced by the large-scale Tyrrhenian dynamics and deserves specific attention in this study.

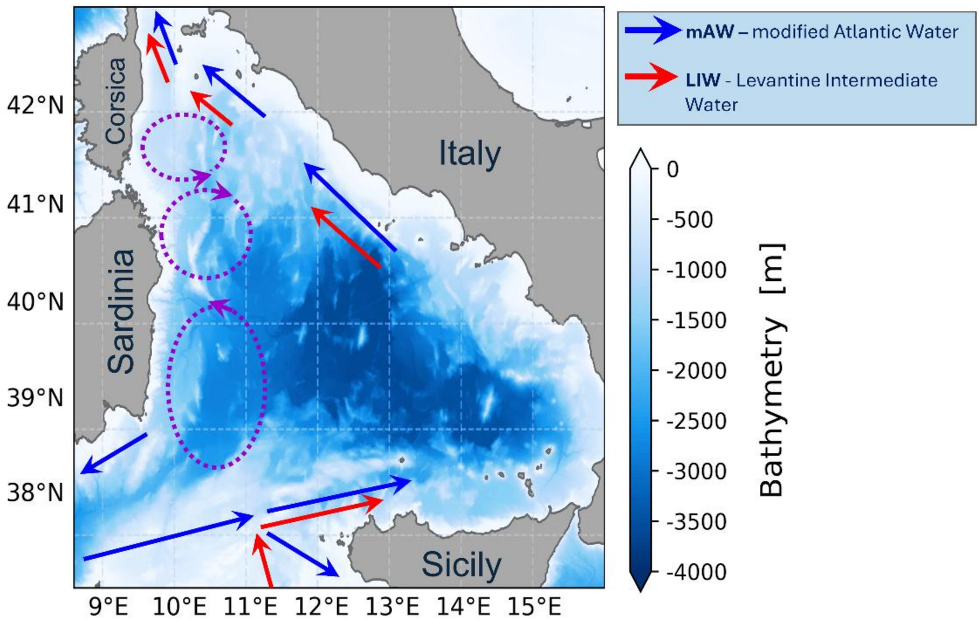

Figure 2. Bathymetric map of the Tyrrhenian Sea. Arrows indicate the main flow of surface (AW, blue) and intermediate (LIW, red) waters. The ovals in the western Tyrrhenian represent the quasi-permanent Bonifacio dipole and the cyclonic circulation between Sardinia and Sicily, both distinctive features of the basin-scale circulation.

2.1.2 Coastal dynamics and circulation in the Gulf of Naples

The GoN, located in the southern TYS, is situated in the central-western Mediterranean and borders the metropolitan area of Naples (Campania, Italy). This semi-enclosed basin, oriented southwestward, spans an area of approximately 900 km^2 with an average depth of about 170 m (Carrada et al., 1980). It extends for around 195 km from Monte di Procida to Punta Campanella, including the Phlegraean coast and the Sorrento Peninsula. The Gulf is partially sheltered from the open sea by the islands of Ischia, Procida, and Capri, which limit direct exchanges with the TYS (Fig.3).

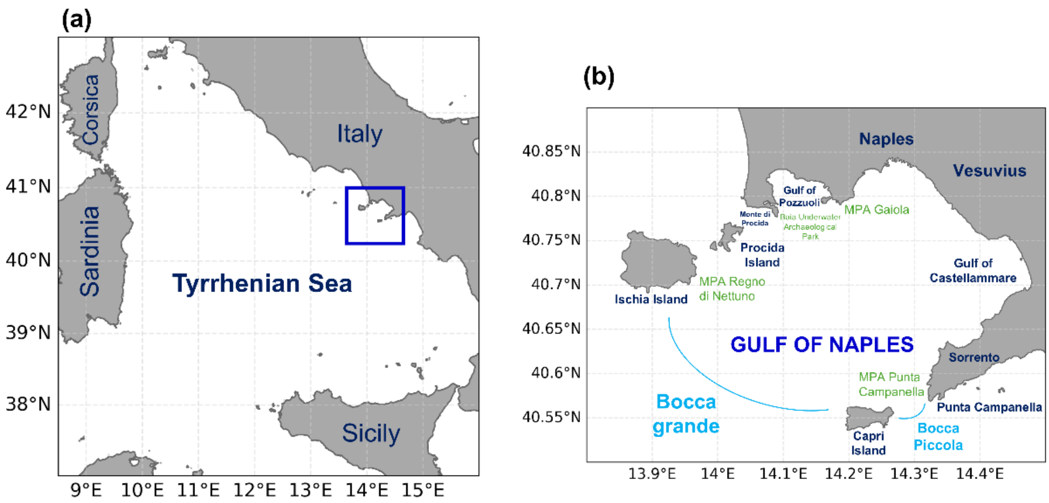

Figure 3. a) General map of the Tyrrhenian Sea. b) General map of the Gulf of Naples, highlighting its main topographic features and marine protected areas (MPA).

Because of its partial isolation, the Gulf acts as a transition zone where open-sea currents interact with local coastal processes. This interaction produces marked spatial variability in both physical conditions (temperature, salinity, currents) and chemical–biological features (nutrient distribution, primary production, and contaminant concentrations) (Uttieri et al., 2011; Kokoszka et al., 2023).

The GoN is an area under intense anthropogenic pressure. Urbanization, port activities, tourism, and industry contribute to significant environmental stress, including the release of untreated or partially treated sewage, industrial effluents, hydrocarbons, and marine litter (Tornero and Ribera d'Alcalà, 2014; De Pippo et al., 2008). As one of the busiest harbours in the Mediterranean, the GoN is particularly vulnerable to the combined effects of local human activities and regional circulation patterns. The presence of sensitive ecosystems and marine protected areas (Gaiola, Regno di Nettuno, Punta Campanella, and Baia Underwater Archaeological Park) further highlights the importance of understanding the Gulf's hydrodynamics (Iacono et al., 2021; Cesarano et al., 2023; Gifuni et al., 2023).

Hydrodynamic processes in the GoN are shaped by both remote and local forcings. The primary remote forcing originates from the large-scale TYS circulation (Pierini and Simioli, 1998; Gravili et al., 2001), while the main local driver is the wind regime, which exhibits marked temporal and spatial variability (Moretti et al., 1976-

1977; de Maio, 1985; Menna et al., 2007). The resulting circulation often involves the formation of cyclonic and anticyclonic gyres, jet currents, and convergence/divergence zones, contributing to a complex and seasonally variable pattern (Cianelli et al., 2011).

Surface circulation in the GoN has been monitored in near real-time since 2004 using a CODAR HF (High-Frequency Coastal Ocean Dynamics Applications Radar) radar system operated by the University of Naples "Parthenope" on behalf of the Regional Environmental Monitoring Centre (Menna et al., 2007; Cianelli et al., 2011). Observational data, in conjunction with modeling efforts (Gravili et al., 2001; Grieco et al., 2005), have provided important insights into the Gulf's circulation patterns (Fig. 4).

As reported by Menna et al. (2007), during winter, dominant NNE–NE winds (8–10 m/s) typically generate an offshore-directed jet current (Fig. 4a), while strong southwesterly winds may reverse this pattern and drive onshore flow (Fig. 4b). In spring and summer, alternating NE and SW breezes create a diurnal land-sea breeze cycle that induces a synchronous clockwise rotation of surface currents across the basin (Fig. 4c-d) (Perusini et al., 1992; Menna et al., 2007; Cianelli et al., 2011).

When the influence of TYS circulation becomes dominant, different scenarios emerge depending on the direction of the Tyrrhenian coastal current (De Maio et al., 1982; de Ruggiero et al., 2020). A north-westward flow (Fig. 4e), drives an intense inflow from the Bocca Piccola and creates a cyclonic gyre in the central basin, accompanied by an anticyclonic structure near Castellammare di Stabia. This pattern is typically observed in autumn and winter. Conversely, in late spring, surface currents strengthen (up to 20 cm/s), promoting a basin-wide anticyclonic circulation, except in the GoP sector.

When the coastal current reverses south-eastward (Fig. 4f), the outer GoN exhibits a cyclonic structure, while anticyclonic gyres dominate the northeastern Bay of Naples and the southeastern Gulf of Castellammare di Stabia.

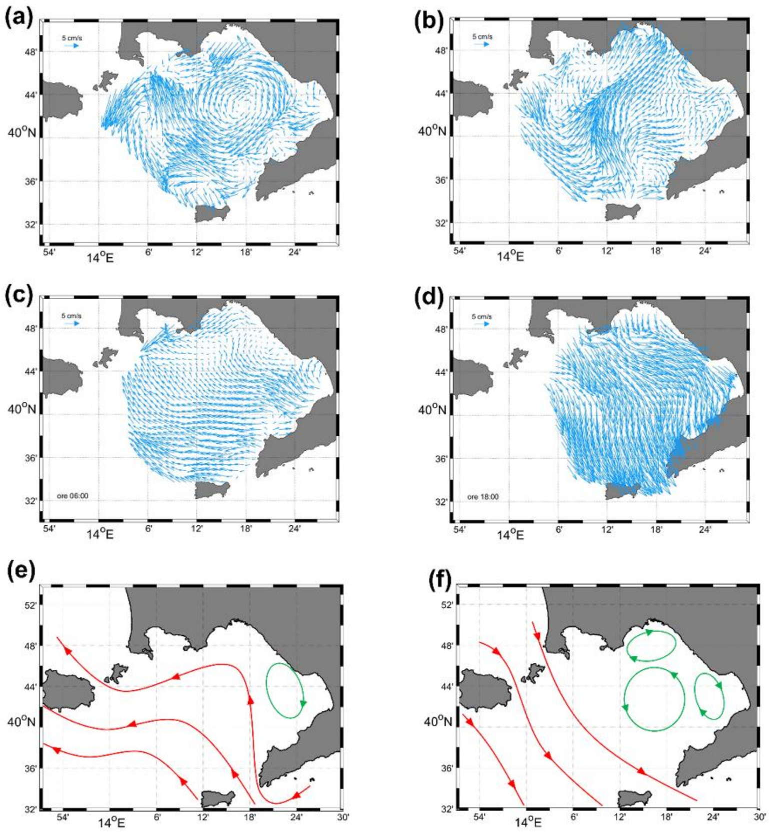

Figure 4. a) Sea surface circulation in the GoN detected by HF radar measurements during NE wind; b) Sea surface circulation in the GoN detected by HF radar measurements during SW wind; c-d) Sea surface circulation in the GoN detected by HF radar measurements during the daily alternation of breeze winds. The two maps show the circulation field: at 06:00 GMT (c) when the flow is mainly directed offshore; at 18:00 GMT (d) when the flow is reversed; e) Schematic circulation in the GoN as driven by a north-westward Tyrrhenian current (red curve line). The green circle is the anticyclonic structure (modified from De Maio et al., 1983); f) Schematic circulation in the GoN as driven by a south-eastern Tyrrhenian current (red curve line). The green circles are the anticyclonic and cyclonic structures (modified from De Maio et al., 1983).

2.1.3 Geographical setting of the Gulf of Pozzuoli

The GoP is a semi-enclosed coastal basin located in the northwestern sector of the GoN within the southern TYS (Fig. 5). It extends from Nisida Island to the city of

Bacoli, covering an area of approximately 33 km². The basin features an average depth of about 60 meters and reaches a maximum depth of approximately 110 meters (Somma et al., 2016; Aiello et al., 2016; Di Martino et al., 2020). The coastal morphology of the GoP is predominantly low-lying and sandy along the western and northern shores, particularly near Bacoli and the adjacent coastal zones (Arienzo et al., 2017). The seabed is primarily composed of muddy and sandy sediments, which can play a significant role in the accumulation and potential remobilization of pollutants (Arienzo et al., 2017; Di Martino et al., 2020). In contrast, the nearby coastline toward the eastern boundary of the Gulf of Naples, including the Posillipo headland, is characterized by rocky and steep profiles, marking a distinct geomorphological transition from the GoP area (Di Crescenzo et al., 2021).

Geologically, the GoP is positioned within the tectonic system of the Campi Flegrei volcanic caldera—an area of high geodynamic complexity associated with intense hydrothermal and volcanic activity (Romano et al., 2004). This setting has significantly influenced the morphology of the seafloor, which includes submerged volcanic banks, pyroclastic deposits, and hydrothermally altered sediments (Aiello et al., 2016; Bruno, 2004). Ongoing bradyseismic phenomena (i.e., vertical ground movements) observed in this area further contribute to changes in the coastal and seabed configuration over decadal time scales (Del Gaudio et al., 2010). Beyond its natural features, anthropogenic pressures have substantially altered the natural landscape and archaeological heritage of the Gulf of Pozzuoli.

Since the mid-19th century, anthropogenic activities have intensified, notably with the establishment of a chemical production plant in Bagnoli in 1854. Over time, the area developed into a major industrial hub, hosting steel production, cement manufacturing, and asbestos processing facilities. Currently, the GoP is undergoing a government-led remediation project, started in 1996 and extended in 2001 to include marine sediments adjacent to the former industrial site (Albanese et al., 2010). The area is also subject to considerable anthropogenic pressures due to its proximity to urban centers, port activities, industrial discharges, tourism pressure and extensive aquaculture. The high population density in the metropolitan Naples region, combined with seasonal tourist influxes, exacerbates anthropogenic stress on coastal and marine environments through increased waste production, coastal infrastructure development, and habitat disturbance.

Mussel farming (*Mytilus galloprovincialis*) is particularly prominent in the northwestern sector of the gulf, where longlines are deployed at fixed sites year-round. These bivalves can also serve as valuable bioindicators of environmental quality and are widely used for monitoring marine contamination (Esposito et al. 2020; Esposito et al. 2017; Mercogliano et al., 2016). Due to its semi-enclosed nature and limited water exchange with the open Tyrrhenian Sea, the GoP is highly sensitive to local meteorological and oceanographic conditions. These features make it a highly relevant site for the study of contaminant accumulation and the long-term environmental effects of industrial and urban activities.

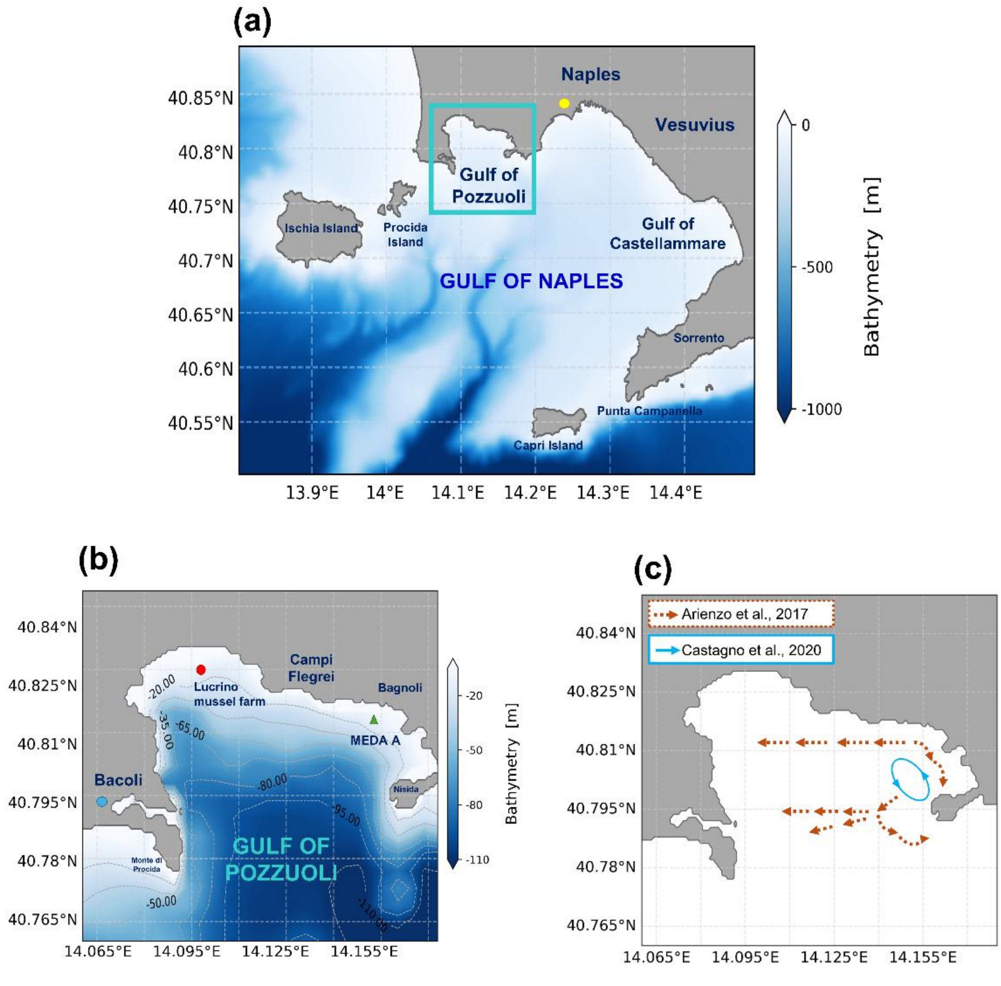

Figure 5. a) Bathymetric map of the GoN highlighting the GoP. The yellow dot is the Napoli Pacanowsky weather station. b) Bathymetric map of the GoP. The red dot corresponds to the position of the Lucrino mussel farm. The light blue dot is the position of the Bacoli weather station. The green triangle is the position of MEDA A;

c) Schematic sediment transport (orange - Arienzo et al., 2017) and sea surface circulation (lightblue - Castagno et al. 2020) at the Bagnoli Bay from previous studies.

2.1.4 Hydrodynamic features of the Gulf of Pozzuoli

Within the broader dynamic system of the GoN, the GoP represents a semi-enclosed sub-basin characterized by limited open exchange with the surrounding waters and by a complex interplay between local forcing and sedimentary processes. Despite its ecological and socio-economic relevance—partly due to nearby aquaculture and historical industrial activity—circulation patterns in the GoP remain relatively understudied, primarily due to the scarcity of basin-scale in situ observations.

Recent advances in hydrographic surveys and numerical modeling (Castagno et al., 2020) have begun to shed light on the hydrodynamics of the GoP, particularly its eastern sector. These studies identified a persistent anticyclonic (clockwise) surface circulation pattern (Fig. 5c), predominantly driven by local wind stress curl, with only a minor contribution from large-scale TYS or GoN forcing. This relatively closed recirculation system may limit the flushing of contaminants and prolong residence times, enhancing the potential for localized accumulation of pollutants.

The sediment dynamics in the GoP are strongly linked to its hydrodynamic behavior and the granulometric characteristics of local sediments. According to Arienzo et al. (2017), fine and very fine sands dominate the sediment composition, and their mobilization is influenced by both wind-driven nearshore currents and basin-scale circulation features. In shallow waters (<10 m), a westward-directed longshore current transports fine sediments, while a cyclonic (anticlockwise) eddy between Bagnoli Bay and the central GoP facilitates lateral redistribution. Very fine sand follows an offshore, east–west transport axis, particularly around the Bagnoli brownfield area (Fig. 5b).

This sediment transport regime plays a crucial role in the redistribution of contaminants. Elevated levels of polycyclic aromatic hydrocarbons (PAHs) have been recorded in surface and bottom sediments near the former industrial area of Bagnoli (Tornero and Ribera d’Alcalà, 2014). Furthermore, monitoring of shellfish in the nearby Lucrino area revealed seasonal exceedances of regulatory limits for both benzo[a]pyrene (BaP) and total PAHs, indicating a link between hydrodynamic and contaminant patterns (Esposito et al., 2017; 2020).

Complementary sediment studies (Albanese et al., 2010; Bergamin et al., 2003; Romano et al., 2004; Arienzo et al., 2020) confirm the presence of widespread contamination, including PAHs, Polychlorinated Biphenyls (PCBs), heavy metals, and hydrocarbons, especially near Bagnoli. While PAHs and PCBs are attributed to historic industrial pollution, the elevated heavy metal concentrations are associated with natural hydrothermal processes linked to the Campi Flegrei volcanic system, adding a geogenic dimension to the contaminant landscape.

In summary, the GoP presents a unique hydrodynamic environment shaped by local wind forcing and sediment characteristics, with limited exchange with the broader GoN. This contributes to the persistence and redistribution of contaminants, underlining the need for targeted monitoring and high-resolution modeling better to understand the basin's vulnerability and support environmental management.

2.2 Marine Pollution and Mussel Farming in the Study Area

2.2.1 Ecological and economic importance of mussel farming

Mussel farming represents a crucial component of coastal aquaculture in the GoP, with *Mytilus galloprovincialis* being the predominant species. The Campania region ranks among the top Italian producers of mussels, with the GoP hosting several aquaculture concessions that contribute significantly to regional seafood supply chains (FAO, 2024). Mussels are farmed using suspended longline systems anchored nearshore, exploiting the sheltered conditions of the semi-enclosed GoP and the availability of nutrient-rich waters influenced by both natural and anthropogenic inputs. Mussel farming areas in the GoP are also strategically important for environmental monitoring, as the semi-enclosed nature of the Gulf amplifies contaminant accumulation, making mussels effective bioindicators of both historical and ongoing pollution.

From an economic perspective, mussel farming represents a key sector for small-scale fisheries and local cooperatives, providing direct employment and supporting ancillary activities such as seed collection, maintenance, and product distribution (MIPAAF, 2020). Italy is one of the leading producers of *M. galloprovincialis* in Europe, with an annual production averaging around 65,000–70,000 tonnes (FAO, 2024; EUMOFA, 2021). The proximity of the GoP to the metropolitan area of Naples facilitates rapid distribution to local markets, fishmongers, and restaurants, reinforcing the economic viability of this traditional activity in a post-industrial coastal context.

Beyond its socio-economic value, mussel farming contributes to ecosystem services through its ecological functions. Mussels are highly efficient filter feeders, capable of filtering up to 5 liters of seawater per hour per individual, depending on size and temperature (Bayne, 2004; Prins et al., 1997). Their filtration activity promotes water clarity, regulates phytoplankton dynamics, and facilitates the recycling of nutrients such as nitrogen and phosphorus (Newell, 2004; Cranford et al., 2007). The structural complexity of mussel ropes also enhances local biodiversity, offering habitat and refuge for invertebrates and juvenile fish species (Mascorda Cabre et al., 2021; Ysebaert et al., 2009).

However, mussel farming is not without environmental consequences. The biodeposition of faeces and pseudofaeces beneath cultivation areas can lead to localized organic enrichment of sediments, potentially triggering hypoxia and altering benthic community composition (Hatcher et al., 1994). These effects are generally confined to areas immediately beneath farm structures and are modulated by hydrodynamic conditions, sediment type, and farm density (Sarà et al., 2004). In the GoP, the limited water renewal and sediment characteristics heighten the need for careful spatial planning of aquaculture to minimize the environmental footprint. “Results from Lagrangian experiments in the Gulf of Naples suggest effective surface water residence times on the order of ∼5–10 days under typical seasonal conditions, with shorter renewal under strong exchange regimes (Gifuni et al., 2025).

Crucially, *M. galloprovincialis* is widely recognized as a bioindicator species due to its capacity to bioaccumulate a range of environmental contaminants, including trace metals, hydrocarbons, and persistent organic pollutants (Bocchetti et al., 2006; Farrington et al., 1983). This capability has been specifically leveraged in the GoP to monitor contaminant transfer from historical industrial sources, such as the Bagnoli brownfield, to aquaculture zones, enabling the evaluation of human and ecosystem exposure risks.

Mussels have been central to global biomonitoring programs such as the Mussel Watch Program (https://coastalscience.noaa.gov/science-areas/pollution/mussel-watch/) and are included in national and European monitoring frameworks (e.g., Marine Strategy Framework Directive – MSFD; Water Framework Directive – WFD). In Italy, mussels are used by ARPA and ISPRA for assessing marine environmental quality, as outlined in legislative decrees such as D.Lgs. 152/2006 and D.Lgs. 190/2010.

In the specific context of the GoP, mussel farming areas are particularly relevant due to the historical contamination linked to the former Bagnoli industrial site. Multiple studies have documented elevated levels of polycyclic aromatic hydrocarbons (PAHs), heavy metals, and PCBs in farmed mussels collected from Lucrino and adjacent sites (Esposito et al., 2017; Esposito et al., 2020; Albanese et al., 2010). These findings highlight the dual role of mussel farming in the GoP. While providing economic benefits, it also offers a natural sentinel system for early warning and long-term surveillance of marine contamination.

In summary, mussel farming in the Gulf of Pozzuoli represents a multifunctional activity at the intersection of food production, environmental monitoring, and ecosystem service provision. Its sustainable management is essential to balance economic interests with the protection of marine habitats in a coastal area marked by ecological sensitivity and a legacy of industrial impact.

2.2.2 Environmental issues and industrial history of the area

The coastal area surrounding the GoP has been significantly impacted by a long-standing industrial legacy, primarily associated with the development of the Bagnoli industrial district. A pivotal moment occurred in 1854 with the establishment of the first chemical production plant in Bagnoli. By the early 20th century, the area had become one of Italy's most important industrial centers, hosting large-scale facilities involved in steel manufacturing, cement production, and asbestos processing. These industrial activities, particularly steel production, contributed to the extensive release of pollutants into the surrounding environment. The Bagnoli steel plant, at the time the second-largest integrated steelworks in Italy, ceased operations in 1990 and was fully dismantled in the early 2000s (Romano et al., 2004).

Among the most concerning pollutants are heavy metals such as lead (Pb), cadmium (Cd), zinc (Zn), and arsenic (As), and Polycyclic Aromatic Hydrocarbons (PAHs). These pollutants are characterized by high persistence and potential for bioaccumulation, with PAHs having a strong affinity for sediments and organic particulates, resulting in long-term contamination hotspots near former industrial sites.

These substances, released into soils and marine sediments over decades, are characterized by high persistence, low degradation rates, and potential for bioaccumulation in marine organisms, posing risks to local ecosystems and economically important aquaculture activities. The contamination is not confined to the industrial site itself but extends into the coastal waters and seabed of the GoP.

The semi-enclosed nature of the Gulf, combined with its limited water exchange, facilitates the accumulation and retention of pollutants, while physical processes such as sediment resuspension and bradyseismic events can promote their redistribution within the basin. Several studies have reported elevated concentrations of PAHs in marine sediments and biota in the coastal zone adjacent to Bagnoli, indicating both historical accumulation and possible ongoing remobilization (Albanese et al., 2010; Armiento et al., 2020).

Despite ongoing remediation efforts—initiated in 1996 and extended in 2001 to include marine sediment treatment near the former industrial site (Albanese et al., 2010)—the environmental consequences of over a century of industrialization remain evident. Monitoring data suggest that sediments continue to act as a secondary source of contamination, particularly under the influence of physical drivers such as coastal currents, resuspension events, and extreme weather conditions. These factors may facilitate the redistribution of PAHs and heavy metals, raising concerns for ecosystem health and the safety of aquaculture operations.

Mussels farmed in the area (*Mytilus galloprovincialis*) are known to accumulate PAHs and heavy metals, making them effective bioindicators for assessing environmental quality and contaminant bioavailability. Continued integrated monitoring—combining in situ sampling, satellite observations, and numerical modeling—is essential to understanding contaminant dynamics, evaluating remediation outcomes, and supporting informed coastal management strategies aimed at protecting the marine environment of the GoP.

2.2.3 Mussels as Environmental Indicators in Coastal Monitoring

Bivalve mollusks, particularly Mytilus galloprovincialis, are widely recognized as effective bioindicators for assessing environmental quality in marine and coastal ecosystems. Their filter-feeding behavior allows them to accumulate and concentrate pollutants such as heavy metals and PAHs from the water column and suspended particulates. This characteristic makes them highly suitable for monitoring both the presence and potential biological effects of contaminants over time, particularly in semi-enclosed basins like the GoP, where water circulation is limited and pollutants tend to accumulate.

Traditional chemical analyses of water and sediments are essential for determining contaminant concentrations with high sensitivity and precision. However, these methods often fail to capture the complexity of environmental contamination, especially in systems exposed to mixtures of pollutants whose combined effects may be synergistic or additive. As Van der Oost et al. (2003) and Phillips & Rainbow (1994) highlight, the identification of specific chemical compounds does not necessarily provide insight into their biological impacts, thus limiting the ecological relevance of chemical quantification alone. For this reason, biological monitoring approaches using living organisms have gained increasing importance in environmental assessments.

Mussels act as integrative indicators of contaminant bioavailability and ecosystem health. Their relatively immobile nature and long lifespan allow them to reflect spatial and temporal trends in pollution exposure, while their wide distribution across marine environments facilitates large-scale comparisons. Le Foche et al. (2005) emphasize that evaluating biological responses within aquatic communities is one of the most effective means of determining ecosystem health, since pollution and environmental stressors influence organisms both directly and indirectly.

As their use as sentinel organisms is well established, mussels have been extensively employed in global monitoring initiatives such as the "Mussel Watch Program" (NOAA, 2023) and European regional programs supported by institutions like the International Council for the Exploration of the Sea (ICES) and the European Union under the Marine Strategy Framework Directive (MSFD).

Several studies in the Mediterranean region confirm the value of *M. galloprovincialis* in monitoring coastal contamination. For example, research conducted in the Gulf of Naples revealed seasonal variations in PAH concentrations, with significantly higher levels detected during winter (Esposito et al. 2020,2017). Similarly, Trinchella et al. (2013) documented the bioaccumulation of cadmium and lead in farmed mussels in the GoN, showing that these organisms are effective in capturing pollution gradients, even between industrial and relatively uncontaminated zones. In the heavily impacted waters near Bagnoli, Mercogliano et al. (2016) found that benzo[a]pyrene concentrations in mussels reached levels up to 36 times higher than EU safety thresholds, indicating ongoing contamination despite remediation efforts. Additional studies in Sardinia's Calich Lagoon demonstrated that mussels accumulate trace elements such as cadmium, lead, cobalt, and nickel with distinct seasonal patterns, further supporting their role as sensitive indicators of temporal variability in contaminant exposure (Meloni et al., 2022).

The integration of mussels into multidisciplinary monitoring programs—combining biological indicators with oceanographic data such as hydrodynamic modeling, sediment transport, and remote sensing—enhances our capacity to assess pollution dynamics in coastal systems. In a complex and semi-enclosed environment like the GoP, where sediment resuspension and limited circulation influence contaminant distribution, the use of *Mytilus galloprovincialis* offers critical data for assessing the effectiveness of remediation strategies and supporting sustainable coastal management practices.

2.2.4 Polycyclic Aromatic Hydrocarbons (PAHs) in the marine environment

PAHs are a class of hydrophobic organic pollutants composed of two or more fused aromatic rings in a generally planar configuration. These compounds are predominantly formed through the incomplete combustion or pyrolysis of organic matter, including fossil fuels, biomass, and various industrial materials (Zhang and Tao, 2009). During combustion, fuel molecules undergo cracking into smaller fragments that, in oxygen-limited environments, can repolymerize to form PAHs. Their formation is thus favored by low oxygen-to-fuel ratios.

Main contributors to PAHs include anthropogenic sources such as vehicular emissions, industrial processes, power generation, oil spills, and urban runoff, whereas natural sources include wildfires and volcanic activity (Bjørseth and Ramdahl, 1985). Nearly 60 % of global PAH emissions are attributed to incomplete fossil fuel combustion (emissions from biomass and coal included) (Zhang and Tao, 2009). Because of their low water solubility, low volatility, and strong affinity for organic matter, PAHs tend to bind to suspended particulates and accumulate in sediments and biota (Oliva et al., 2020; Abdel-Shafy & Mansour, 2016; Sverdrup et al., 2002). This sediment affinity is particularly critical in semi-enclosed coastal areas like the GoP, where limited water exchange and local hydrodynamics favor the prolonged retention of PAHs and their subsequent uptake by filter-feeding organisms such as mussels.

Recognizing their toxicity, the U.S. Environmental Protection Agency (USEPA) designated 16 priority PAHs in the 1970s (Wise et al., 2015; Srogi, 2007; Baumard et al., 1997). The European Union subsequently established a list of 15+1 priority PAHs, focusing on food safety, which includes eight compounds from the USEPA list **(Table 1)**, and an additional compound identified due to its relevance in food contamination contexts (Wenzl et al., 2006). Among them, benzo[a]pyrene (BaP) is classified by the International Agency for Research on Cancer (IARC) as a Group 1 human carcinogen, while others are listed as probable (Group 2A) or possible (Group 2B) human carcinogens.

In response to these concerns, EU regulations such as EC 1881/2006 (amended by 835/2011) and the latest 2023/915 legislation define maximum permissible PAH concentrations in food products—especially molluscs—setting 5 μg/kg for BaP and 30 μg/kg for the sum of the four marker PAHs.

In coastal ecosystems, PAHs enter via atmospheric deposition, riverine inputs, industrial discharges, sewer overflows, and the handling of fossil fuels. Their distribution is influenced by meteorological conditions (precipitation amount, wind patterns), seasonal sunlight (UV) exposure, and physicochemical factors affecting photodegradation (Wang et al., 2008; Manoli et al., 2000; Wortham et al., 1993). Once adsorbed, PAHs settle into sediments and bioaccumulate in organisms, with potential remobilization driven by sediment mixing or hydrodynamic shifts (Sun et al., 2018; Readman et al., 1984).

A recent global modeling study (Wu et al., 2024) showed that PAH concentrations remain elevated over industrialized regions like China, Europe, and India, and that while some declines occurred between 2013 and 2018, reductions lag those of particulate matter. This underscores the persistent environmental impact of PAHs even amid emission-control efforts. Given their toxicological impact and persistence, PAHs are considered critical contaminants in coastal monitoring programs. Regular analysis of PAHs in bivalves and sediments provides essential data for assessing environmental contamination, supporting environmental risk assessments, and guiding coastal management and policy decisions.

Substance	Total molecular formula	Molecular weight	Carcinogenic activity
Naphthalene	$C_{10}H_8$	128	+
Phenanthrene	$C_{14}H_{10}$	178	-
Anthracene	$C_{14}H_{10}$	178	±
Fluoranthene	$C_{16}H_{10}$	202	-
Pyrene	$C_{16}H_{10}$	202	-
Chrysene	$C_{18}H_{12}$	228	±
Benzo(a)anthracene	$C_{18}H_{12}$	228	+
Benzo(b)fluoranthene	$C_{20}H_{12}$	252	++
Benzo(k)fluoranthene	$C_{20}H_{12}$	252	+
Benzo(e)pyrene	$C_{20}H_{12}$	252	±
Benzo(a)pyrene	$C_{20}H_{12}$	252	+++
Perylene	$C_{20}H_{12}$	252	±
Benzo(ghi)perylene	$C_{22}H_{12}$	276	±
Dibenzo(ah)anthracenes	$C_{22}H_{14}$	278	+++
Indeno(cd)pyrene	$C_{22}H_{12}$	276	+
Coronene	$C_{24}H_{12}$	300	±

Table 1. USA EPA priority list of PAH. + (++) There is sufficient evidence that the substance is carcinogenic to experimental animals; ± The available data are inadequate to permit an evaluation of the carcinogenicity of the substance to experimental animals; - The available data provide no evidence that the substance per se is carcinogenic to experimental animals.

2.2.5 Integrated approaches to marine contamination studies: in situ, satellite, and model data

Understanding and managing marine pollution in coastal areas, particularly in semi-enclosed basins, demands a multidisciplinary and integrative approach that combines in situ measurements, remote sensing technologies, and numerical modelling. Each of these methods contributes uniquely to the comprehensive assessment of marine contamination, offering complementary perspectives that improve the detection of pollution sources, evaluate environmental risks, and support remediation strategies.

In situ observations remain a key approach in contamination assessment. They provide direct measurements of pollutant concentrations in water, sediments, and biota, providing high-resolution insights into local environmental conditions. For instance, *Casas and Bacher (2006)* developed a dynamic bioaccumulation model integrating in situ chemical analyses and physiological parameters to estimate mercury and lead uptake in *Mytilus galloprovincialis*. Such methods are critical for validating model simulations and calibrating remote sensing data.

Remote sensing, particularly using satellite sensors, extends observational capacity over wide spatial scales and at higher frequencies than traditional sampling. *Pavlakis et al. (2001)* successfully applied synthetic aperture radar (SAR) imagery to detect illegal oil discharges in the Mediterranean Sea, highlighting the utility of satellites in pollution surveillance. More recently, multispectral data from Sentinel-2 satellites have been combined with artificial intelligence techniques to map suspended particulate matter, chlorophyll concentrations, and turbidity in coastal waters, contributing to pollution source tracking and eutrophication assessments (Kong et al., 2025).

Numerical modelling serves as a predictive and integrative tool to simulate contaminant transport, dispersion, and accumulation in marine systems. Hydrodynamic models offer a mechanistic understanding of pollutant behaviour under various environmental scenarios. Gifuni et al. (2023) developed a hydrodynamic model coupled with a Lagrangian particle tracking system to simulate the seasonal transport of microplastics in the Gulf of Naples. Likewise, Guerrini et al. (2022) employed a coupled Eulerian–Lagrangian model to simulate the distribution and transport of microplastics and associated contaminants in the Mediterranean Sea, highlighting the role of particles as vectors of pollution in marine ecosystems.

The synergy among these approaches enhances the effectiveness of monitoring strategies. In summary, the integration of field data, remote sensing, and numerical modelling is now considered the gold standard in marine pollution studies. This multifaceted approach supports accurate environmental assessments, guides remediation efforts, and informs sustainable coastal management and public health protection.

Chapter III

3. DATA AND METHODS

3.1 Experimental design

This study investigates how meteorological and oceanographic dynamics influence PAH contamination in farmed mussels (*Mytilus galloprovincialis*) in the GoP, southern TYS. The research integrates biological, chemical, meteorological, and oceanographic data across two key years—2016 and 2024—to explore the environmental drivers of PAH bioaccumulation in mussel tissues.

The year 2016 was selected retrospectively due to the availability of high frequency in situ measurements and validated hydrodynamic model outputs. Four contamination events occurring during late autumn and winter were analyzed to evaluate conditions favouring the transport of PAHs from known polluted coastal areas—particularly the decommissioned industrial site of Bagnoli—to the Lucrino mussel farming site.

The year 2024 marks a new phase of research, characterized by active data collection under the project "Un approccio multidisciplinare alla contaminazione da idrocarburi nei mitili allevati nel Golfo di Pozzuoli," funded by the University of Naples Parthenope. Starting in early 2024, oceanographic campaigns were conducted to acquire new in situ measurements; at the same time, both the spatial and temporal resolution of chemical and biological samplings of sediments, water, and mussels were enhanced. These datasets were designed to validate and expand the 2016 findings and to support the development of predictive tools for contamination risk management. Additionally, water column properties and currents were described during different seasons in the GoP, filling one of the gaps in local circulation knowledge.

Within the broader framework of this PhD project, two complementary methodological approaches were implemented (Fig. 6). These two approaches are not intended for direct quantitative comparison. Rather, they were designed to isolate and interpret different transport mechanisms operating under distinct observational constraints, spatial scales, and data-availability conditions. Together, they offer complementary perspectives on PAH dispersion pathways in the GoN.

The 2016 model-based approach focused on the local scale of the GoP, examining the transport of PAHs from the Bagnoli industrial area to the Lucrino mussel farm. This approach was supported by an environmental survey on marine sediments conducted by the Regional Agency for Environmental Protection of Campania (ARPAC), which revealed very similar PAH compositions at both sites (De Maio et al., 2021- sampling activities report), strongly suggesting a common contamination source and highlighting the connectivity of sediment-borne pollutants at the local scale.

In contrast, the 2024 altimetry-based approach was implemented to overcome limitations in data availability encountered during the 2016 study. This approach was conducted at a broader, regional scale covering the entire GoN. It aimed to assess contamination patterns linked to nautical fuel emissions, with particles originating from areas of intense maritime traffic and dispersing toward the Pozzuoli aquaculture zone. During 2024, two contamination events were recorded in the winter months (January and February), providing the opportunity to investigate PAH transport and accumulation under seasonal winter conditions. Chemical analyses of mussels confirmed that PAHs detected during this campaign were predominantly associated with nautical fuel, supporting the focus on regional-scale marine sources. Unfortunately, a detailed description of PAH contamination of mussels in 2016 is not available.

The 2024 analysis further benefited from the integration of altimetric data derived from the Surface Water and Ocean Topography (SWOT) mission, which represents a major technological advance in ocean observation. SWOT provides high-resolution, wide-swath measurements capable of resolving coastal and mesoscale circulation features with unprecedented spatial detail (Fu et al., 2012; Morrow et al., 2019; Fu et al., 2024). This capability allows a more accurate reconstruction of surface geostrophic current variability even in coastal and semi-enclosed basins such as the Gulf of Naples, where traditional altimetry often lacks resolution. Consequently, SWOT data enabled the characterization of fine-scale transport dynamics essential for understanding pollutant dispersion and accumulation in nearshore environments (Fortunato et al., 2025; Verger Miralles et al., 2025).

To achieve these objectives, environmental and oceanographic datasets were obtained from multiple complementary sources:

- Meteorological data included continuous measurements from the Bacoli and Napoli weather station and gridded reanalysis products (e.g., NCEP-CFSR for 2016 and ERA5 for 2024), characterizing both local wind regimes and larger-scale atmospheric conditions.
- Oceanographic data consisted of water column profiles from the "MEDA A" platform (ADCP, CTD) in 2016, with extended surveys in 2024 to increase both spatial and vertical resolution.
- Numerical modeling was performed using the Campania Regional Ocean Model (CROM), based on the Princeton Ocean Model, to describe sea surface circulation and support particle transport simulations in 2016.
- Satellite remote sensing provided Chlorophyll-a data from the Copernicus Marine Environment Monitoring Service (CMEMS) in 2016, complemented in 2024 by observations from the Surface Water and Ocean Topography (SWOT) mission.
- Lagrangian simulations were conducted using the GNOME model for 2016 and using the Python-based Parcels tool for 2024 to simulate forward particle trajectories and dispersion patterns.

By combining past contamination events with newly acquired field data, this two-phase experimental framework enables both retrospective interpretation and forward-looking forecasting. It provides a comprehensive understanding of the physical processes governing pollutant dispersion and accumulation, with direct implications for environmental monitoring and management.

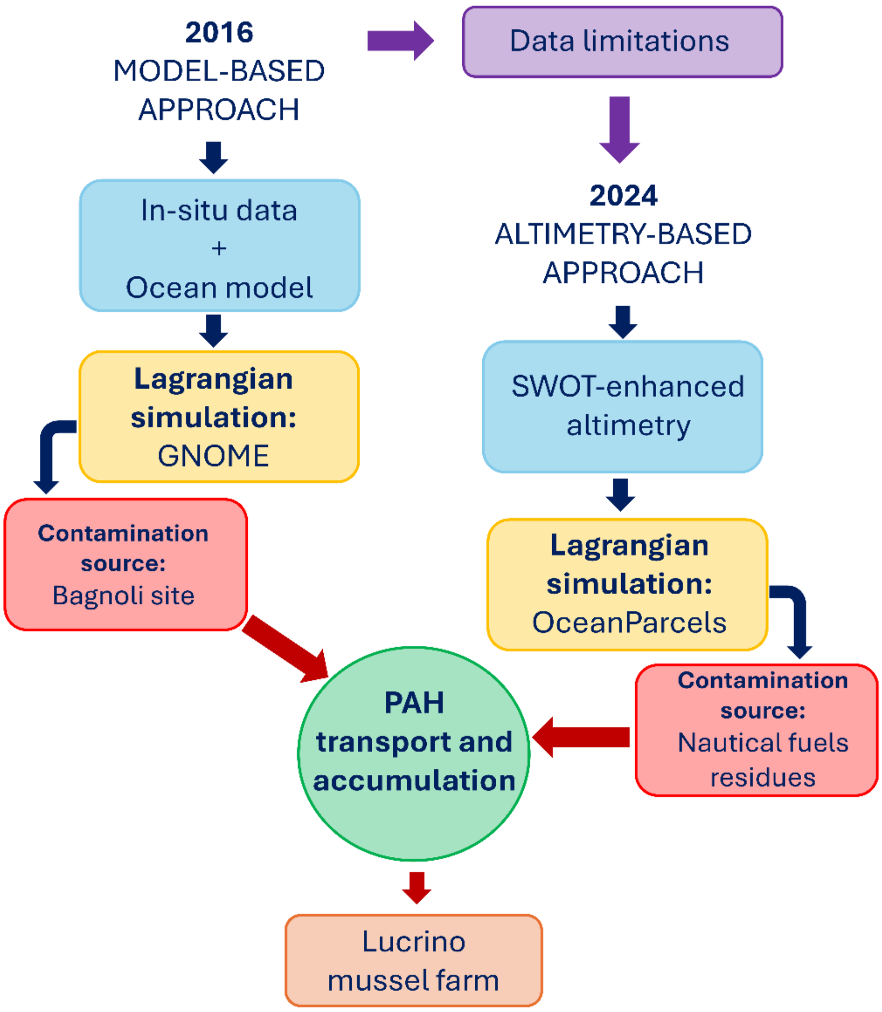

Figure 6. Conceptual map of the experimental design illustrating the datasets, modeling components, and analytical approaches adopted in this study. The 2016 model-based approach investigates the potential transport of contaminants originating from the Bagnoli site, while the 2024 altimetry-based approach focuses on the dispersion of pollutants derived from nautical fuel residues. Both approaches aim to assess the exposure and transport pathways affecting the Lucrino mussel farm.

3.2 Standard PAHs concentration measurements and analysis in farmed mussels

To assess contamination levels of polycyclic aromatic hydrocarbons (PAHs) in farmed mussels (*Mytilus galloprovincialis*), samples are regularly collected by authorized personnel from the Istituto Zooprofilattico Sperimentale del Mezzogiorno

(IZSM), following standardized protocols. The Lucrino mussel farm site, within the GoP site is monitored by regional health authorities due to its proximity to historically contaminated coastal areas, including the decommissioned industrial site of Bagnoli.

Each sample consists of approximately 1 kg of commercial-sized mussels, randomly collected along the longline system at depths ranging from 3 to 4 meters. Selected specimens are characterized by similar biometric parameters: valve length (5–7 cm), weight (3–5 g), and age (9–11 months).

After collection, mussels are immediately transported on ice to IZSM laboratories, where soft tissues from 20 to 40 individuals are dissected, individually wrapped in aluminium foil, and stored at −20 °C until chemical analysis. These procedures ensure sample integrity and compliance with official monitoring protocols. PAH quantification is performed using High-Performance Liquid Chromatography (HPLC) according to Serpe et al. (2010) and in compliance with Commission Regulation (EU) No 836/2011. The method includes the analysis of mussel tissues, without considering the PAH content in seawater inside mussels, sediment, seawater or interstitial samples. The analytical procedure involves homogenization of soft tissues, saponification, extraction with cyclohexane, and clean-up using Sep-Pak silica cartridges. The final extract is analysed by HPLC with a specific chromatographic column and gradient elution using an acetonitrile/water mobile phase. Identification and quantification are based on retention times and external standard calibration. The method allows for the detection of the four EU-regulated PAHs in bivalve molluscs: benzo(a)pyrene (BaP), benz(a)anthracene (BaA), benzo(b)fluoranthene (BbF), and chrysene (CHR). Analytical performance met EU criteria, with quantification limits of 0.2 μg/kg and recovery rates of 50–120%. These analyses are part of a broader chemical monitoring program to ensure compliance with Regulation (EU) No 2023/915, which sets the maximum permissible levels of BaP (5.0 μg/kg) and the sum of BaP, BaA, BbF, and CHR (30.0 μg/kg) in molluscs intended for human consumption.

During 2016, a total of 15 mussel samples were collected throughout the year at the Lucrino farm. Among these, four samples exceeded the legal limits for PAHs, representing high-PAH sampling (hereafter "pollution events") collected on 25 January, 17 February, 22 November, and 14 December.

Since 2024, under the University of Naples Parthenope project "Un approccio multidisciplinare alla contaminazione da idrocarburi nei mitili allevati nel Golfo di Pozzuoli", the official monitoring strategy has been complemented with additional samplings performed by the University staff to include additional contaminants and biological endpoints. The project initially focused on PAH exposure and accumulation, with particular attention to oxidative stress and cellular damage mediated by reactive oxygen species (ROS), but also includes seasonal monitoring of seawater inside and outside the mussels and sediment, as well as quantification of heavy metals and metalloids.

The biological and ecological research of this project develops along three main lines:

- Morphological and ecological analysis: collection of biometric parameters (shell length, biomass) to assess growth and health; study of the benthic community associated with mussels to provide insights into biodiversity and ecological quality.
- Environmental chemical analyses: sampling of soft tissues and inter-valvular water analysed by ICP-MS for 14 trace elements (Al, V, Cr, Mn, Fe, Co, Ni, Cu, Zn, As, Mo, Cd, Pb, U); seasonal sampling of water and sediments to characterize environmental quality and identify contamination sources; integration of chemical data with physiological responses for ecotoxicological interpretation.
- Physiological assessment of environmental stress: analysis of gill tissues for oxidative stress biomarkers (ROS levels, lipid peroxidation [HPs], protein oxidation [CO], oxidant susceptibility [ΔHPs], and total antioxidant capacity [TAC]), providing early-warning signals of sub-lethal responses and contributing to the evaluation of mussel health.

Sampling is conducted on three ropes deployed at ~8 m depth. Each rope is subdivided into three vertical sections (upper, central, and lower), from which 30 cm portions were collected to investigate potential vertical gradients in contaminant accumulation and physiological responses. In 2024, 18 mussel samples were collected over the course of the year at the same site. Only two of these samples exceeded the

EU legal limits for PAHs, corresponding to pollution events on 24 January and 14 February.

3.3 Meteorological Data Collection and Processing

Meteorological data were used to investigate the potential atmospheric drivers of PAH transport toward the mussel farming area and to characterize weather conditions preexisting the contamination events.

For 2016, wind direction and speed were analyzed to understand their influence on sea surface circulation within the GoP. Local meteorological observations were obtained from the Bacoli weather station (lightblue dot in Fig. 5b), which is part of the Campanialive network (https://www.campanialive.it/). This station, located in the western GoP (40° 47' 31.38" N, 14° 4' 40.11" E) at an elevation of 3 meters above sea level, was the only site in the area providing uninterrupted records throughout 2016. The station collects data at 10-minute intervals, including air temperature, humidity, atmospheric pressure, wind speed and direction, heat index, and ultraviolet (UV) radiation.

To complement local observations and assess synoptic-scale meteorological conditions, gridded reanalysis data from the NCEP Climate Forecast System Reanalysis (CFSR) were used. These data provide a broader atmospheric context with a spatial resolution of 0.5° × 0.5°, allowing the identification of large-scale weather patterns (e.g., cyclonic activity, pressure systems, fronts passages) during the days preceding high PAH concentration events. Additionally, in situ rainfall data from two automatic weather stations located in Pozzuoli and Nisida Island were analyzed to evaluate the potential contribution of atmospheric deposition or runoff as secondary PAH sources. However, before and during most contamination events analyzed in 2016, no significant precipitation was recorded, suggesting that wind-driven transport and resuspension likely played a more critical role.

For the year 2024, local meteorological data were provided by the Naples Pacanowsky weather station (yellow dot in Fig. 5a), located at the University of Naples Parthenope (40° 49′ 55.6″ N, 14° 14′ 42.9″ E). This station is part of Fondazione Osservatorio Meteorologico Milano Duomo (Fondazione OMD, https://www.fondazioneomd.it/rete-meteo) and provides high-frequency measurements recorded every 10 minutes, including air temperature, humidity, atmospheric pressure, wind speed and direction, solar radiation, and precipitation intensity. Wind direction and wind speed were used for this study.

To complement local observations and assess synoptic-scale meteorological conditions, gridded data from the reanalysis dataset *ERA5 hourly data on single levels from 1940 to present* (Copernicus Climate Change Service (C3S) Climate Data Store, Hersbach et al., 2023; accessed on 14-Apr-2025), were incorporated to support Lagrangian transport simulations. ERA5 provides hourly atmospheric variables on a global grid with a horizontal resolution of 0.25° × 0.25°, representing a substantial improvement over previous-generation reanalysis product. For this study, 10 m wind speed and direction were extracted over the Gulf of Pozzuoli domain and used as forcing inputs for particle-tracking models aimed at reproducing the transport pathways of surface plumes and their potential connectivity with mussel farming areas. In-situ wind data were used to combine ERA5 reanalysis wind fields over the Gulf of Naples with observed values at the station, implementing a spatially weighted approach to maintain continuity of the wind field across the domain. The combination of high-resolution ERA5 data with station observations allowed for the realization of a more accurate representation of local atmospheric forcing conditions, particularly for reproducing near-surface currents and assessing wind-driven transport toward aquaculture sites. All meteorological datasets were quality-controlled and processed using MATLAB and Python, with particular focus on stick plots and wind roses for visualizing directional wind patterns; temporal matching with oceanographic and contamination events; correlation with sea surface currents and wave parameters from in situ and model data.

3.4 Oceanographic Observations and Datasets

A comprehensive characterization of the physical marine environment in the Gulf of Pozzuoli (GoP) was essential to assess the mechanisms of pollutant transport and the variability of contamination patterns observed in farmed mussels. The oceanographic data used in this study were obtained from three main sources: in situ measurements, numerical ocean model outputs, and satellite remote sensing. These datasets provide complementary spatial and temporal resolutions and were analyzed for both 2016 and, where available, 2024, as part of a multi-scale experimental framework.

3.4.1 In Situ Oceanographic Measurements

In situ oceanographic data were primarily acquired through the “MEDA A” coastal monitoring platform, operated by the Stazione Zoologica Anton Dohrn. The platform is located in the Bagnoli Bay (40° 48.550' N, 14° 09.300' E) at a depth of approximately 19 meters and is equipped with a suite of autonomous sensors for real-time monitoring of sea state and water properties.

Current measurements were obtained using an upward looking Acoustic Doppler Current Profiler (ADCP) operating at 600 kHz. The ADCP records vertical profiles of current speed and direction every 15 minutes, with a resolution of 0.5 m. The instrument provides data across 49 bins, with the 31st bin (located ~1.4 m below the surface) selected as representative of surface current conditions in this work. Wave data—including height, period, and direction—are recorded hourly. Water column properties were measured with a CTD multiparametric probe installed on an automatic vertical profiler. Parameters include temperature, salinity, dissolved oxygen, fluorescence (chlorophyll-a) and irradiance, all of which are collected at 5-minute intervals. Data at 15 m depth, characterized by the highest data density and relevance for sediment resuspension processes affecting contaminant transport have been used.

In 2016, the dataset spans from January 1st to December 6th, with partial interruptions in December.

In 2024, new oceanographic surveys were launched as part of the ongoing monitoring initiative in the Gulf of Pozzuoli, expanding both the spatial and vertical coverage of in situ measurements and enabling more direct observations of near-bottom dynamics and any possible plume transport. These surveys were conducted seasonally within the framework of the already cited University of Naples Parthenope research project. The oceanographic component of the project focused on 17 monitoring stations distributed across the study area (Fig. 7). At each station, surface current measurements were obtained using a Nortek Aquadopp 300 current meter, while vertical profiles of water column properties were collected with a Seabird SBE 19plus V2 multiparametric CTD probe. The CTD was equipped with sensors for pressure, temperature, conductivity, fluorescence (chlorophyll-a), dissolved oxygen, Ph and turbidity, enabling high-resolution assessment of physical–chemical conditions.

These new datasets provide seasonal observations of current patterns and water column variability, supporting the characterization of near-bottom circulation processes and their role in the resuspension and transport of contaminants from the Bagnoli sediments towards the mussel farming areas of Lucrino.

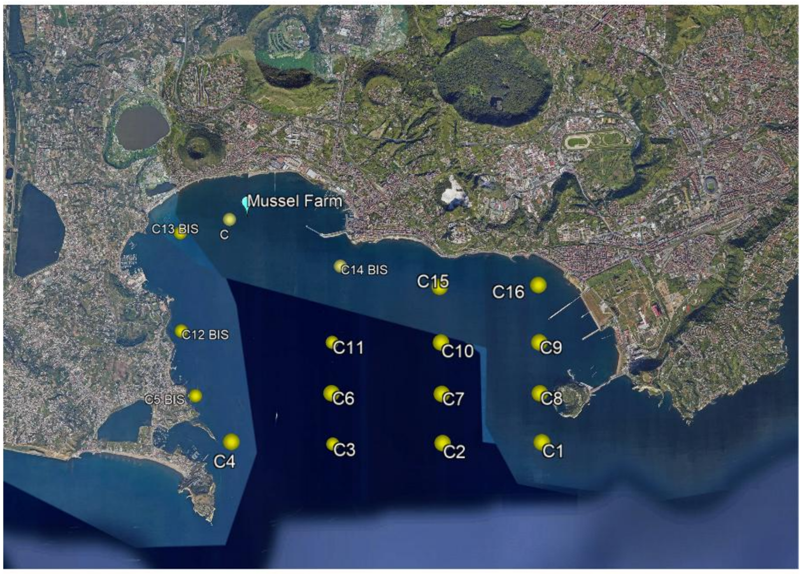

Figure 7. Location of 2024 in situ monitoring stations in the Gulf of Pozzuoli. Map generated using *Google Earth*. Yellow dots indicate sampling stations, and the lightblue symbol indicates the Lucrino mussel farm positions.

3.4.2 Satellite Data

Satellite-based remote sensing was employed to complement model and in situ data, particularly for the detection of sea surface features indicative of circulation structures (e.g., fronts, eddies, and filaments).

For 2016, we incorporated satellite-derived chlorophyll-a (CHL) concentration data covering the study area. While CHL data do not provide a direct measurement of surface currents, they offer valuable qualitative insights into hydrodynamic patterns, as chlorophyll distribution is influenced by water mass movements, mixing processes, and frontal dynamics (Mattei and Scardi, 2022; Dohan, 2017; Forget and André, 2007). This makes it a useful indicator of surface circulation features.

Satellite CHL observations have been widely used to study oceanographic processes and assess surface circulation patterns. In this study, CHL satellite data provided an additional observational component to evaluate the consistency between modelled circulation fields and features visible in ocean color imagery.

For this purpose, we used the *Mediterranean Sea, Bio-Geo-Chemical, L4, monthly means, daily gap-free and climatology Satellite Observations* product (Product ID: OCEANCOLOUR_MED_BGC_L4_MY_009_144) from the Copernicus Marine Environment Monitoring Service (CMEMS, https://marine.copernicus.eu/). This dataset provides daily, gap-free CHL concentration data at a 1 km spatial resolution and a Level 4 processing level, ensuring high-quality, temporally consistent estimates for the Mediterranean Sea (Volpe et al., 2018, 2019). The dataset was accessed through CMEMS and is available at https://doi.org/10.48670/moi-00300. This choice was driven by the limited availability of higher-resolution satellite data (Levels 1 and 2), which are significantly affected by cloud cover, particularly during the winter months. While Kd490 (the diffuse attenuation coefficient at 490 nm) could have been a valuable proxy for sediment transport in this study, its spatial resolution and temporal coverage during the period of interest were insufficient for our analysis. Consequently, we relied exclusively on CHL data for comparison with observed sea current patterns. Satellite data were processed, analysed, and visualized using MATLAB and SeaDAS, a specialized image analysis package developed by NASA for processing, displaying, analysing, and ensuring the quality control of ocean color data.

For 2024, the observational framework was enhanced with altimetry data from the Surface Water and Ocean Topography (SWOT) satellite, launched in late 2022 by the National Aeronautics and Space Administration (NASA) and the French Space Agency (CNES), with contributions from the Canadian Space Agency (CSA) and the United Kingdom Space Agency (UKSA). Specifically, we employed the *Experimental multimission gridded L4 sea level heights and velocities with the SWOT product* (DOI: https://doi.org/10.24400/527896/A01-2024.007). This dataset is derived from Level-3 along-track altimetry (DOI: doi.org/10.48670/moi-00147) and combines observations from conventional nadir missions (Jason-3, CryoSat-2, Saral/AltiKa, Sentinel-3A/B, Sentinel-6A, HaiYang-2B) with SWOT nadir and KaRIn measurements (DOI: https://doi.org/10.24400/527896/A01-2023.018). The gridded fields are produced using the MIOST (Multiscale Interpolation of Ocean Surface Topography) approach (Ubelmann et al., 2021, 2022; Ballarotta et al., 2025), which explicitly separates different dynamical modes (e.g., geostrophic, barotropic, equatorial wave processes) by constructing independent covariance components. This allows for a more detailed reconstruction of mesoscale and submesoscale structures, making the product particularly suitable for assessing the added value of SWOT observations. The dataset provides daily fields at 1/10° × 1/10° spatial resolution and is distributed by AVISO (SSALTO/DUACS, CNES). Sea surface height (SSH) gradients derived from this dataset can be used to estimate geostrophic surface currents, offering a novel observational layer for the GoP, where fine-scale circulation is critical for pollutant dispersion. The integration of SWOT-derived SSH fields with model and in situ observations is expected to improve the interpretation of dynamic features (e.g., nearshore eddies or jets) that influence particle transport, including the delivery of PAHs to aquaculture zones.

3.4.3 Ocean Model Outputs

In situ observations in the Gulf of Pozzuoli are extremely limited, with the "MEDA A" fixed-point station representing the only continuous monitoring location. Consequently, to obtain a basin-scale perspective of water mass properties and circulation dynamics in both the GoP and GoN during 2016, this study relies on outputs from the high-resolution Campania Regional Ocean Model (CROM; de Ruggiero et al., 2016), which is based on the Princeton Ocean Model (POM; Blumberg and Mellor, 1987; Mellor, 2004; Giunta et al., 2007). CROM solves the primitive equations of motion using sigma-coordinate vertical discretization and finite-difference schemes on Arakawa B grids, including free surface calculations, thermodynamics, and turbulence closure parameterizations.

The model domain extends from 40°N to 41.43°N latitude and from 13°E to 15.36°E longitude, covering the full GoP and GoN regions along with a surrounding buffer zone to ensure smooth nesting with the larger-scale NEMO-OPA Mediterranean model (Madec, 2008; Oddo et al., 2009), which provides initial and boundary conditions (Fig. 8). The horizontal grid resolution is 1/144° in both latitude and longitude ($\Delta y \approx 772$ m, $\Delta x \approx 579$–591 m), while the vertical discretization consists of 40 sigma levels, refined near the surface and in intermediate layers. Atmospheric forcing is supplied by the non-hydrostatic SKIRON/Eta model at 5 km resolution, accounting for momentum, heat, freshwater, and radiative fluxes.

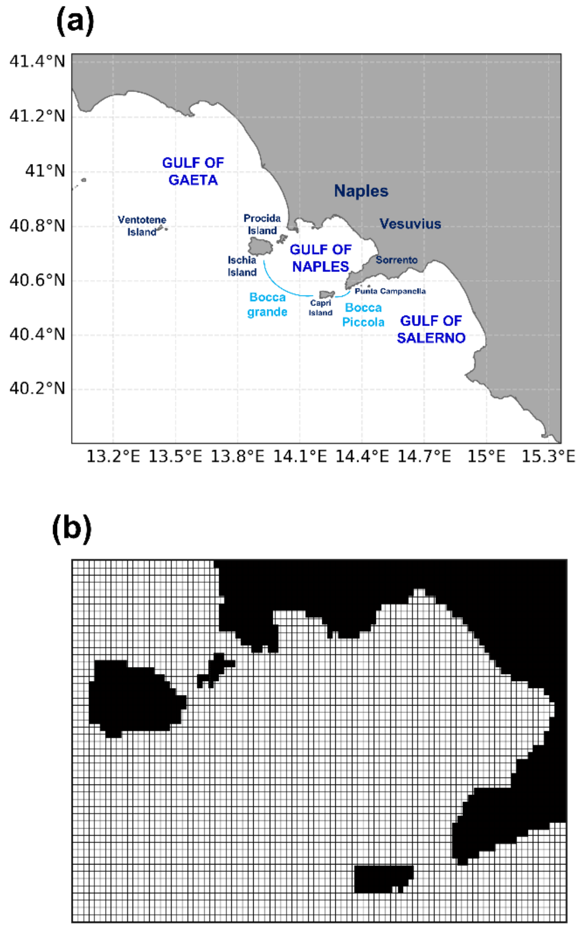

Figure 8. Domain of integration (a) and computational grid (b) of CROM.

CROM generates hourly outputs of temperature, salinity, currents, and sea level. The model has been extensively validated for both surface and subsurface dynamics in the Gulf of Naples, using a combination of satellite altimetry, turbidity maps, high-frequency radar measurements, and in situ CTD/ADCP datasets (de Ruggiero et al., 2016, 2020; Gifuni et al., 2022). While SKIRON/Eta adequately reproduces basin-scale wind patterns, its coarse resolution tends to underestimate local wind intensity in the GoP, as confirmed by comparisons with Bacoli weather station data (Gifuni et al., 2022).

To improve the representation of local winds, SKIRON/Eta outputs were blended with Bacoli station observations (lightblue dot in Fig. 5b), which were assumed to be representative of the entire target domain (black box in Fig. 8a: 40.76°N–40.83°N, 14.06°E–14.18°E). Within this area, the SKIRON-simulated wind was replaced by a spatially uniform field derived from Bacoli measurements, using a 20-grid-point blending buffer (cyan box in Fig. 8a) to ensure a smooth transition. Within this zone, the wind field was computed as a weighted combination of modelled and observed winds via a Hann function (Eq. 1):

$$W(d) = \frac{1}{2}\left(1 + cos\left(\pi \cdot \frac{d}{R}\right)\right) \quad for\ d < R \qquad \textbf{[1]}$$

where d is the distance from the boundary of the black box, and R is the relaxation distance defining the width of the transition. This function ensures that the observed wind has full weight at the boundary of the target area ($W = 1$ at $d = 0$) and smoothly fades to zero ($W = 0$ at $d = R$), avoiding artificial discontinuities.

The final wind components (Uadj, Vadj) were then computed according to the following equations:

$$Uadj = W \cdot Uobs + (1 - W) \cdot Ucrom \qquad \textbf{[2]}$$

$$Vadj = W \cdot Vobs + (1 - W) \cdot Vcrom \qquad \textbf{[3]}$$

CROM outputs in this study were employed to: describe sea surface current patterns preceding high PAH concentration events; identify potential transport pathways from likely source areas (e.g., Bagnoli) to the Lucrino mussel farm; provide Eulerian current fields to drive forward and backward Lagrangian simulations of particle transport.

3.5 Lagrangian Simulators for Particle Tracking

To investigate the transport pathways of contaminants in the coastal environment, forward Lagrangian transport simulations were conducted for two distinct study periods using different modeling tools. The adoption of two Lagrangian frameworks reflects differences in data availability, spatial scale, and methodological objectives between the two phases of the study, rather than a direct comparison of models.

For the 2016 analysis, the General NOAA Operational Modeling Environment (GNOME) was employed (Beegle-Krause, 1999; 2001; Zelenke et al., 2012). This choice was driven by the availability of high-frequency hydrodynamic outputs from the Campania Regional Ocean Model (CROM) and by the suitability of GNOME for event-based simulations at the local scale, aimed at reconstructing short-term transport pathways from known coastal contamination sources toward the mussel farming area.

In contrast, the 2024 analysis was conducted using Parcels (Probably A Really Computationally Efficient Lagrangian Simulator), a Python-based toolbox specifically designed for flexible and large-scale particle tracking using outputs from different ocean circulation products (OceanParcels project, 2019). Parcels were selected to support the integration of satellite-derived geostrophic currents from the SWOT mission and to enable simulations over a broader spatial domain, consistent with the regional-scale focus of the 2024 investigation.

3.5.1 GNOME - General NOAA Operational Modeling Environment

The simulations were driven by the Eulerian surface current fields produced by the CROM and forced with the blended wind field. GNOME applies a mixed Eulerian-Lagrangian approach to simulate the particles' advection (Lagrangian Elements, LEs) driven by time-varying surface currents and/or wind forcing, using a forward Euler integration scheme (equivalent to a first-order Runge-Kutta method).

Each particle’s trajectory follows the Lagrangian equation of motion:

$$\frac{d\vec{x}}{dt} = \vec{u} \qquad \textbf{[4]}$$

where $\vec{x}$ is the particle position vector and $\vec{u}$ is the total surface velocity. For the 2016 simulations, particles are modeled as passive tracers, and transport is constrained to a single surface layer, neglecting vertical motions and shear. In GNOME, the displacement (Δx, Δy, Δz) at time *t* of a generic passive tracer (identified by its spatial coordinates) is calculated using Equation 5 (Zelenke et al., 2012):

$$\Delta x = \frac{\frac{u}{111{,}120.00024} \cdot \Delta t}{\cos(y)}, \ \Delta y = \frac{v}{111{,}120.00024} \cdot \Delta t, \text{ and } \Delta z = 0 \qquad \textbf{[5]}$$

where $\Delta t = t - t_1$ is the time elapsed between time steps i (set to 15 minutes), y is the latitude in radians, and 111120.00024 is the distance in meters per degree of latitude (assuming 1 arcminute equals 1 nautical mile everywhere). (Δx, Δy) are the 2D longitudinal and latitudinal displacements at the surface layer z, while (u, v) are the zonal and meridional components of the surface current field provided by CROM.

Following Uttieri et al. (2011), the horizontal diffusion was set equal to 10^4 cm^2/s, a typical value for coastal areas (Okubo,1971). Diffusive processes were also included in the transport equations, using GNOME's random walk algorithm. The horizontal diffusion is represented as (Zelenke et al., 2012):

$$\frac{\partial C}{\partial t} = D_x \cdot \frac{\partial^2 C}{\partial x^2} + D_y \cdot \frac{\partial^2 C}{\partial y^2} \qquad \textbf{[6]}$$

Where C is the concentration of the material and D_x, D_y are the horizontal diffusivity coefficients.

Considering the diffusive processes, the calculation of the zonal (Δx) and meridional displacement (Δy) of the i-th particle is computed according to the following equation:

$$\Delta x = \frac{dx \cdot \frac{\sqrt{6 \cdot \frac{D}{10{,}000} \cdot \Delta t}}{111{,}120.00024}}{\cos(y)} \qquad \Delta y = dy \cdot \frac{\sqrt{6 \cdot \frac{D}{10{,}000} \cdot \Delta t}}{111{,}120.00024} \qquad \textbf{[7]}$$

GNOME then calculates the horizontal displacements using the diffusion coefficient D, and at each time step, it randomly selects *dx* and *dy* from a uniform distribution ranging between -1 and 1.

In a more compact Lagrangian form, the particle velocity can be expressed as the sum of the advective, wind-induced drift, and stochastic diffusive components:

$$\vec{u} = \vec{u}_c + \alpha\vec{u}_w + h(\mathrm{t}) \quad \textbf{[8]}$$

where $\vec{u}_c$ is the surface velocity provided by CROM, $\alpha\vec{u}_w$ represents the wind-induced drift (windage term), and η(t) is a stochastic term accounting for horizontal turbulent diffusion. The coefficient α defines the fraction of the wind velocity contributing to the surface drift; in this study, it was set to 3% (α=0.03), following typical values adopted for surface floating PAH-bearing particles in coastal environments (Ko et al., 2020; Stolzenbach et al., 1977).

The stochastic displacement follows the random walk formulation:

$$h(\mathrm{t}) = \sqrt{2D\,\Delta t}\,x(t) \quad \textbf{[9]}$$

where $D$is the horizontal diffusivity and $\boldsymbol{\xi}(t)$is a random vector, whose components are drawn from a standard normal distribution ($\xi_x, \xi_y \sim \mathcal{N}(0,1)$).

The resulting discrete position of the particle can be written as:

$$\vec{\mathrm{x}}_{\mathrm{t}+\Delta\mathrm{t}} = \vec{\mathrm{x}}_{\mathrm{t}} + (\vec{\mathrm{u}}_{\mathrm{c}} + \alpha\vec{\mathrm{u}}_{\mathrm{w}})\Delta\mathrm{t} + \sqrt{2\mathrm{D}\,\Delta\mathrm{t}}\,\mathrm{x}(\mathrm{t}) \quad \textbf{[10]}$$

This stochastic formulation corresponds to the two-dimensional advection–diffusion equation implemented in GNOME and allows the representation of unresolved turbulent motions as an effective horizontal diffusion process (Zelenke et al., 2012; Okubo, 1971).

Regarding particle beaching, GNOME automatically checks whether the new particle position is located on land or in water. The beaching algorithm traces the entire line on the bitmap between the old and new points to ensure that the particle does not skip over land and instead stops it at the first land cell encountered.

Based on the analysis of observed meteo-marine conditions for each event, we hypothesize that PAH-bearing sediments are resuspended during high-energy wave events and subsequently transported by surface currents from Bagnoli to the Lucrino mussels farm (red dot in Fig. 5b). To simulate this process, 4000 virtual particles were randomly released within the Bagnoli coastal zone (see the black dots in Fig. 9). In this framework, each particle represents a resuspended, sediment-associated PAH contaminant originating from the Bagnoli brownfield area. The particles act as passive tracers to explore plausible transport pathways toward the Lucrino mussel farm, without implying precise predictions of contaminant concentrations.

Releases were triggered one day after each peak wave event to account for a time lag between sediment resuspension and the onset of transport. Table 2 summarizes the timing and duration of each simulation experiment (in hours). To account for uncertainties in the simulated current field, a 30% error estimate was applied to both the along-current and cross-current components. This approach enables the calculation of both a *best-guess trajectory* (based on the unperturbed current field) and a corresponding *minimum regret trajectory* that captures the range of plausible transport pathways under uncertain conditions. Simulating the minimum regret solution helps assess transport outcomes that are less probable but potentially more harmful than the best-guess scenario.

Pollution event	**Release (day)**	**End (day)**	**Duration (hours)**	**Total particles**
25 Jan	16 Jan	25 Jan	240	4000
17 Feb	11 Feb	17 Feb	168	4000
22 Nov	13 Nov	22 Nov	240	4000
14 Dec	9 Dec	14 Dec	144	4000

Table 2. Details of each Lagrangian forward transport simulation with GNOME.

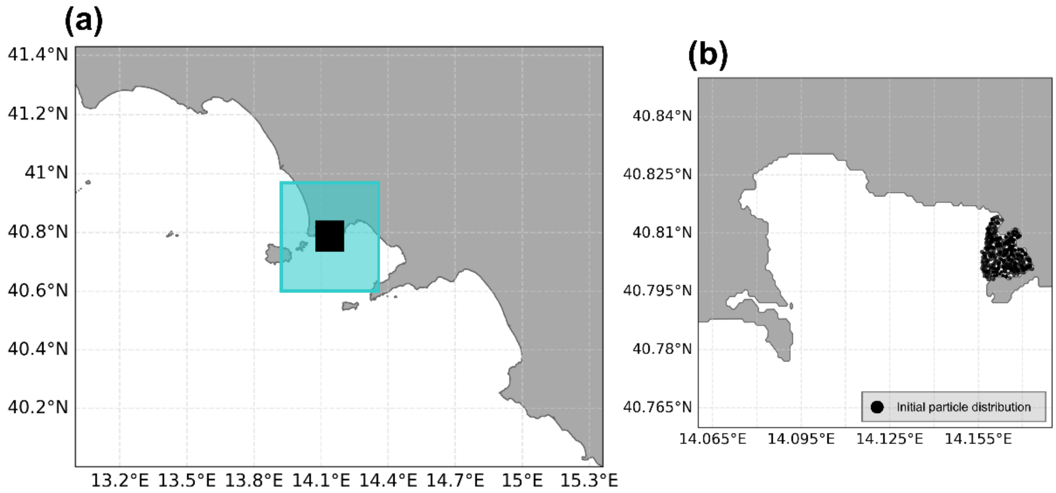

Figure 9. a) Target area (black box) and the surrounding buffer zone (cyan box) used for the computation of the blended wind field. b) Initial particle distribution adopted for Lagrangian transport simulations with GNOME. Particles represent resuspended, sediment-associated PAHs released near the Bagnoli area.

3.5.2 Parcels - Probably A Really Computationally Efficient Lagrangian Simulator

For the year 2024, Lagrangian particle tracking simulations were conducted using OceanParcels v3.1.1 (Delandmeter and van Sebille, 2019) to investigate the transport pathways of polycyclic aromatic hydrocarbons (PAHs) potentially released from maritime traffic in the Gulf of Naples. OceanParcels allows the simulation of both passive particles, such as contaminants or microplastics, and active particles, such as plankton or fish, within three-dimensional oceanic velocity fields. Particles were released in areas of the Gulf characterized by intense maritime traffic, reflecting likely sources of PAH dispersion (Fig. 10a). This choice was supported by chemical analyses performed during the 2024 project campaigns, which showed that PAHs detected in mussels were primarily derived from nautical fuels, confirming the link between maritime activity and contamination in the Lucrino farming area. In the 2024 Parcels simulations, particles represent near-surface PAH-bearing residues derived from nautical fuel, advected by ocean currents and wind forcing. As with the GNOME simulations, these particles serve as diagnostic tracers to identify likely transport pathways and accumulation zones, rather than to predict exact contaminant concentrations.

Four Lagrangian experiments were conducted to represent seasonal conditions (January–February, April, July, and October). Particles were released every 12 hours at locations characterized by intense maritime traffic **(Fig.9b)**. The Lagrangian trajectories were computed by integrating the general equation of motion:

$$\frac{d\vec{x}}{dt} = \vec{u} \qquad \textbf{[11]}$$

where $\vec{x}$ is the particle position vector and $\vec{u}$ is the total surface velocity. The advection equation governs the motion of each particle:

$$\vec{\mathrm{x}}_{\mathrm{t}+\Delta\mathrm{t}} = \vec{\mathrm{x}}_{\mathrm{t}} + \int_{t}^{t+\Delta t} \vec{u}(\vec{\mathrm{x}}(\tau), \tau) d\tau \qquad \textbf{[12]}$$

where $\vec{\mathrm{x}}_{\mathrm{t}}$ represents the position of the particle at time *t* and $\vec{u}$ is the Eulerian velocity field at time *t* interpolated from the ocean data. The velocity field used in the simulation was derived from altimetry data, and the simulation was restricted to the surface layer (2D simulation). The integral in Equation 12 is evaluated using a time step (*Δt)* of 15 minutes, meaning each particle's position was updated every 900 s based on the velocity fields. This combination of short integration time steps and regular particle release ensures both numerical accuracy and a representative sampling of potential transport pathways over the month-long period. No stochastic diffusion was applied in these simulations, as the resolution of the altimetry-derived velocity fields was considered sufficient to capture the dominant mesoscale and sub-mesoscale transport processes. Prior studies using Parcels have shown that for high-resolution velocity fields, the addition of random walk diffusion contributes minimally to particle displacement compared to deterministic advection (Van Sebille et al., 2018; Reijnders et al., 2022). By focusing exclusively on advective transport, the simulations provide a clear representation of the dominant pathways and accumulation zones of floating PAHs without introducing artificial dispersion that could obscure the influence of coherent currents and wind forcing.

In the present study, since particles were restricted to surface transport, the integral was solved using a 2D fourth-order Runge–Kutta (RK4) advection scheme (Butcher, 2016), which approximates the position at the next time step as:

$$\vec{x}_{t+\Delta t} = \vec{x}_t + \frac{\Delta t}{6}\,(k_1 + 2k_2 + 2k_3 + k_4) \qquad \textbf{[13]}$$

With:

$$k_1 = \vec{u}(x_t, t) \qquad \textbf{[14]}$$

$$k_2 = \vec{u}\left(\vec{x}_t + \frac{\Delta t}{2} k_1, t + \frac{\Delta t}{2}\right)$$

$$k_3 = \vec{u}\left(\vec{x}_t + \frac{\Delta t}{2} k_2, t + \frac{\Delta t}{2}\right)$$

$$k_4 = \vec{u}(\vec{x}_t + \Delta t k_3, t + \Delta t)$$

This approach ensures accurate interpolation of the velocity field and smooth particle tracking over complex coastal geometries.

To represent realistic coastal processes, a high-resolution land mask derived from GEBCO bathymetry was applied. Particles encountering grid cells with elevation above zero were considered beached, halting their motion to prevent unphysical penetration into land. Mathematically, this is expressed as:

$$\vec{x}_{t+\Delta t} = \begin{cases} \vec{x}_t & if\ landmask\,(x_t + \Delta t) \geq 0.5 \\ \vec{x}_{t+\Delta t} & otherwise \end{cases} \qquad \textbf{[15]}$$

This formulation ensures that once a particle reaches land, its position remains fixed at the previous time step, effectively simulating beaching. By stopping particles at land points, the model reproduces realistic accumulation along coastlines and avoids unphysical scenarios where particles would cross terrestrial boundaries. Since the velocities are given in linear units (m/s), a conversion to geographic coordinates (degrees latitude and longitude) was applied to advect particles on the Earth's curved surface:

$$\Delta lat = \frac{v \cdot \Delta t}{R} \cdot \frac{180}{\pi} \quad [16]$$

$$\Delta lon = \frac{u \cdot \Delta t}{R \cdot cos(\phi)} \cdot \frac{180}{\pi} \quad [17]$$

where v and u are the meridional and zonal velocities, Δt is the time step in seconds, R=6.371×10^6m is the Earth's radius, and ϕ is the particle latitude. The factor 180/π converts radians to degrees, while the cos(ϕ) term accounts for the convergence of meridians toward the poles. This formulation ensures that particle trajectories respect the curvature of the Earth and the spatial structure of the velocity field.

Particle density was evaluated on a structured 60×60 grid in longitude and latitude, with each grid cell spanning approximately 1.3 km in longitude and 1.2 km in latitude. This discretization allows quantitative assessment of local particle accumulation and transport pathways while balancing spatial resolution and computational efficiency.

In the first scenario, particles were advected solely by surface geostrophic currents derived from altimetric L4 sea level products (*Experimental multimission gridded L4 sea level heights and velocities with SWOT product*). The particle advection equation in this case reduces to:

$$\vec{u} = \vec{u}_c \quad [18]$$

where $\vec{u}_c$ represents the geostrophic surface velocity provided by the altimetry.

In the second scenario, the effect of wind forcing was incorporated in addition to the SWOT-derived surface currents. Wind data were obtained from the ERA5 reanalysis product, which was locally corrected using observations from the Naples weather station. A spatially weighted approach was applied to combine ERA5 reanalysis and station wind data, meaning that wind measurements from the Naples Pacanowski station were given greater influence close to the station, while ERA5 values gradually dominated farther away **(Fig. 9c)**. This ensured a smooth transition across the Gulf of Naples and avoided discontinuities in the wind field used for particle simulations. A windage factor of 3% was applied to account for the contribution of wind at 10 meters height to the drift of floating PAH-bearing particles (Ko et al., 2020; Stolzenbach et al., 1977). Wave-related processes, including Stokes drift and radiation stress, were not explicitly included in the simulations. Although wave-induced dynamics, particularly those associated with radiation stress and wave–current interactions, can play an important role in coastal environments, these processes could not be resolved by the available hydrodynamic and altimetric datasets. The simulations were therefore designed to isolate the circulation- and wind-driven components of transport, acknowledging that wave-related effects may contribute to nearshore dispersion and represent a source of uncertainty in the reconstructed pathways. Moreover, the simulated particles represent small, floating contaminants, for which wave-induced drift components are not explicitly resolved by the available datasets. The simulations, therefore, focus on transport driven by geostrophic currents and wind-induced drift.

The total advection velocity was obtained by vectorially summing the ocean currents and the wind-induced velocity scaled by the windage factor:

$$\vec{u} = \vec{u}_c + \alpha \vec{u}_w \qquad [19]$$

where $\vec{u}_c$ represents the surface geostrophic velocity provided by the altimetry, and $\alpha \vec{u}_w$ is the wind-induced velocity at 10 m height scaled by the windage factor $\alpha = 0.03$. The surface current field implicitly includes the oceanic response to atmospheric forcing, while the windage term accounts for the direct action of wind on floating particles. The total linear velocity was then converted to geographic coordinates (degrees latitude and longitude) using the same relations as in the first scenario:

$$\Delta lat = \frac{(\vec{u}_c + \alpha \vec{u}_w) \cdot \Delta t}{R} \cdot \frac{180}{\pi} \qquad [20]$$

$$\Delta lon = \frac{(\vec{u}_c + \alpha \vec{u}_w) \cdot \Delta t}{R \cdot cos(\phi)} \cdot \frac{180}{\pi} \qquad [21]$$

This formulation ensures that the combined effect of ocean currents and wind forcing is properly represented on the curved Earth surface.

For each scenario, four Lagrangian simulations were performed to represent different seasonal conditions in 2024. Each simulation covered one month (January–February, April, July, and October). The winter simulation (January–February) was extended to 60 days to encompass the two high-PAH contamination events detected in mussel samples (24 January and 14 February). Particles were released continuously every 12 hours, with 150 particles per release, resulting in a total of 18,000 particles for the 60-day simulation and 9,000 particles for each 30-day run. **Table 3** summarizes each simulation detail. This configuration ensures dense spatial coverage while maintaining computational efficiency. The four simulation periods thus provide a representative picture of seasonal variability in transport dynamics within the Gulf of Naples, linking modelled dispersion patterns with observed contamination events.

In summary, the Lagrangian framework implemented with Parcels allowed simulation of continuous particle release and transport over one month, capturing the interplay between ocean currents and wind forcing while providing a detailed spatial representation of particle density, transport pathways, accumulation zones, and potential areas of environmental concern.

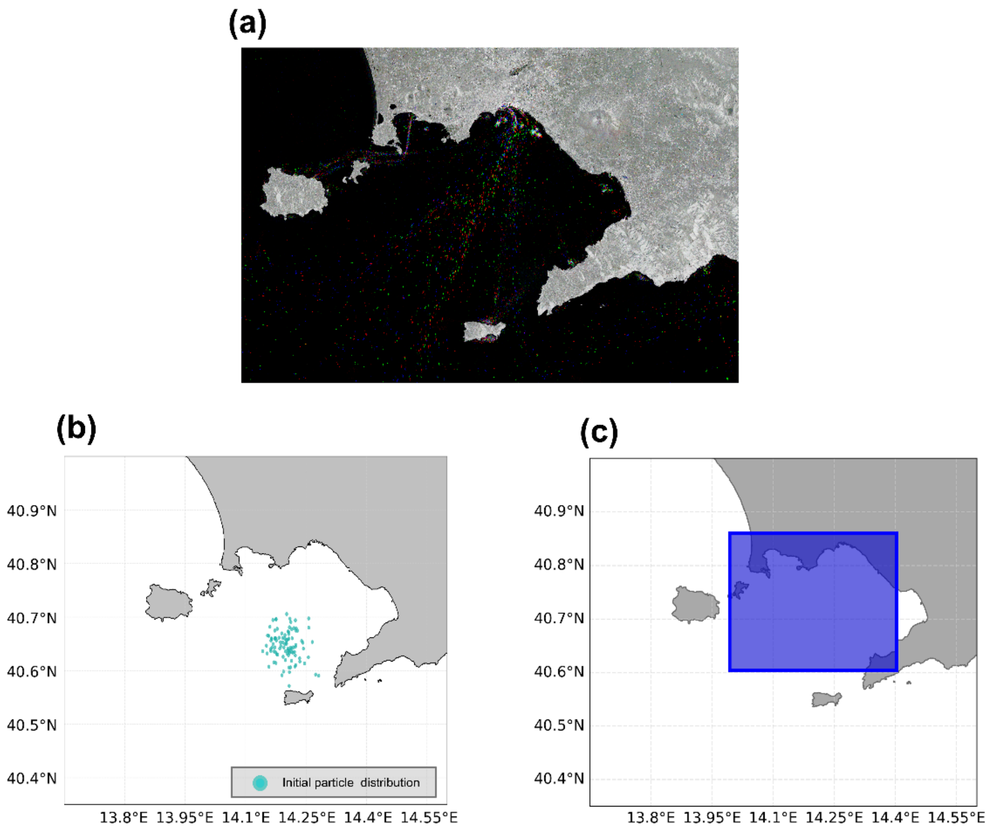

Figure 10. a) Maritime traffic in the Gulf of Naples captured by ESA's Copernicus Sentinel-1 satellites. This composite image condenses three years of radar data (2017 in blue, 2018 in green, 2019 in red), revealing ship movements across the Tyrrhenian Sea between the Port of Naples, Pozzuoli, the islands of Ischia, Procida, and Capri, as

well as the Sorrento Peninsula and the Amalfi Coast. The sea appears dark, while urban areas and Mount Vesuvius reflect the radar signal in bright white. b) Initial particle distribution adopted for Lagrangian transport simulations with OceanParcels. c) Buffer zone (blue box) used for the computation of the blended wind field. Particles represent near-surface PAH residues from maritime traffic, advected by currents and wind.

Season	Release (day)	End (day)	Duration (hours)	Total particles
Winter	1 Jan	29 Feb	1440	18000
Spring	1 Apr	30 Apr	720	9000
Summer	1 Jul	30 Jul	720	9000
Autumn	1 Oct	30 Oct	720	9000

Table 3. Details of each Lagrangian forward transport simulation with OceanParcels.

3.5.3 Comparison between Lagrangian modeling approaches

The two Lagrangian modeling approaches adopted in this study — GNOME and Parcels — share the same fundamental formulation, based on the integration of particle trajectories within a prescribed velocity field, as expressed in Equations [4] and [11].

However, they differ substantially in terms of spatial scale, input data, and physical parameterization, providing complementary perspectives on the dispersion dynamics within the Gulf of Naples.

GNOME, applied to the 2016 contamination events, was designed as a local-scale model to simulate the short-term transport of passive tracers released near Bagnoli under high-energy wave conditions. It relies on CROM-derived surface currents and blended wind fields, incorporating a stochastic diffusion term to represent unresolved turbulent processes. The model thus captures both the deterministic advection and the sub-grid diffusion typical of nearshore environments.

In contrast, Parcels, applied to the 2024 scenarios, operates at a regional scale, driven by SWOT-enhanced geostrophic currents and ERA5 wind supplemented by in situ wind measurements. It was configured as a deterministic, advection-only model, assuming that the spatial and temporal resolution of the velocity fields is sufficient to explicitly resolve mesoscale variability. This configuration allows investigation of seasonal and wind-driven transport pathways under realistic synoptic forcing.

Together, the two approaches provide a consistent multi-scale framework for assessing pollutant transport and potential exposure of coastal aquaculture areas.

While GNOME was applied to investigate short-term, nearshore dispersion processes, and Parcels was implemented to extend the analysis to broader spatial and temporal scales, these differences reflect the specific modeling setups adopted in this study rather than intrinsic limitations of the respective tools. This approach allowed the identification of persistent circulation features that may influence the connectivity between source and receptor areas.

It is important to emphasize that both GNOME and Parcels are used in a diagnostic sense: they are intended to identify plausible transport pathways and patterns of connectivity between source and receptor areas, rather than to predict exact contaminant concentrations. The complementary scales of the two frameworks —

local nearshore processes with GNOME and basin-scale seasonal circulation with Parcels — provide a more robust mechanistic understanding of PAH transport, allowing key features of exposure and accumulation to be consistently identified despite inherent uncertainties in the velocity fields and forcing data.

Chapter IV

4. RESULTS

4.1 Local model-based approach for 2016

Due to the general scarcity of continuous, depth-resolved oceanographic observations in the Gulf of Pozzuoli, the initial phase of this research focused on the year 2016, for which a relatively comprehensive dataset was available. This dataset combined in situ measurements from the *MEDA A* oceanographic station with outputs from the CROM circulation model and satellite observations, providing a first opportunity to investigate the coupled role of meteorological forcing and coastal hydrodynamics in driving PAH transport.

The rationale for focusing on 2016 is twofold. First, historical mussel monitoring at the Lucrino site shows a clear seasonal pattern in PAH concentrations — high values in late autumn/early winter and low (often near-zero) values in spring–summer — a pattern that persists across the 2014–2022 record (Fig. 11) and was already suggested in earlier studies (Perugini et al., 2007a,b; Esposito et al., 2017). Second, for 2016, we had access to a corresponding set of observations and model outputs that permits a first, integrated analysis of atmospheric forcing, water column characteristics, and bottom-layer dynamics:

- Chemical monitoring: A total of 15 mussel samples were collected throughout 2016 at the Lucrino site, four of which (25 January, 17 February, 22 November, and 14 December) exceeded the legal PAH limits. Time series of BaP and the sum of the four priority PAHs are reported in Fig. 12.
- In-situ hydrography: CTD casts from the *MEDA A* station provided temperature–salinity (T–S) information.
- Sea-current and wave measurements: ADCP from MEDA A records of current components (zonal u and meridional v) over the vertical range 1.4 m – 18.5 m, and simultaneous wave parameters (wave height H_s, peak period T_p, and direction). Hovmöller diagrams of daily-averaged u and v for the whole year

gave a depth-resolved view of the circulation preceding each sampling event. Wave time series and directional statistics are shown in Fig.14.

- Meteorology: wind time series from the Bacoli meteorological station are used to build stick diagrams and to relate local atmospheric forcing to ocean response.
- Numerical model and satellite products: sea surface currents from the CROM circulation model and satellite imagery examined for the week preceding each high-PAH sampling to obtain a synoptic and spatially continuous view of surface transport pathways.

This combination — although not equivalent to a sustained, multi-year, depth-resolved observational network — enabled a robust process analysis for 2016 that links observed mussel contamination to identifiable marine-weather conditions (Fortunato et al. 2025).

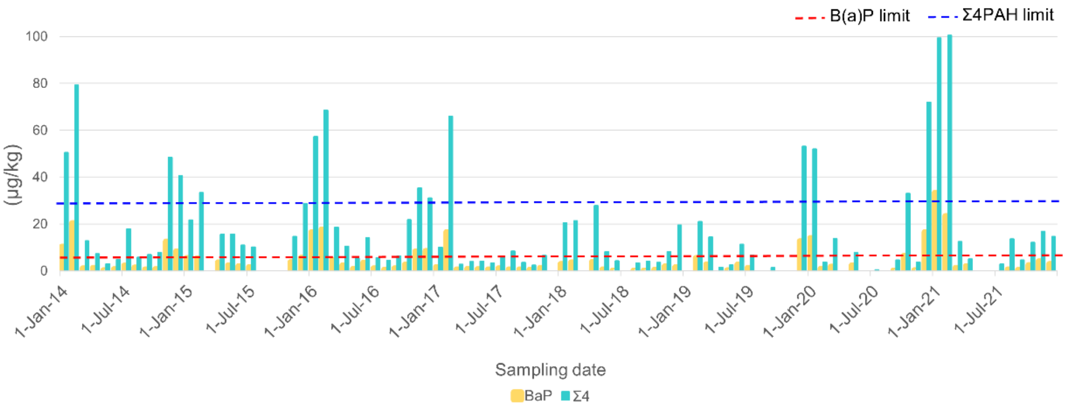

Figure 11. BaP concentration levels and the sum of 4PAH concentration in *Mytilus galloprovincialis* tissues from Lucrino farm between 2014 and 2022. The red and blue dotted lines indicate the PAH's legal limit.

4.1.1 Mussel contamination in 2016

The monitoring record confirms the seasonal behaviour already reported in previous studies: PAH concentrations in mussels are highest during late autumn and winter and drop to nearly undetectable levels in spring–summer (**Fig. 12**; Esposito et al., 2017). In 2016, out of 15 sampled events, four samples exceeded legal limits, occurring on 25 January, 17 February, 22 November, and 14 December. These discrete contamination peaks provide case studies to examine antecedent meteo-oceanographic conditions and to test transport and resuspension hypotheses.

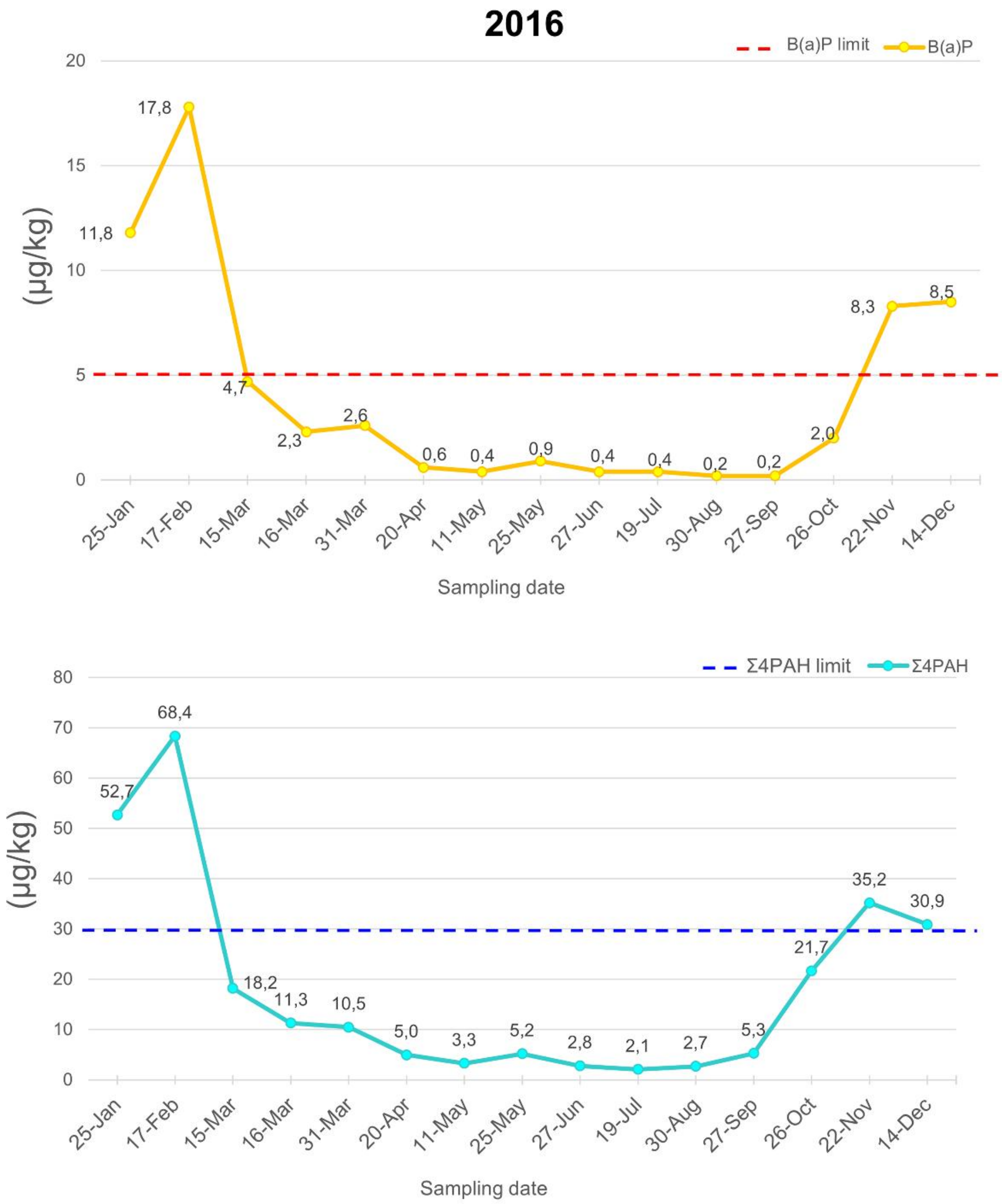

Figure 12. BaP concentration levels (upper panel) and the sum of 4PAH concentration (lower panel) in Mytilus galloprovincialis, tissues from Lucrino farm in 2016. The red and blue dotted lines indicate the PAH's legal limit. Dates refer to each PAH concentration analysis performed on sampled mussels.

4.1.2 Hydrographic context: temperature, salinity and seasonal stratification

MEDA A CTD data (T–S diagram, Fig. 13) indicate pronounced seasonal variability in water masses. Winter samples are characterized by colder and saltier waters (observed minimum temperature 14.24 °C, maximum salinity 38.19 PSU), while summer is dominated by warmer and fresher waters (maximum temperature 27.82 °C, minimum salinity 34.10 PSU). The freshest water mass (early May) is consistent with a regional freshwater input associated with increased rainfall (maximum daily rainfall 27.2 mm recorded at Pozzuoli) and is visible as the low-salinity cluster on the T–S diagram. Seasonal development of the mixed layer (Cianelli et al., 2011) and the vertical stratification inferred from these profiles are central to understanding why transport pathways and vertical exchange processes differ markedly between the warm and cold seasons.

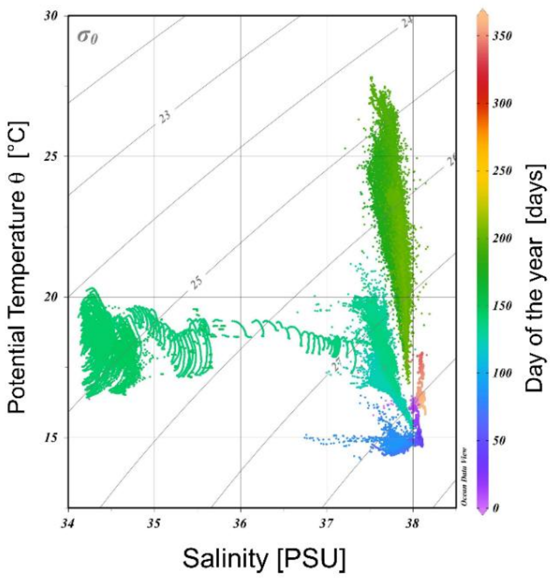

Figure 13. Potential temperature-Salinity (θ-S) diagram for the 2016. The colorbar indicates the days of the year. Data were collected at a depth of 15m from the "MEDA A" CTD probe.

4.1.3 Sea currents, waves, and the physical precursors of contamination events

ADCP-derived Hovmöller diagrams of the zonal (u) and meridional (v) components (daily means, 1.4–18.5 m) provide a clear view of the depth-resolved circulation for the full year (Fig.14a). Two distinct regimes emerge:

- Winter contamination events: in the days preceding the late autumn/early winter PAH peaks, the entire water column shows negative zonal velocities (westward) and positive meridional velocities (northward) — i.e., a northwestward displacement of water masses. This depth-extended signal suggests strong wind-driven and/or barotropic responses capable of transporting pollutants from the decommissioned Bagnoli area toward the western GoP mussel farms. Model surface fields (CROM) support these observations, showing the development of northwestward surface currents about one week before the contamination events.
- Summer conditions: the northwestward pattern is largely restricted to surface layers during summer; deeper layers remain relatively less impacted. The limited vertical influence of surface forcing in stratified conditions reduces the probability of efficient transport of sediment-bound PAHs into the mussel feeding layer and across broader areas.

Wave measurements recorded by the ADCP show a notable association with contamination peaks. The wave data (Fig. 14b) reveal that, prior to pollution events, wave heights were generally higher, with peak wave periods (T_p) longer than 8 s and a predominant direction from the south. Significant wave heights (H_s) exceeding 1.2 m consistently preceded the most significant PAH contamination episodes. These wave conditions indicate enhanced hydrodynamic forcing capable of mobilizing surface sediments. To quantify the potential for sediment resuspension, wave-induced bottom shear stress (τ_β) was estimated using the Soulsby (1997) and Nielsen (1992) formulation, based on ADCP-measured wave parameters (H_s = 1.2 m, T = 8 s) and a representative site depth of 19 m. Assuming a wave friction factor appropriate for sandy seabed (f^w = 0.04), the calculated τ_β (~2.9 Pa) clearly exceeds the critical shear stress for fine sand resuspension ($\tau c \approx$ 0.05–0.1 Pa). This quantitative evidence confirms that the wave energy thresholds required to trigger sediment resuspension were surpassed, supporting the role of wave dynamics in enhancing PAH release into the water column and increasing their bioavailability. These findings align with the unified sediment transport framework proposed by Van Rijn (2007), which emphasizes the combined effects of currents and waves in controlling sediment mobilization and transport dynamics. The predominance of fine sand in the study area, as documented by Arienzo et al. (2017), justifies the use of these τc values and supports the application of this framework to interpret sediment resuspension and contaminant dynamics at the Lucrino site.

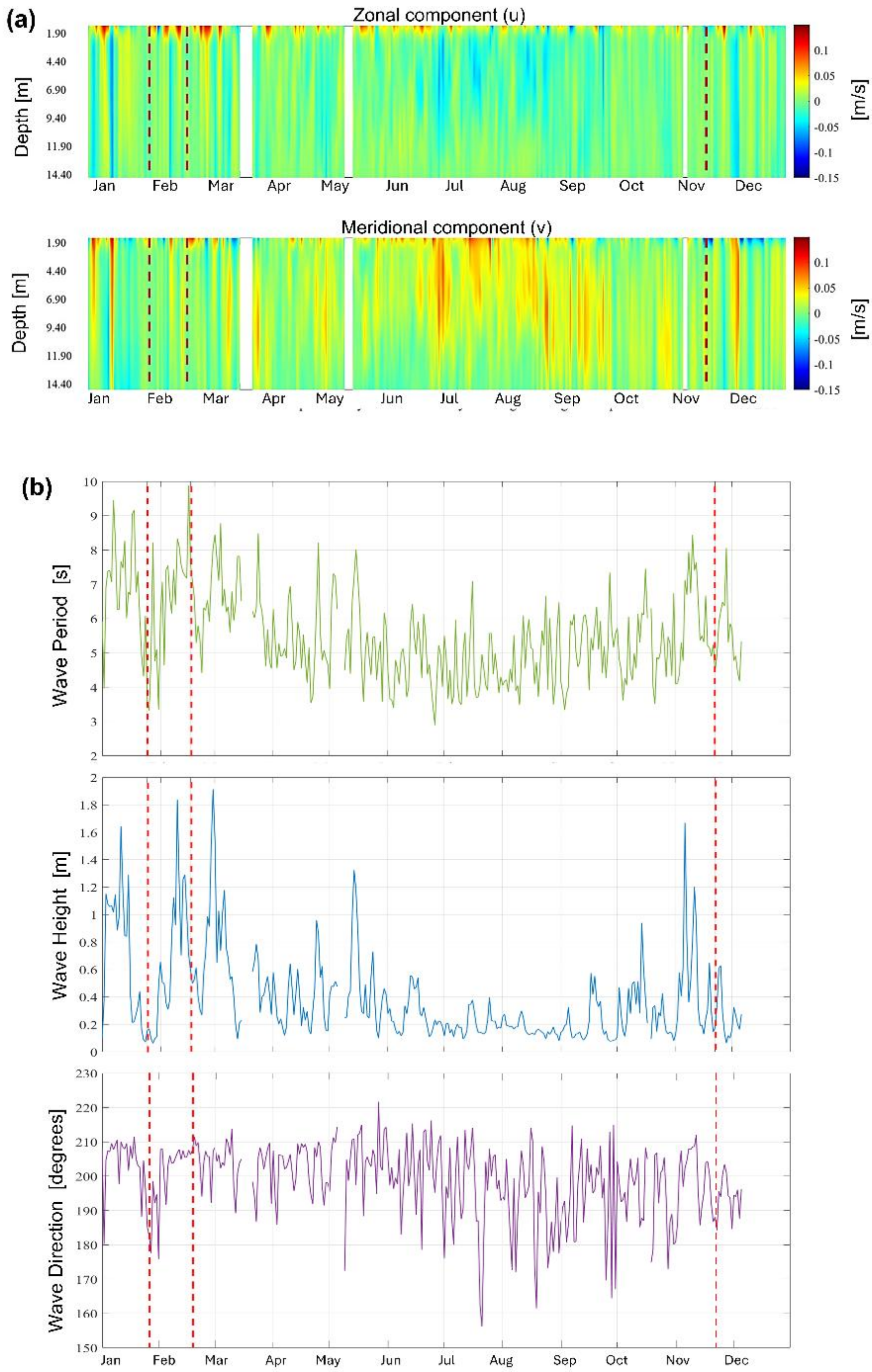

Figure 14. a) Hovmöller diagram for sea current data. The labels on the x-axis are the dates of mussel sampling and relative PAH analyses. b) Wave period, wave height, and wave direction recorded by "MEDA A" ADCP in 2016. The dotted red lines indicate events with higher contamination.

4.1.4 Atmospheric forcing and synoptic context

Meteorological records from the Bacoli station indicate that the hydrodynamic patterns described above coincide with episodes of intensified wind forcing from the southwest sector. Stick diagrams from wind and ADCP current observations illustrate the temporal coherence between wind increases and the onset of the northwestward surface flow patterns (see stick diagrams in Figs 15a-18a). Thus, contamination episodes appear to be driven by synoptic situations that simultaneously generate sustained northwesterly surface transport in the GoP and produce southerly waves capable of mobilizing bottom sediments.

4.1.5 Event-based analysis for 2016

To better understand the physical mechanisms underlying the episodic contamination of mussels observed in 2016, a detailed analysis for each contamination event was conducted. This approach integrates meteorological, oceanographic, and model-derived information to reconstruct the environmental conditions preceding each high-PAH sampling and to assess their causal relationships. The analysis focuses on four discrete contamination episodes (25 January, 17 February, 22 November, and 14 December), each representing a distinct hydrodynamic and atmospheric configuration.

For each event, time series of wind and current data, modelled surface circulation, and satellite chlorophyll maps were examined. Stickplots and Hovmöller diagrams provided depth-resolved insights into current evolution, while meteorological data were used to identify the large-scale synoptic forcing. This multi-source framework allowed the identification of recurring patterns — notably, the coupling between southerly winds, enhanced wave activity, and northwestward nearshore transport — that collectively drive the resuspension and advection of PAH-contaminated sediments toward the Lucrino mussel farm.

The following sections describe, in chronological order, the four contamination events, highlighting the interplay between atmospheric conditions, sea-state evolution, and nearshore circulation responsible for each pollution episode. The results presented in this section have been published in Fortunato et al. (2025).

25 January pollution event

The PAH levels measured on 25 January 2016 were 11.8 µg/kg for BaP and 52.7 µg/kg for the sum of the four PAHs. Wind data of the entire month indicate a single episode of strong SSE winds (around January 20), with peak speeds reaching 10.8 m/s, approximately one week prior to the pollution event. This is evident in Fig 15a where the arrows indicate the direction the wind is pointing at. This convention is applied to similar diagrams (figures from 15 to 18) for wind and current data. On a larger scale, from January 18th to 22nd, the study region was affected by a weak atmospheric trough, resulting in a northeastern flow associated with minor precipitation events. Specifically, a brief rainfall episode occurred on the 21st, attributed to the passage of an instability line (i.e., a non-frontal band of convective activity). Following this, a gradual rise in atmospheric pressure was observed as a high-pressure system migrated into the Central Mediterranean basin, ensuring stable meteorological conditions until 25th January. During this period, northerly winds still prevailed, except on the 25th, when winds shifted from the northwest due to the presence of the anticyclonic area.

ADCP data (Fig 15b) indicate that sea currents were predominantly directed towards NW during January 2016, with a temporary change in current direction about ten days before the pollution event. The Hovmöller diagram derived from ADCP data (Fig 15c) provides crucial insights into the currents preceding the pollution event. Approximately ten days before the event, across all the analyzed depths, the zonal component (u) was observed to be negative, while the meridional component (v) was positive, indicating a prevailing movement of sea currents towards the NW. During this timeframe, the zonal component reached its maximum negative value (− 0.089 cm/s), while the meridional component reached a maximum value of 1.1 cm/s.

Fig 15d illustrates the mean current during this period, recorded with a value of 0.06 cm/s. The analysis of model outputs shows a southwestward current in the central and offshore areas of the GoN (Fig 15e,f) one week prior to the pollution event. Moreover, the satellite CHL maps (Fig 15g) reveal a lower concentration in the Bocca Piccola area of the GoN, which aligns with the circulation pattern described by CROM that shows an entering flow from Bocca Piccola. This confirms that despite the model's limitations in near coastal coverage, it might still capture significant circulation patterns affecting the distribution of CHL and, potentially, other particles.

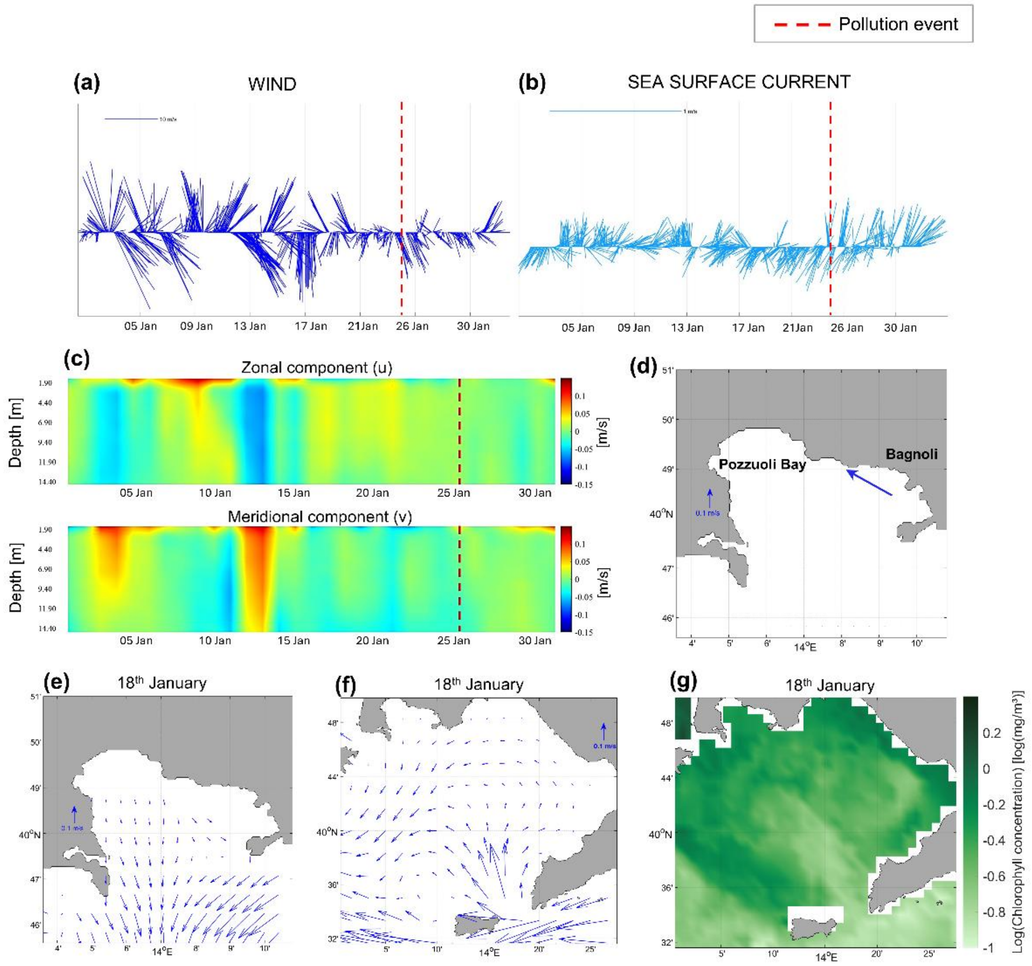

Figure 15. a) Stickplot diagram for wind data in January 2016; b) Stickplot diagram for sea surface current data recorded by the ADCP probe in January 2016; c) Hovmöller diagram for sea current data in January 2016; d) Mean current velocity map; e) Daily map of surface current simulated by CROM one week before the pollution event on 25th January zoomed in GoP. The arrows indicate the direction and intensity of the sea surface currents; f) Daily map of surface current simulated by CROM one week before the pollution event on 25th January over the GoN; g) Daily Level 4 CHL maps at 1 km of spatial resolution to describe the conditions of the enquired area about a week before the pollution event on 25th January.

17 February pollution event

The PAH levels measured on 17th February were 17.8 µg/kg for BaP and 68.4 µg/kg for the sum of the four PAHs. Large-scale atmospheric circulation analysis shows that during the period from 10th to 13th February, the Central Mediterranean area was affected by a western flow, embedded in a wide trough that embraced a large part of Central and Northern Europe. This led to several moderate rainfall episodes in the study area, especially on February 11th and 13th. On the 14th, a notable meridional oscillation of the polar front occurred over the western Mediterranean basin, triggering a southern and mild flow over the Italian Peninsula. Such meridional flow caused additional weak rainfall events on the 14th and 15th February. In the subsequent days, the Rossby wave evolved to the cutoff stage between the Balearic Islands and northern Africa, leading to warm advection over Southern Italy without generating significant precipitation events.

The local wind data analysis (Fig 16a) indicates that strong SSE-S winds were observed one week prior to the pollution event, with peaks reaching a maximum of 16.9 m/s.

In this scenario, the sea surface current pattern at the "MEDA A" site (Fig 16b) exhibited more variability compared to January. However, the current field is directed towards NE in both the surface and the immediate subsurface layers. Below approximately 4 meters, a predominant direction towards NW was observed. (Fig 16c). During this period, the zonal component of the current reached a maximum value of 0.6 cm/s, while the meridional component reached a maximum value of 0.4 cm/s. The resulting mean current intensity was reported as 0.06 cm/s (Fig 16d).

The sea surface circulation simulated by CROM one week before the pollution event (Fig 16e,f) shows a flow mainly directed towards the eastern area of the GoP.

The CHL concentration map (Fig 16g) shows a minimum concentration near the Gulf of Castellammare di Stabia that could be associated with the presence of a gyre that is consistent with the Eulerian current field simulated by CROM.

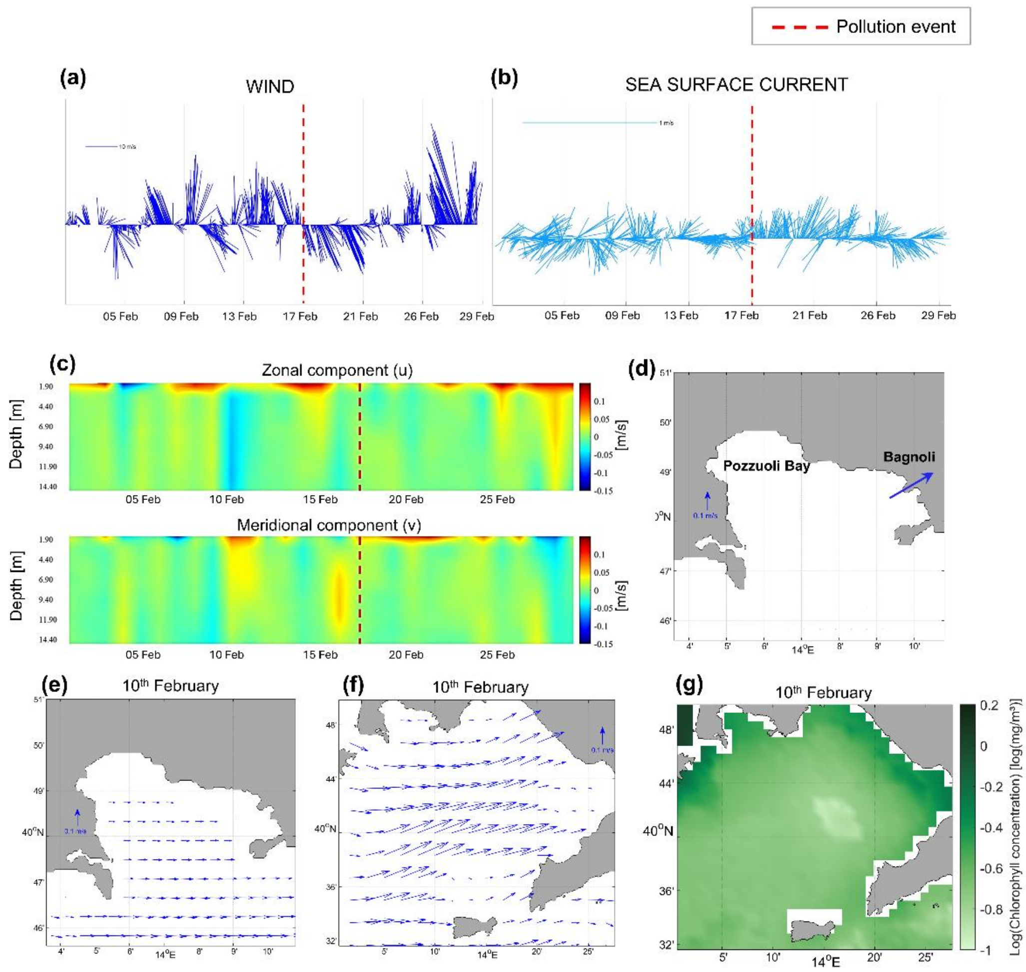

Figure 16. a) Stickplot diagram for wind data in February 2016; b) Stickplot diagram for sea surface current data recorded by the ADCP probe in February 2016; c) Hovmöller diagram for sea current data in February 2016; d) Mean current velocity map; e) Daily map of surface current simulated by CROM one week before the pollution event on 17th February zoomed in GoP.The arrows indicate the direction and intensity of the sea surface currents; f) Daily map of surface current simulated by CROM one week before the pollution event on 17th February over the GoN; g) Daily Level 4 CHL maps at 1 km of spatial resolution to describe the conditions of the enquired area about a week before the pollution event on 17th February.

22 November pollution event

The PAH levels measured on 22nd November were 8.3 µg/kg for BaP and 35.2 µg/kg for the sum of the four PAHs. In situ wind data (Fig 17a) showed a variable regime with relatively weak winds throughout the month, except for the week preceding the pollution event during which winds peaked at a maximum of 11.6 m/s, blowing from the SE-SSE.

Initially, the meteorological conditions were modulated by a high-pressure area until the 17th. Subsequently, a wide trough formed over Western Europe, affecting the western side of the Mediterranean region between the 20th and the 22nd of November. This meteorological configuration led to a warm southeastern flow over the Tyrrhenian Sea, determining a rise in air temperature. As for the rainfall, from the 15th to the 22nd of November, no precipitation events occurred in the investigated area. Regarding sea surface currents, variable patterns were observed during the first two weeks of November, as shown by the stickplot diagram in Fig 17b. Then, after the 13th of November, intense currents directed towards SSW-SW persisted for a continuous two-week period. Around ten days before the pollution event, sea currents were towards the NW, as illustrated by the Hovmöller diagram in Fig 17c. During this period, the zonal component of the current reached a maximum value of 0.2 cm/s, while the meridional one reached a maximum value of 0.2 cm/s, resulting in a mean current of 0.06 cm/s (Fig 17d).

The sea surface circulation simulated by CROM one week before the pollution event showed a southwestward current in the central and offshore areas of the GoN (Fig 17e,f). Additionally, the satellite CHL maps (Fig 17g) revealed a lower concentration in the Bocca Piccola area of the GoN and a higher concentration near the coast, which aligns with the circulation pattern described by CROM that showed a flow entering from Bocca Piccola. This suggests that, despite the model's limitations in coastal areas, it still provides valuable insights into the circulation patterns that influence the distribution of CHL and, potentially, other particles.

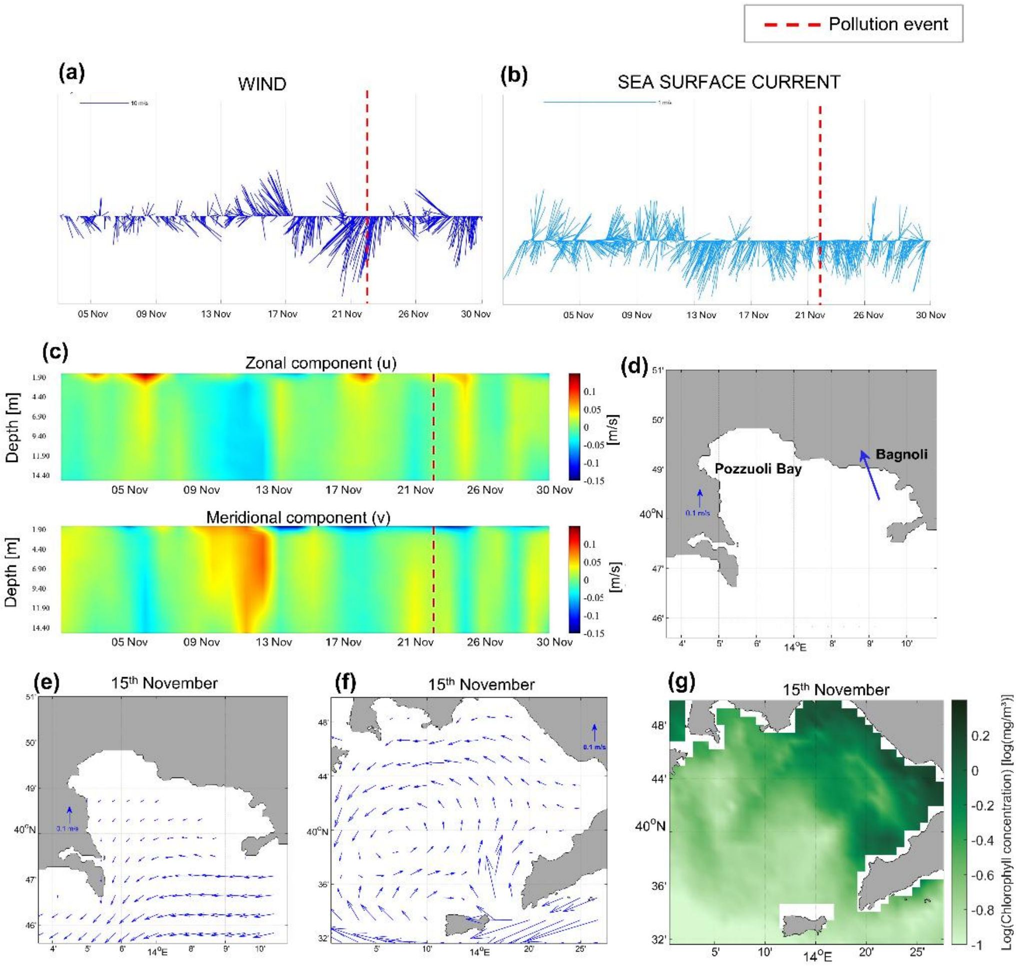

Figure 17. a) Stickplot diagram for wind data in November 2016; b) Stickplot diagram for sea surface current data recorded by the ADCP probe in November 2016; c) Hovmöller diagram for sea current data in November 2016; d) Mean current velocity map; e) Daily map of surface current simulated by CROM one week before the pollution event on 22nd November zoomed in GoP. The arrows indicate the direction and intensity of the sea surface currents; f) Daily map of surface current simulated by CROM one week before the pollution event on 22nd November over the GoN; g) Daily Level 4 CHL maps at 1 km of spatial resolution to describe the conditions of the enquired area about a week before the pollution event on 22nd November.

14 December pollution event

The PAH levels measured on 14th December were 8.5 µg/kg for BaP and 30.9 µg/kg for the sum of the four PAHs. From the 8th to the 10th of December, the atmospheric conditions in the study area were modulated by a high-pressure system, which determined stable weather, light winds and an absence of precipitation events. On the 11th of December, a wide trough affected Eastern Europe and the Balkan Peninsula, weakening the high-pressure system. Consequently, a weak low-pressure area formed over the Ligurian Sea, driving a moist western flow over the investigated area, leading to light rainfall around the 11th and 12th of December. In the following days, the synoptic configuration was characterized by an anticyclonic area over the Central Mediterranean region and Central Europe, along with a trough elongated from Eastern Europe to the Eastern Mediterranean. Stable weather conditions prevailed over the study area, associated with moderate northeastern winds. Prior to the pollution event, strong SE-SSE winds were locally observed, with peaks reaching 16.1 m/s, as shown in the stickplot diagram in Fig 18a. Unfortunately, current data were only collected until December 6th by “MEDA A”, limiting the discussion of the current pattern for the entire month. Nevertheless, the observation period included the week before the pollution event on December 14th. Analysis of sea surface currents (Fig 18b) indicated that they were predominantly directed towards the SSW-SW direction. The Hovmöller diagram (Fig 18c) showed that the period preceding the pollution event was characterized by a column of water with a negative zonal component (u) and a positive meridional component (v). During this period, the zonal component reached a maximum value of 9.7 cm/s, while the meridional component reached a maximum value of 9.6 cm/s. The average of the prevailing directions of marine currents is represented in Figure Fig 18d.

The sea surface current simulated by CROM one week before the pollution event (Fig 18e,f) showed a flow mainly directed towards the eastern area of the GoP. This flow aligns with the observed CHL patterns (Fig 18g), indicating a high concentration of CHL in the GoN, where the entering flow is consistent, and a lower CHL concentration in the GoP.

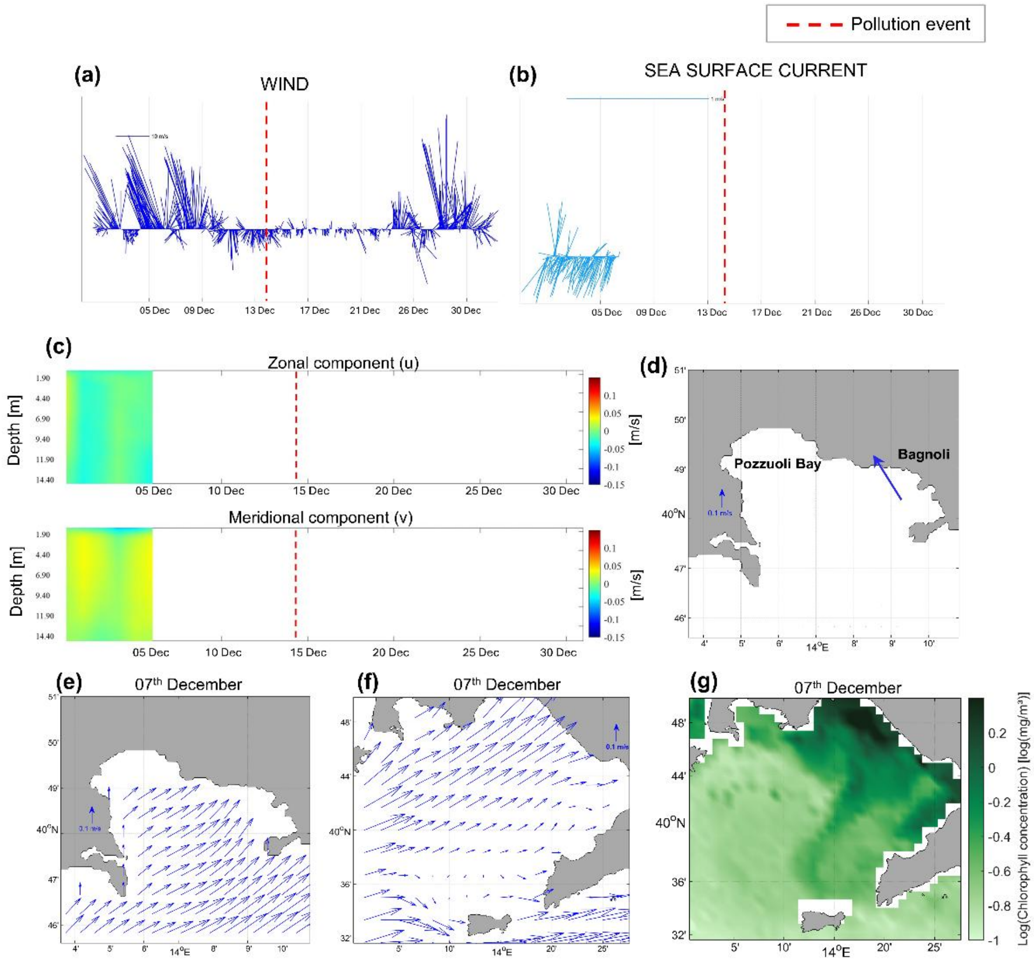

Figure 18. a) Stickplot diagram for wind data in December 2016; b) Stickplot diagram for sea surface current data recorded by the ADCP probe in December 2016; c) Hovmöller diagram for sea current data in December 2016; d) Mean current velocity map; e) Daily map of surface current simulated by CROM one week before the pollution event on 14th December, zoomed in GoP. The arrows indicate the direction and intensity of the sea surface currents; f) Daily map of surface current simulated by CROM one week before the pollution event on 14th December over the GoN; g) Daily Level 4 CHL maps at 1 km of spatial resolution to describe the conditions of the enquired area about a week before the pollution event on 14th December.

4.1.6 Lagrangian transport simulations

Once the atmospheric forcing over the study area before and during the pollution events, together with the corresponding in situ current measurements, have been presented, we report here the results of forward Lagrangian transport simulations aimed at identifying potential sources of PAHs (Polycyclic Aromatic Hydrocarbons) observed in mussels from the Lucrino farm. These diagnostic simulations were not intended to reproduce the exact observed concentrations but to identify plausible transport pathways consistent with the observed contamination timing.

This section presents the outcomes of simulations designed to test the hypothesis that the Bagnoli area may act as a primary source of PAHs. For details regarding the timing and duration of each simulated scenario, see Table 1.

Fig. 19 illustrates the spatial distribution of particle trajectories for each pollution event. The maps combine particle density plots based on the 'best estimate' trajectories (shown in grayscale) with the minimum-regret solution (pink shading in Figure 18), which accounts for uncertainty in the surface current simulations. Density maps were constructed by dividing the domain into 50 m bins and calculating a two-dimensional histogram of the number of particles passing through each bin during the simulation, thereby highlighting the dominant transport pathways and areas of higher particle accumulation. The pink-shaded area represents the uncertainty envelope of the modelled currents, with a 90% probability that particles will be found within this region (Zelenke et al., 2012).

For all the scenarios, forward simulations indicate that particles released near Bagnoli (Fig. 11b) can reach the Lucrino mussel farm (red dot in Fig. 19), though the extent and intensity of this transport vary according to the specific event. In January 2016 (Fig. 19a), the particle plume disperses broadly toward the northwest, with Lucrino located at the plume’s edge, suggesting limited exposure. For February 2016 (Fig. 19b), the best estimate trajectories remain confined to the northeastern Gulf of Pozzuoli, not directly impacting Lucrino. However, when model uncertainties are included (pink area), the simulations reveal a potential for particles to reach the mussel farm, indicating a non-negligible risk.

For November 2016 (Fig. 19c), a dense, well-defined plume extends westward from Bagnoli, resulting in significant particle accumulation near the Lucrino mussel farm. In December 2016 (Fig. 19d), a broader plume develops, extending toward Lucrino, further supporting the likelihood of contaminant transport under favourable oceanic and meteorological conditions.

Overall, the simulation outcomes are consistent with field observations and strongly support the hypothesis that, under specific atmospheric and hydrodynamic conditions, contaminants resuspended near Bagnoli can be advected toward the Lucrino mussel farm, contributing to the observed PAH concentrations.

It is important to acknowledge the main sources of uncertainty in these simulations, including the representation of coastal currents, wind forcing, particle parameterization, and nearshore processes such as sediment resuspension and vertical mixing. The combined use of best-guess and minimum regret trajectories allows capturing the range of plausible transport outcomes under these uncertainties. Despite these limitations, the principal conclusions — namely the identification of dominant transport pathways, the role of wind-driven coastal convergence, and the potential for sediment-borne PAHs to reach the Lucrino mussel farm — remain robust, as they are consistently supported across multiple simulations and event scenarios.

To provide a systematic quantitative synthesis of the four PAH contamination events analyzed in 2016, Table 4 summarizes the main meteorological forcing, wave conditions, current characteristics, inferred source type, and the outcomes of the Lagrangian transport simulations.

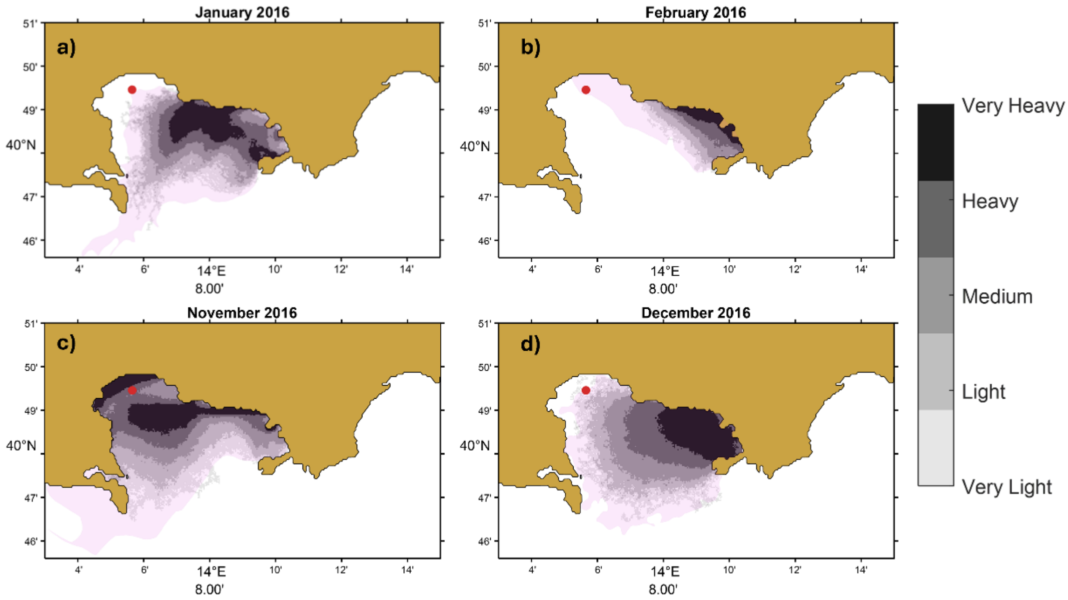

Figure 19. Results of Lagrangian simulations for four high-PAH contamination events: (a) January, (b) February, (c) November, and (d) December 2016. The red dot marks the location of the Lucrino mussel farm. The grayscale shading represents the particle density map obtained considering the 'best guess' solution. The pink-shaded areas indicate the potential spread of particles under uncertain current conditions, obtained by introducing a 30% random perturbation to both the both along and cross current directions.

Date	BaP / Σ4PAH (μg/kg)	Dominant wind	Wind max (m/s)	Wave height H_s (m)	Peak Wave period T_p (s)	Main current direction	Mean Sea Current Magnitude (cm/s)	Source	Main modelling outcome
25 Jan 2016	11.8 / 52.7	SSE	10.8	>1.2	>8	NW (entire water column)	0.06	Contaminated marine sediment from the Bagnoli site	NW plume reaches Lucrino marginally; exposure possible but limited
17 Feb 2016	17.8 / 68.4	SSE–S	16.9	>1.2	>8	NE (surface), NW (below ~4 m)	0.06	Contaminated marine sediment from the Bagnoli site	Direct impact unlikely in best guess; Lucrino reached under uncertainty envelope
22 Nov 2016	8.3 / 35.2	SE–SSE	11.6	>1.2	>8	NW (entire water column)	0.06	Contaminated marine sediment from the Bagnoli site	Dense plume from Bagnoli reaches Lucrino; strong accumulation
14 Dec 2016	8.5 / 30.9	SE–SSE	16.1	>1.2	>8	NW (entire water column)	9.7	Contaminated marine sediment from the Bagnoli site	Broad plume extends toward Lucrino; high transport potential

Table 4. Summary of contamination events in 2016 and modelling outcomes.

4.1.6 Final considerations on the model-based approach

The analyses presented in this chapter highlight the potential and limitations of model-based approaches for studying contaminant transport in semi-enclosed coastal systems such as the GoP. While the 2016 simulations provided valuable insights into the main hydrodynamic drivers of PAH dispersion, several data gaps and model uncertainties remain, particularly concerning nearshore processes and small-scale circulation patterns that strongly influence pollutant dispersion.

As already described, to address these limitations, in 2024 a dedicated project was launched aiming to expand the current understanding of the factors controlling PAH contamination in mussels farmed in the GoP, through the integration of chemical, physical, and biological measurements.

Within the Approccio Multidisciplinare alla Contaminazione da Idrocarburi nei Mitili Allevati nel Golfo di Pozzuoli – AMICA project, six oceanographic field campaigns have been conducted so far, strategically distributed to cover all seasons. These campaigns combine measurements of hydrodynamic, physicochemical, and biological parameters across 13 monitoring stations throughout the Gulf of Pozzuoli. Collected data include current profiling using a Nortek Aquadopp 300 current meter, CTD casts with a SEABIRD SBE 19plus V2 multiparametric probe (measuring temperature, salinity, fluorescence, dissolved oxygen, and turbidity), and water and sediment sampling via Niskin bottles and grab samplers.

The monitoring campaign provided additional insights into the biogeochemical status of the Lucrino area. Specifically, the distribution of trace and macro elements — aluminum (Al), vanadium (V), chromium (Cr), manganese (Mn), iron (Fe), cobalt (Co), nickel (Ni), copper (Cu), zinc (Zn), arsenic (As), molybdenum (Mo), cadmium (Cd), lead (Pb), and uranium (U) — was analyzed in both mussel tissues (Mytilus galloprovincialis, expressed in µg/g dry weight) and inter-valvular water (µg/L), together with oxidative stress biomarkers in gill tissues. Results revealed marked variability among the sampled ropes (R1, R2, R3), reflecting micro-environmental differences and exposure gradients within the farm area.

The observed biomarker responses and rope-scale variability provide an independent line of evidence supporting the physical transport interpretation: higher stress responses in certain ropes correspond to locations and periods where particle retention, resuspension, and nearshore convergence are predicted by hydrodynamic and Lagrangian simulations. This integration of biological and physical data strengthens the mechanistic understanding of PAH exposure pathways in the mussel farm. It should be noted, however, that oxidative stress biomarkers reflect general physiological responses and are not specific to PAH exposure alone. Their interpretation, therefore, benefits from a combination of chemical analyses and physical transport diagnostics, allowing a more robust attribution of contaminant sources and transport mechanisms.

The integrated analysis of bioaccumulation, environmental chemistry, and physiological stress responses revealed a close relationship between chemical composition, accumulation behaviour in mussels, and activation of antioxidant mechanisms — depicting a diffuse exposure scenario consistent with the current anthropogenic pressure characterizing the Gulf of Pozzuoli.

Ultimately, this integrated observational effort aims to establish a high-resolution, observation-constrained modeling framework capable of reproducing both physical transport and biogeochemical interactions. By coupling field data, chemical analyses, and numerical simulations, the AMICA project provides a process-based foundation for understanding PAH dynamics in the GoP and represents a key step toward more effective environmental management and risk mitigation strategies.

4.2 Regional altimetry-based approach for 2024

The altimetry-based approach focused on the year 2024, leveraging high-resolution satellite observations and Lagrangian particle tracking to investigate the dispersion of PAHs across the broader GoN and their potential accumulation at the Lucrino mussel farm. This approach aimed to complement the 2016 model-based analysis by examining contamination patterns originating primarily from nautical fuel emissions, identified through chemical analyses of mussels.

The year 2024 has been selected in order to take advantage of new satellite altimery data collected by the SWOT mission and made available in 2025 for the year 2024.

The 2024 investigation combined four complementary datasets:

- Chemical monitoring: A total of 18 mussel samples were collected throughout 2024 at the Lucrino site, two of which (24 January and 14 February) exceeded the legal PAH limits. Time series of BaP and the sum of the four priority PAHs are reported in Fig. 20. The new chemical analyses available confirmed that the PAHs detected during the two winter events were predominantly associated with nautical fuel, highlighting the importance of maritime activity as a regional contamination source.
- Meteorology: Wind fields from the Naples Pacanowky stations and ERA5 reanalysis, used to characterize the local and regional wind fields driving surface transport. A windage factor of 3% was applied in particle tracking simulations to account for the effect of winds on floating PAH-bearing particles. This integration allowed assessment of the combined influence of ocean currents and wind-driven drift on contaminant dispersion
- Satellite altimetry: Geostrophic velocity fields were obtained from the Surface Water and Ocean Topography (SWOT) mission, complemented by multimission gridded L4 altimetry products. These datasets provided high-resolution information on mesoscale and submesoscale circulation patterns, supporting the identification of surface transport pathways.
- Lagrangian simulations: Forward particle tracking was conducted using the Parcels Python toolbox. Particles were continuously released in locations characterized by high maritime traffic to simulate PAH

dispersion across the GoN toward the Lucrino farm. Particle trajectories were advected by altimetry-derived geostrophic velocities, and the effect of wind forcing was included as described above.

This approach allows, for the first time, the integration of chemical, meteorological, and oceanographic evidence over multiple temporal scales to interpret contamination mechanisms at the regional level. The altimetry-based framework thus complements the 2016 model-based analysis, extending the focus from local sediment connectivity to surface transport dynamics associated with nautical fuel emissions and wind-driven advection.

Four one-month simulations were conducted to represent seasonal variability:

- January–February (winter), encompassing the two observed contamination events;
- April (spring), marking the onset of weaker and more stable circulation;
- July (summer), characterized by minimal contamination and reduced atmospheric forcing;
- October (autumn), reflecting the transition to stronger cyclonic circulation and episodic wind events.

Each simulation was performed under two forcing scenarios: first, in which particles were advected by geostrophic currents derived from SWOT-enhanced altimetry; second, where wind forcing from ERA5 (locally corrected by station data) was added with a 3 % windage factor to represent near-surface drift.

The following sections describe the outcomes for each simulation period, highlighting the dominant transport patterns, accumulation zones, and their correspondence with observed contamination levels in mussel tissues.

4.2.1 Mussel contaminations in 2024

During the 2024 field campaigns in the Gulf of Pozzuoli, mussel tissues were analyzed as part of the multidisciplinary project “Un approccio multidisciplinare alla contaminazione da idrocarburi nei mitili allevati nel Golfo di Pozzuoli”. The results showed a clear predominance of iron (Fe, 74.6–81.8%), followed by zinc (Zn, 11.8–17.5%) and vanadium (V, 2.4–3.1%), while other elements, including copper (Cu, 0.5–0.7%), arsenic (As, 2.2–3.2%), lead (Pb), cadmium (Cd), chromium (Cr), selenium (Se), and molybdenum (Mo), were present at <1% of the total metal burden. This distribution is consistent with values reported for mussels in Mediterranean port and lagoon environments, where Fe and Zn typically dominate soft tissues (Moschino et al., 2012; Meloni et al., 2022; Barre et al., 2024; ISPRA, 2017).

Vanadium reached slightly higher percentages than those commonly observed in non-industrial environments, aligning with studies that identify V as a tracer of heavy fuel combustion and intense maritime traffic (Amiard et al., 2008; Boatta et al., 2013; Gillio Meina et al., 2020). Analysis of mussels across different size classes confirmed that Fe, Zn, and V remained within consistent ranges (Fe: 68–82%, Zn: 10–20%, V: 2–4%), indicating a stable contamination pattern with no significant size-dependent bioaccumulation.

These metal profiles mirrored the dissolved metal composition in surrounding waters, where Zn accounted for 54–62% (mean ≈ 58%), V for 22–35% (mean ≈ 27%), and Fe for 9–16% (mean ≈ 13%), with all other elements collectively below 2–3%. The concordance between tissue and water compartment confirms that mussels reliably integrate environmental contamination signals, reflecting a diffuse yet persistent port-related pressure (ARPAL–ICRAM, 2005; ISPRA, 2017).

Naval emissions emerged as a significant source of co-contaminants, particularly V, nickel (Ni), and PAHs, which often co-occur in port systems and can interact at the cellular level to induce oxidative stress. The 2024 mussel analyses suggest that these pollutants are transported toward the Lucrino farm via wind-driven surface advection from high-traffic zones, highlighting the combined influence of regional transport and local sources. These results provide essential evidence of the interplay between industrial legacy and contemporary maritime sources, reinforcing the importance of integrated monitoring frameworks to capture complex contamination dynamics in semi-enclosed coastal systems.

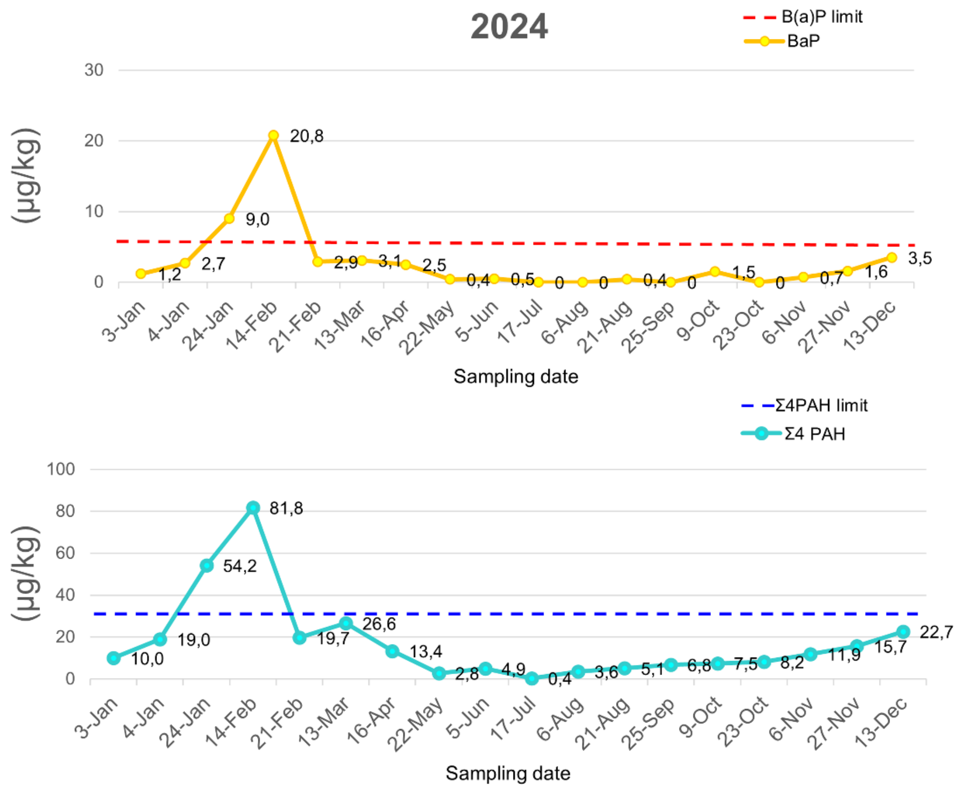

Figure 20. BaP concentration levels (upper panel) and sum of 4PAH concentration (lower panel) in Mytilus galloprovincialis, tissues from Lucrino farm in 2024. The red and blue dotted lines indicate the PAHs legal limit. Dates refer to each PAH concentration analysis performed on sampled mussels.

4.2.2 Event-based analysis in 2024

A detailed event-based analysis was carried out to investigate the environmental drivers and transport mechanisms leading to PAH accumulation at the Lucrino mussel farm. The approach integrated Lagrangian simulations, meteorological and oceanographic observations, and chemical monitoring. Specifically, forward particle-tracking experiments were performed under two configurations: (i) using only geostrophic circulation, and (ii) including wind forcing. For each simulation, connectivity maps were derived to identify likely source-to-target (mussel farm) pathways and areas of high arrival probability, and beaching probability maps were generated at the end of the run to quantify the likelihood of deposition along the coastline.

The combined analysis of trajectories, connectivity, and beaching maps allowed assessment of how different circulation and wind regimes modulate transport pathways, nearshore convergence, and potential coastal deposition, and to directly compare these patterns with the observed contamination peaks.

Winter event (January–February 2024)

The PAH levels measured on 24 January 2016 were 9.0 μg/kg for BaP and 54.2 μg/kg for the sum of the four PAHs; on 14 February were respectively 20.8 μg/kg and 81.8 μg/kg. The altimetry-based Lagrangian simulations for winter 2024 revealed distinct transport patterns depending on the inclusion of wind forcing. In the first scenario (Fig. 21), where particles were advected solely by the geostrophic currents derived from SWOT-enhanced altimetry, particle motion was mainly zonal, with trajectories extending eastward along the Gulf's central axis. Particles remained largely confined within the coastal and nearshore sectors of the Gulf, favouring retention and accumulation processes, particularly in the Pozzuoli area.

In contrast, when wind forcing was added, the distribution of surface particles changed substantially (Fig. 22). The inclusion of the wind field enhanced particle convergence along the northern coast and promoted a strong onshore transport toward the Lucrino mussel farming area. These patterns are consistent with the prevailing southerly winds (mean direction ≈ 210°, mean speed 3.2 m s^{-1}) recorded during this period (see wind rose in Fig. 22). The wind regime during the winter period was dominated by persistent southerly to southwesterly winds, with the SW component showing the highest persistence, followed by NE. These winds were not only frequent but also sustained over multiple consecutive days, producing a quasi-continuous forcing toward the northern Gulf. Their persistence and moderate strength favored coastal convergence and onshore advection of surface pollutants toward the Lucrino area. Such conditions, coupled with the energetic winter circulation, favored the advection of PAH-contaminated material toward the coast, particularly during mid- and late January, coinciding with the contamination peaks observed in mussel tissues on 24 January and 14 February 2024.

By the end of February, particle dispersion extended westward and offshore, suggesting a weakening of wind influence and the reestablishment of a more open-gulf circulation. Overall, the winter simulations emphasize the crucial role of southerly wind-driven advection in promoting pollutant transport and nearshore accumulation under typical seasonal conditions.

The connectivity and beaching probability maps (Figs. 23a–d) further support these results, revealing well-defined transport pathways from high maritime traffic zones toward the Lucrino area and localized accumulation near the mussel farm. This spatial coherence between model outputs and observed contamination patterns reinforces the link between hydrodynamic conditions and PAH delivery. The beaching probability distributions (Figs. 23c,d) clearly illustrate the role of wind forcing in enhancing coastal particle retention. Under the current-only scenario (Fig. 23c), beaching is confined to a limited sector west of Pozzuoli, reflecting weak nearshore transport driven solely by geostrophic circulation. In contrast, the inclusion of wind forcing (Fig. 23d) produces a pronounced increase in beaching probability along the northern coast, particularly near Lucrino. Such enhancement is consistent with the prevailing S–SW winds during January–February, which promoted onshore advection and favored pollutant accumulation along the shoreline. Overall, these results indicate that the combined action of currents and southerly winds effectively drives the delivery and retention of PAH-contaminated material near the coast, in agreement with the contamination peaks detected in mussel tissues during winter 2024.

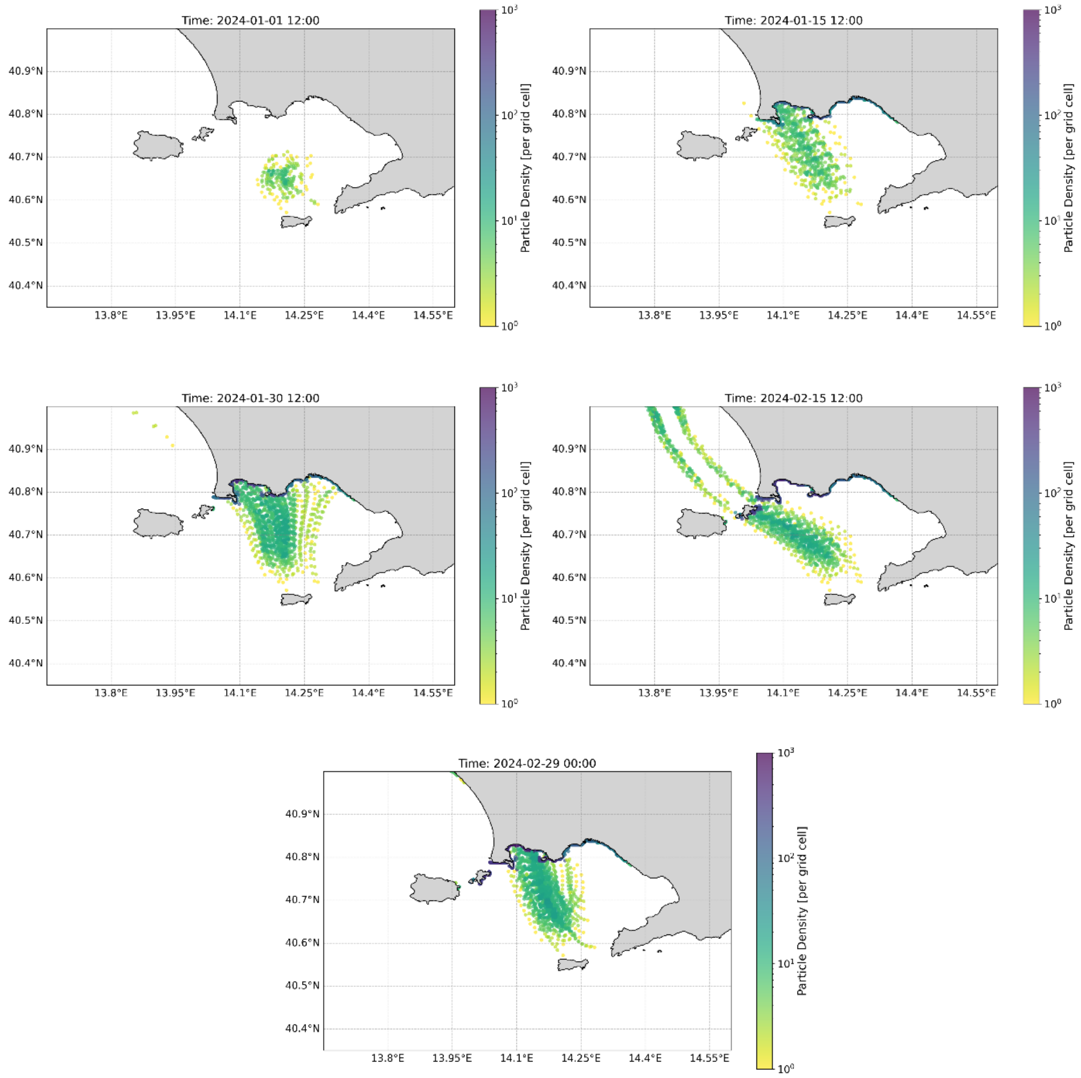

Figure 21. Dispersion of PAH-bearing particles in the Gulf of Naples during the January–February 2024 simulation, using only geostrophic currents derived from SWOT-enhanced altimetry and L4 altimetry products. Particles were continuously released every 12 hours from high maritime traffic zones. Colors represent particle density per grid cell, highlighting areas of higher and lower concentration

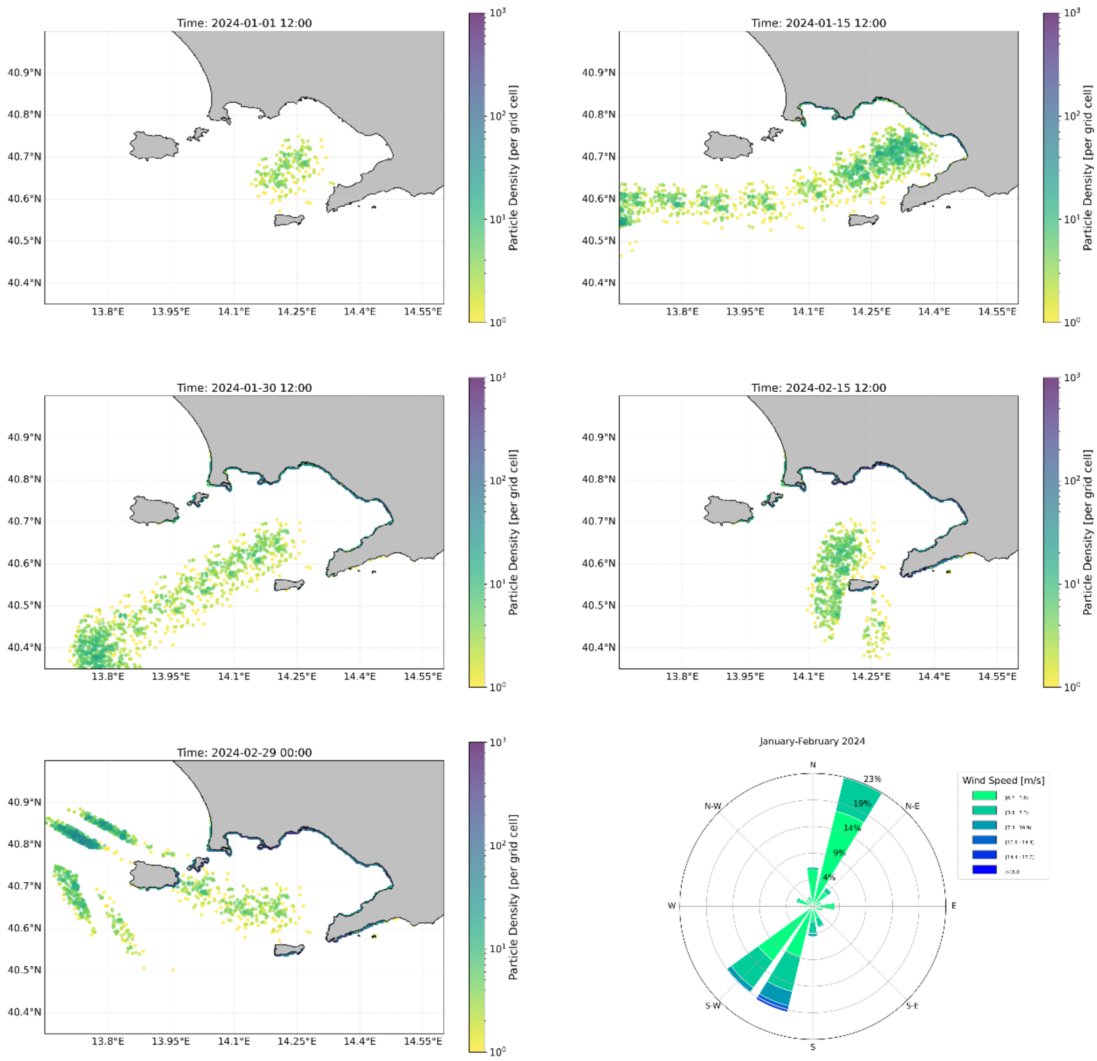

Figure 22. Dispersion of PAH-bearing particles in the Gulf of Naples during the January–February 2024 simulation, using geostrophic currents derived from SWOT-enhanced altimetry, combined with wind forcing. Particles were continuously released every 12 hours from high maritime traffic zones. Colors represent particle density per grid cell, highlighting areas of higher and lower concentration. The wind rose shows the mean wind direction and speed measured at the Naples Pacanowsky weather station during the simulation period.

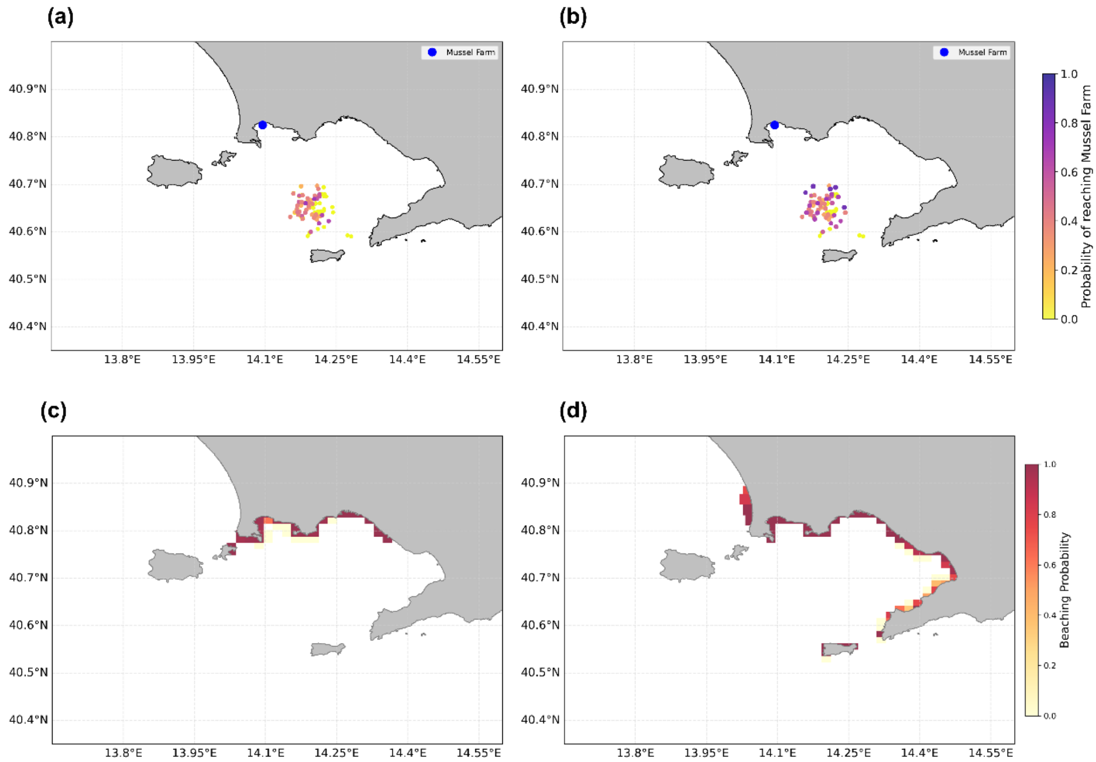

Figure 23. Connectivity and beaching probability maps for the January–February 2024 simulations. (a–b) Connectivity maps showing the probability of PAH-bearing particles reaching the Lucrino mussel farm under (a) geostrophic-current forcing only and (b) combined geostrophic and wind forcing. (c–d) Corresponding beaching probability maps at the end of the simulation, representing the likelihood of particles stranding along the coastline under (c) current-only and (d) current-plus-wind scenarios. Colors indicate the relative probability of particle arrival at the target area or coastal grid cells.

Spring event (April 2024)

The altimetry-based Lagrangian simulations for April 2024 revealed markedly weaker and more localized transport dynamics compared to the winter scenario, reflecting the more stable and subdued circulation regime typical of the spring season. Results from both scenarios indicate limited dispersion and no significant particle accumulation near the Lucrino mussel farm.

In the first scenario (Fig. 24), particles released from high maritime traffic zones remained relatively confined throughout the simulation period. By mid-month (10 April), dispersion extended modestly toward the northeast. By April 30, particles had dispersed further offshore and along the northern Gulf coast, yet with no evident transport toward the Lucrino area. The simulated trajectories remained largely offshore, and no convergent structures emerged along the western coastline. These patterns align with the weak and unstructured surface circulation observed during spring.

When wind forcing was included (Fig. 25), particle dispersion slightly increased, particularly during the second half of the month. Trajectories expanded mainly southward and eastward across the central Gulf, with only a few particles approaching the nearshore areas. The Lucrino sector remained largely unaffected, showing no significant accumulation near the mussel farm.

The April wind rose (Fig. 25) indicates prevailing southwesterly winds (mean direction ≈ 229°, mean speed 2.6 m s^{-1}), which were weaker and less persistent than those observed in winter. The SW direction remained dominant, but persistence was significantly lower, and secondary components from the NE and E sectors reflected the more variable and transitional atmospheric regime. Mean speed indicates gentle southwesterly breezes rather than synoptic-scale winds. As a result, wind forcing induced only minor modifications to particle trajectories, with most remaining offshore. These moderate and intermittent winds contributed little to coastal transport, consistent with the absence of PAH exceedances in mussel samples during spring.

Overall, the April simulations reveal low transport efficiency of PAH-bearing particles toward the Lucrino mussel farm. The weak dispersion and lack of coastal accumulation align with chemical monitoring results, reinforcing the hypothesis that contamination events are primarily associated with persistent and stronger southerly winds, which were not present during the spring period.

The connectivity and beaching probability maps (Figs. 26a-d) confirm these results, showing that particles released from high maritime traffic zones remain largely confined offshore, with negligible transport toward the Lucrino area (Figs. 26a,b). This visual evidence reinforces the low risk of PAH accumulation in mussels under the prevailing spring circulation and wind conditions.

Under the geostrophic current-only scenario (Fig. 26c), beaching occurs primarily in the northeastern sectors of the Gulf of Naples, particularly along the Gulf of Castellammare, reflecting weak nearshore transport driven solely by geostrophic circulation. When wind forcing is included (Fig. 26d), particles are redirected toward the northern Gulf coasts, including both the northeastern coast and the areas of Capri and Punta Campanella. This indicates that even moderate spring winds can impact particle retention across multiple coastal sectors, although nearshore accumulation near Lucrino remains negligible.

Notably, particles advected by combined currents and wind exit through Bocca Piccola, confirming the limited impact on mussel farms in spring. These patterns, though weaker than in winter, highlight the role of wind-driven advection in shaping coastal particle distribution under spring circulation conditions.

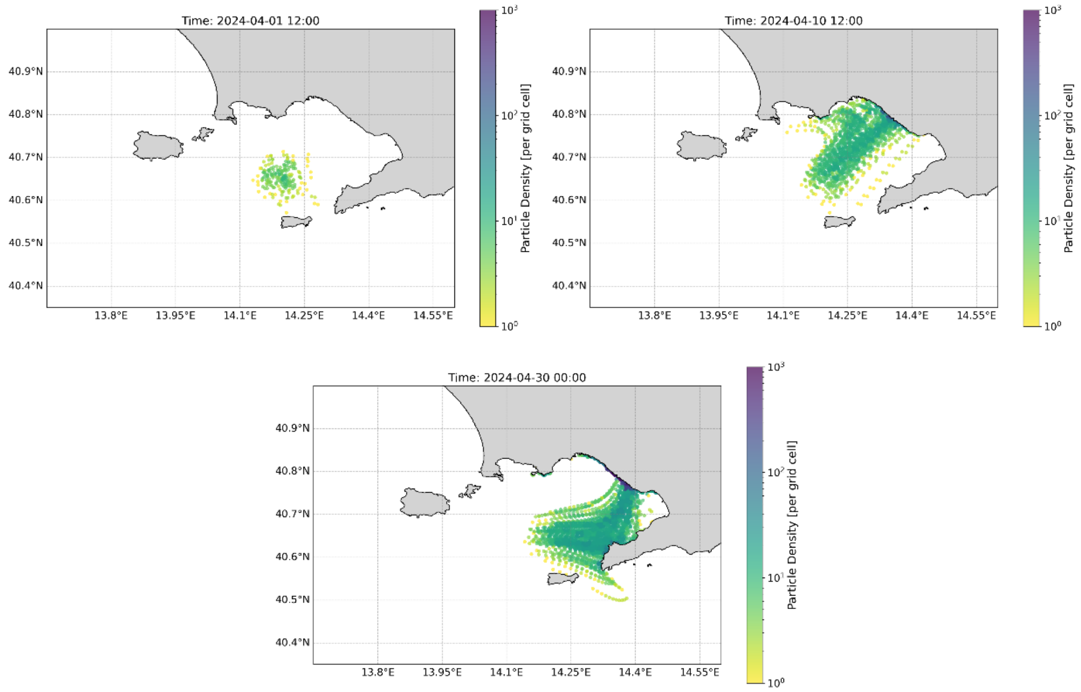

Figure 24. Dispersion of PAH-bearing particles in the Gulf of Naples during the April 2024 simulation, using only geostrophic currents derived from SWOT-enhanced altimetry and L4 altimetry products. Particles were continuously released every 12 hours from high maritime traffic zones. Colors represent particle density per grid cell, highlighting areas of higher and lower concentration

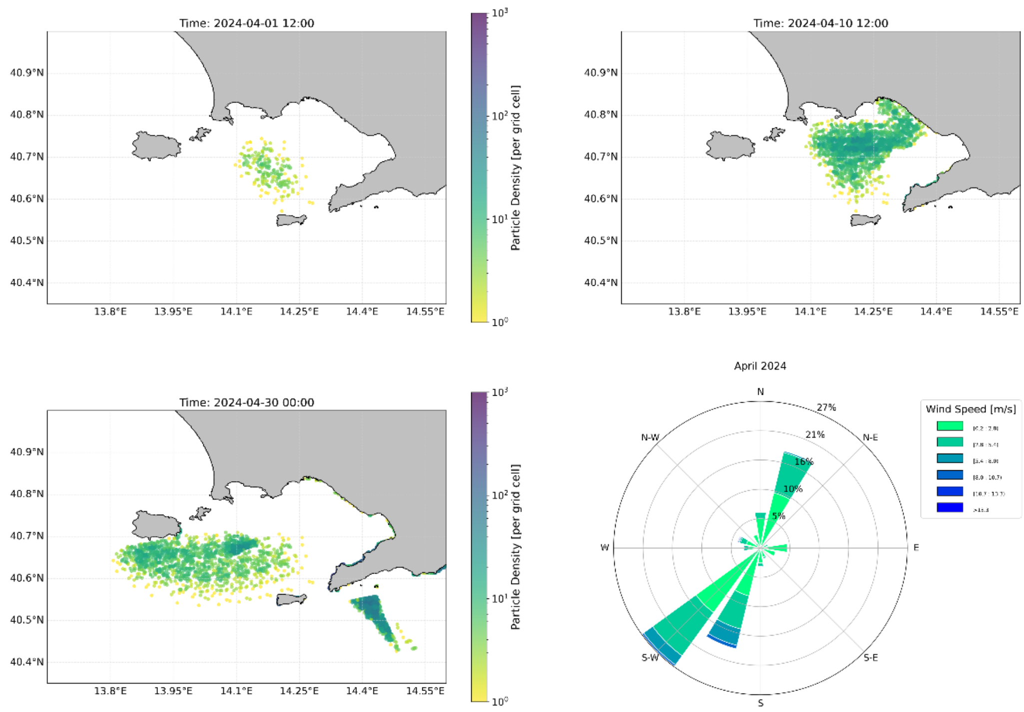

Figure 25. Dispersion of PAH-bearing particles in the Gulf of Naples during the April 2024 simulation, using geostrophic currents derived from SWOT-enhanced altimetry, combined with wind forcing. Particles were continuously released every 12 hours from high maritime traffic zones. Colors represent particle density per grid cell, highlighting areas of higher and lower concentration. The wind rose shows the mean wind direction and speed measured at the Naples Pacanowsky weather station during the simulation period.

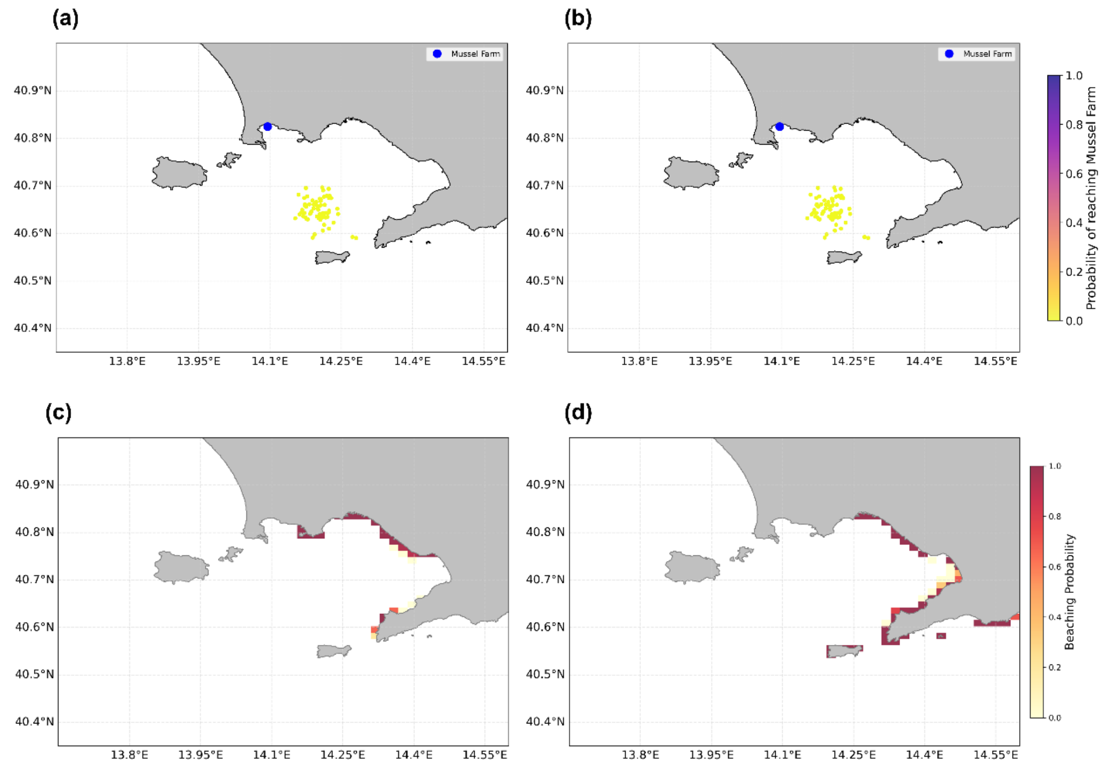

Figure 26. Connectivity and beaching probability maps for the April 2024 simulations. (a–b) Connectivity maps showing the probability of PAH-bearing particles reaching the Lucrino mussel farm under (a) geostrophic-current forcing only and (b) combined geostrophic and wind forcing. (c–d) Corresponding beaching probability maps at the end of the simulation, representing the likelihood of particles stranding along the coastline under (c) current-only and (d) current-plus-wind scenarios. Colors indicate the relative probability of particle arrival at the target area or coastal grid cells.

Summer event (July 2024)

The altimetry-based Lagrangian simulations for July 2024 revealed markedly different transport conditions compared to the winter period, consistent with the absence of PAH contamination observed in mussel tissues during summer.

In the first scenario, where particles were advected solely by geostrophic currents derived from SWOT-enhanced altimetry (Fig. 27), dispersion remained limited and largely confined to the central sector of the Gulf of Naples. Particle trajectories displayed a preferential east–northeastward orientation, with motion mostly parallel to the coastline and no significant accumulation near the Lucrino mussel farm. The temporal evolution indicated a gradual offshore spreading and weak mesoscale activity, reflecting the stable and low-energy circulation regime typical of summer months.

In the second scenario, when wind forcing was included, some changes in particle dispersion were observed (Fig.28). The addition of the wind field promoted a slightly broader south–southeastward spreading, consistent with the prevailing SW winds (mean direction ≈ 218°, mean speed ≈ 2.4 m s^{-1}). During summer, the wind regime was characterized by low intensity and steady sea-breeze circulation, with SW winds again prevailing but at weak mean speeds. Secondary components (NE, E, and N) exhibited very low persistence, confirming the dominance of local thermally-driven winds. This pattern led to minimal wind-induced transport and maintained particles dispersed offshore, preventing any significant onshore accumulation. The low persistence and gentle character of summer winds thus explain the minimal PAH levels measured in mussels during this period.

Trajectories remained largely confined to the central Gulf, dominated by stable summer circulation, with no significant accumulation observed near the Lucrino area. The weak and persistent westerly flow limited coastal convergence and reduced the potential for pollutant retention along the northern coast.

Overall, the July simulations indicate a low efficiency of coastal transport and the absence of favorable conditions for contaminant advection toward the Lucrino mussel farm. These findings are consistent with chemical monitoring results showing the lowest PAH concentrations in mussels during summer 2024, confirming that stable circulation and weak winds strongly limit nearshore contamination.

The connectivity and beaching maps for July 2024 (Figs. 29a-d) show a very low probability of PAH-bearing particles reaching the Lucrino mussel farm. In both scenarios— sea surface currents only and currents plus wind forcing—the majority of particles remain dispersed offshore, with minimal nearshore convergence (Figs. 29a,b).

Under the current-only scenario (Fig. 29c), beaching occurs mainly in the northeastern sector of the Gulf and along Punta Campanella, reflecting weak nearshore transport driven solely by geostrophic currents. When wind forcing is included (Fig.

29d), particle retention is further reduced and confined to the areas near Punta Campanella, along the Sorrento coast, and Capri Island, indicating that even summer winds induce only minor coastal convergence. In both scenarios, particles fail to reach the Lucrino mussel farm.

These patterns confirm that the combination of stable summer circulation and weak, persistent winds strongly limits coastal transport and nearshore retention, consistent with the very low PAH levels measured in mussel tissues during July 2024. Overall, the summer connectivity maps reinforce the conclusion that conditions during this season are unfavorable for pollutant delivery to sensitive coastal areas such as Lucrino.

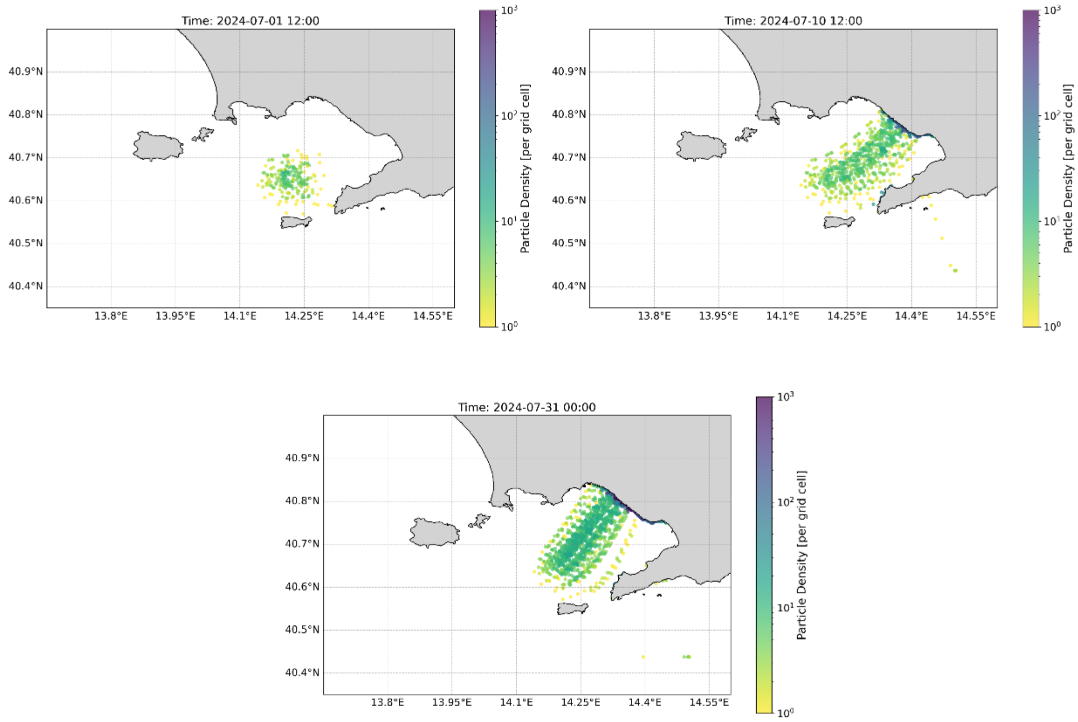

Figure 27. Dispersion of PAH-bearing particles in the Gulf of Naples during the July 2024 simulation, using only geostrophic currents derived from SWOT-enhanced altimetry and L4 altimetry products. Particles were continuously released every 12 hours from high maritime traffic zones. Colors represent particle density per grid cell, highlighting areas of higher and lower concentration.

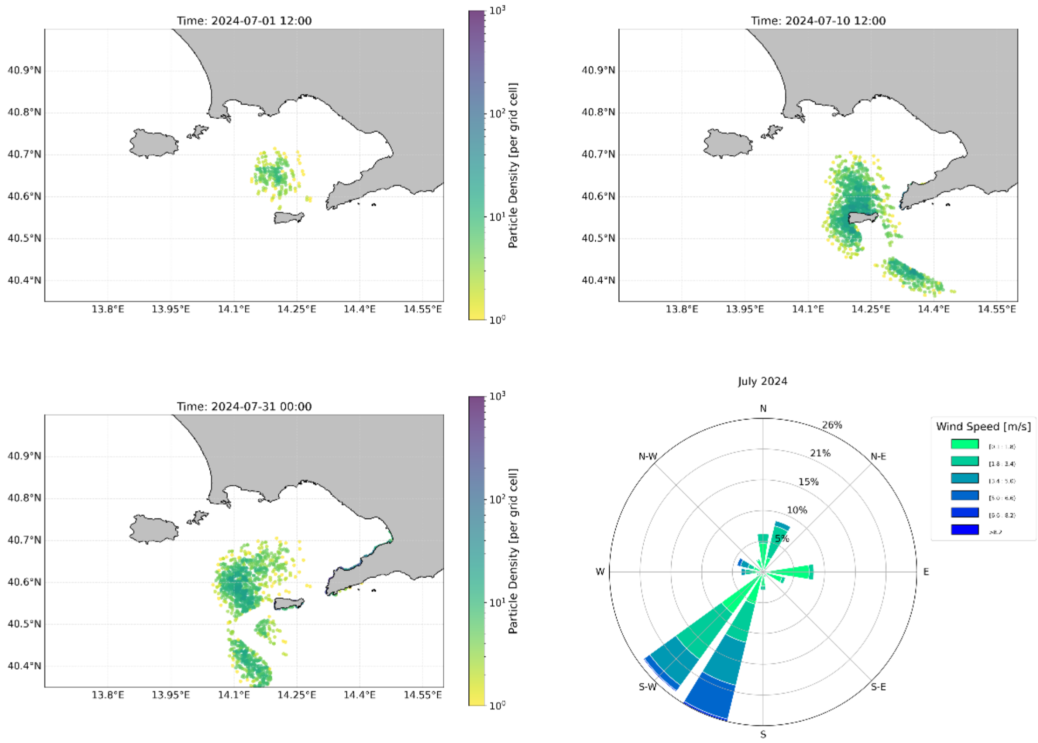

Figure 28. Dispersion of PAH-bearing particles in the Gulf of Naples during the July 2024 simulation, using geostrophic currents derived from SWOT-enhanced altimetry, combined with wind forcing. Particles were continuously released every 12 hours from high maritime traffic zones. Colors represent particle density per grid cell, highlighting areas of higher and lower concentration. The wind rose shows the mean wind direction and speed measured at the Naples Pacanowsky weather station during the simulation period.

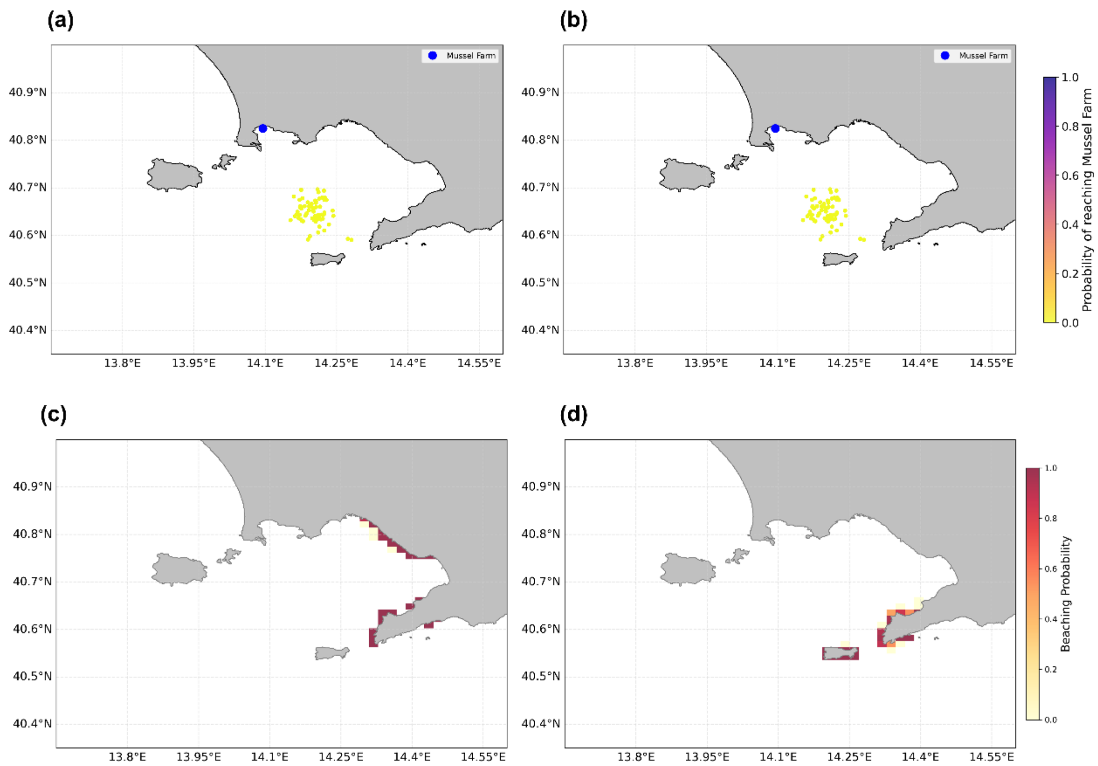

Figure 29. Connectivity and beaching probability maps for the July 2024 simulations. (a–b) Connectivity maps showing the probability of PAH-bearing particles reaching the Lucrino mussel farm under (a) geostrophic-current forcing only and (b) combined geostrophic and wind forcing. (c–d) Corresponding beaching probability maps at the end of the simulation, representing the likelihood of particles stranding along the coastline under (c) current-only and (d) current-plus-wind scenarios. Colors indicate the relative probability of particle arrival at the target area or coastal grid cells.

Autumn event (October 2024)

The altimetry-based Lagrangian simulations for October 2024 represent the transition from the weakly energetic summer circulation to the more variable autumnal regime. Despite the seasonal shift, results from both scenarios indicate limited potential for coastal contamination transport toward the Lucrino area, in agreement with the absence of PAH exceedances in mussel tissues during this period.

In the first scenario (Fig. 30), where particles were advected solely by geostrophic currents, trajectories displayed a predominant westward dispersion pattern. From the initial release points, particles were transported along the central Gulf and progressively displaced toward the western offshore sector, without significant inflow into the Gulf of Pozzuoli. The overall motion remained consistent with a large-scale, basinward flow regime, characterized by the absence of convergent features along the northern coast. These results confirm that the autumn circulation was mainly dominated by mesoscale eddies and open-sea transport processes rather than coastal retention.

When the wind field was incorporated into the simulation (Fig. 31), particle trajectories exhibited a markedly different evolution. Initially, dispersion extended eastward across the central Gulf toward the Capri sector, followed by a progressive offshore advection during the latter part of the month. The southern to southwesterly winds (mean direction ≈ 217°, mean speed ≈ 2.6 m s^{-1}), occasionally alternating with calm periods, slightly increased dispersion variability but did not enhance onshore transport. In autumn, the atmospheric forcing shifted toward a more variable and transitional regime, with SW and NE as the most persistent directions. Despite their moderate persistence, these winds alternated between opposing directions, reducing the net momentum toward the coast. As a result, dispersion patterns remained largely offshore, with weak or transient convergence near Lucrino. This variability explains the absence of contamination peaks in mussels during October, as alternating wind patterns hindered sustained pollutant advection.

As a result, the Lucrino area remained largely unaffected, with no modeled convergence or stagnation zones capable of enhancing pollutant retention near the coast. The simulated distribution remained predominantly offshore, indicating limited wind influence on nearshore transport.

Overall, the October simulations highlight a circulation regime unfavorable to nearshore contamination. Both scenarios point to the dominance of offshore and divergent transport pathways, consistent with the meteorological conditions characterized by weak, variable easterly winds and low hydrodynamic energy. These results confirm that, in the absence of persistent southerly winds and strong coastal currents, the advection of PAH-contaminated particles toward the Lucrino mussel farm is unlikely during the autumn season.

The connectivity maps for October 2024 (Figs. 32a,b) illustrate the distinct transport potential under the two scenarios. In the current-only scenario (Fig. 32a), there is a minimal probability of particles reaching the Lucrino mussel farm, reflecting limited but possible nearshore transport driven by geostrophic currents. In contrast, when wind forcing is included (Fig. 32b), particles are diverted offshore and toward other sectors, with no connectivity to Lucrino, indicating that even moderate and variable autumn winds prevent significant pollutant delivery to the target area.

The beaching probability maps (Figs. 32c,d) further support these results. Under the current-only scenario (Fig. 32c), beaching occurs along the Gulf of Pozzuoli near Lucrino, as well as Procida, Ischia, and the Gulf of Gaeta. When wind forcing is included (Fig. 32d), particle retention shifts toward the northeastern sector of the Gulf of Naples, Capri, Punta Campanella, and the northeastern part of the Gulf of Pozzuoli, including Bagnoli, and Ischia island, with negligible accumulation near Lucrino. These patterns align with chemical monitoring data showing no PAH exceedances in mussel tissues during October 2024. Overall, the autumn simulations highlight how wind forcing can strongly modify particle trajectories and nearshore retention, reducing the likelihood of pollutant delivery to sensitive mussel farming areas.

To provide a systematic quantitative overview of the 2024 contamination events at the Lucrino mussel farm, Table 5 summarizes observed PAH levels, prevailing wind and conditions, inferred sources, and the main outcomes of Lagrangian particle tracking simulations using SWOT-enhanced altimetry, with and without wind forcing.

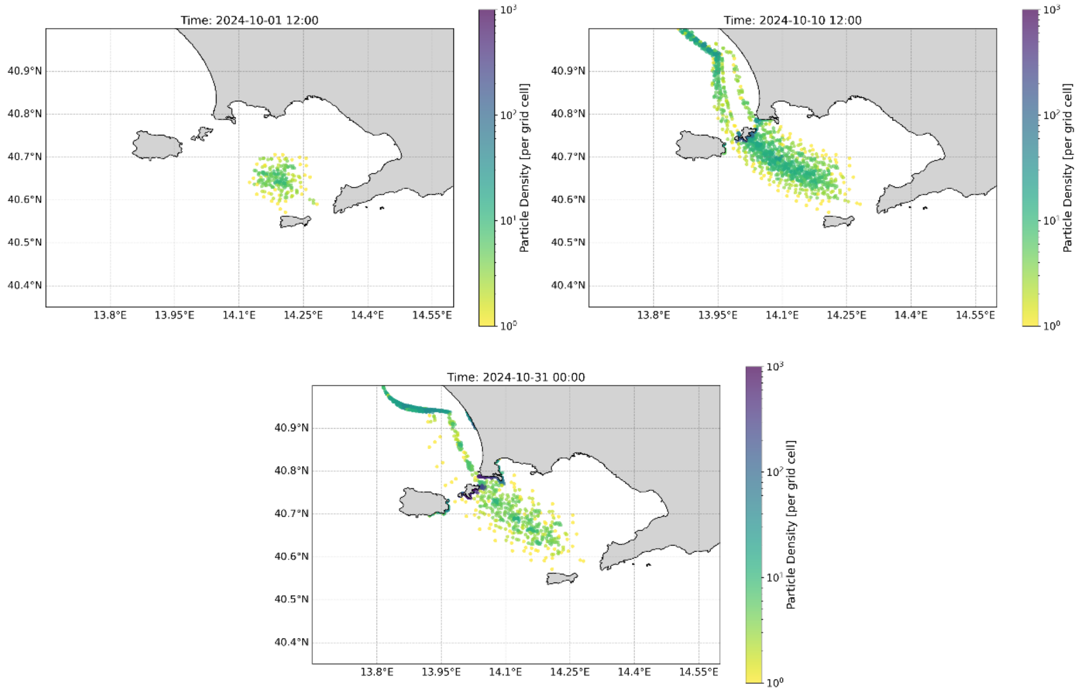

Figure 30. Dispersion of PAH-bearing particles in the Gulf of Naples during the October 2024 simulation, using only geostrophic currents derived from SWOT-enhanced altimetry and L4 altimetry products. Particles were continuously released every 12 hours from high maritime traffic zones. Colors represent particle density per grid cell, highlighting areas of higher and lower concentration.

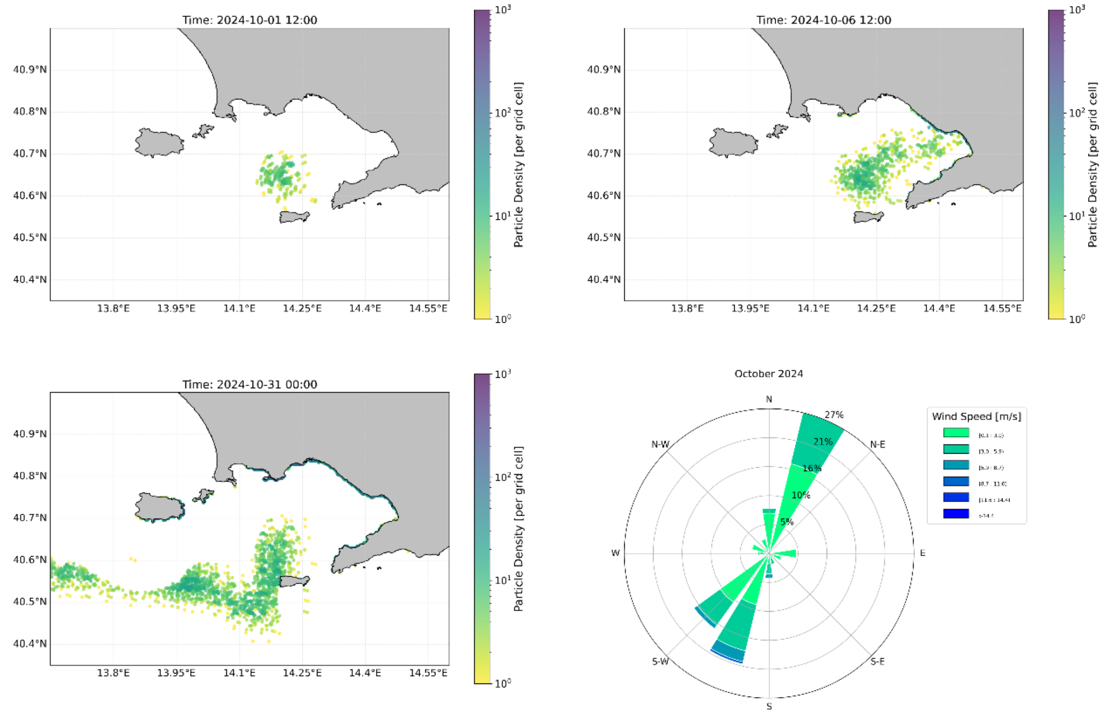

Figure 31. Dispersion of PAH-bearing particles in the Gulf of Naples during the October 2024 simulation, using geostrophic currents derived from SWOT-enhanced altimetry, combined with wind forcing. Particles were continuously released every 12 hours from high maritime traffic zones. Colors represent particle density per grid cell, highlighting areas of higher and lower concentration. The wind rose shows the mean wind direction and speed measured at the Napoli station during the simulation period.

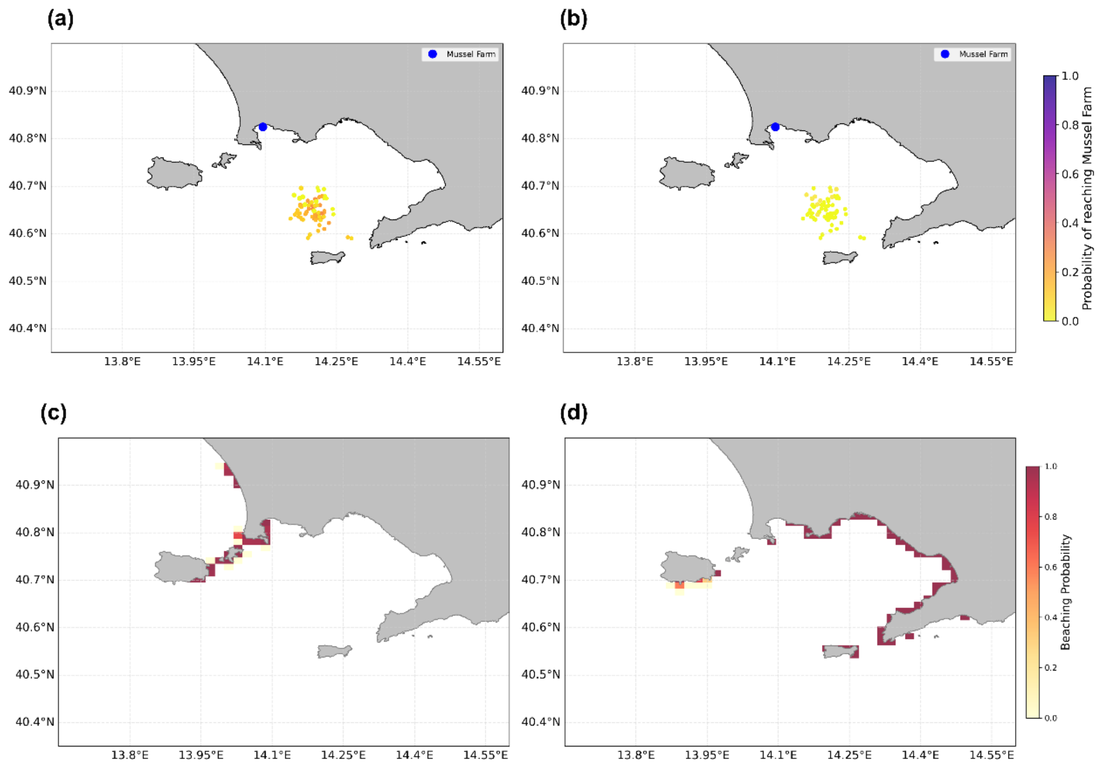

Figure 32. Connectivity and beaching probability maps for the October 2024 simulations. (a–b) Connectivity maps showing the probability of PAH-bearing particles reaching the Lucrino mussel farm under (a) geostrophic-current forcing only and (b) combined geostrophic and wind forcing. (c–d) Corresponding beaching probability maps at the end of the simulation, representing the likelihood of particles stranding along the coastline under (c) current-only and (d) current-plus-wind scenarios. Colors indicate the relative probability of particle arrival at the target area or coastal grid cells.

Period	BaP / Σ4PAH (µg/kg)	Dominant wind	Wind speed (m/s)	Main Sea Current direction	Source	Main modelling outcome
Jan 2024	9.0 / 54.2	S–SW	3.2	Zonal	Nautical fuel	Particles converge along the northern coast, strong onshore transport to Lucrino; geostrophic currents alone produce coastal retention west of Pozzuoli
Feb 2024	20.8 / 81.8	S–SW	3.2	Eastward with nearshore convergence	Nautical fuel	Enhanced convergence and coastal accumulation at Lucrino with wind forcing; trajectories offshore with geostrophic-only forcing
Apr 2024	< limit	SW	2.6	Limited offshore–onshore mixing	No exceedance	Minor coastal influence; particles largely offshore; negligible accumulation near Lucrino
Jul 2024	< limit	SW	2.4	East-northeastward	No exceedance	Stable summer circulation; minimal offshore convergence; no transport to Lucrino
Oct 2024	< limit	SW–S	2.6	Westward, mostly offshore	No exceedance	Offshore and divergent transport; wind forcing modifies trajectories but does not deliver particles to Lucrino

Table 5. Summary of contamination events in 2024 and modelling outcomes.

4.3 Summary of findings

This chapter combined two complementary analytical designs — a local model-based approach (2016) and a regional altimetry-based one (2024) — to investigate the physical and environmental mechanisms driving PAH contamination in mussels farmed in the GoP. Together, these analyses provide a coherent picture of how meteorological forcing, hydrodynamic variability, and human activities interact to generate pollutant transport across multiple spatial and temporal scales.

The 2016 local analysis focused on event-scale processes, exploiting a combination of all the in-situ measurements, numerical model outputs, and satellite observations available for that year. This approach revealed that contamination episodes were systematically associated with specific meteorological–oceanographic conditions: (i) the occurrence of southerly and south-easterly winds, (ii) the development of northwestward nearshore currents, and (iii) enhanced wave activity capable of activating sediment resuspension.

These coupled forcings generated short-lived but intense transport pathways from the Bagnoli coastal sector — a known source of legacy contamination — toward the Lucrino mussel farm. Lagrangian transport simulations confirmed that under such conditions, particles released near Bagnoli could reach the farm area within a few days, supporting the hypothesis that PAH peaks in mussels are linked to resuspension and advection of contaminated sediments. The analysis also demonstrated the strong seasonality of contamination, with events concentrated in late autumn and winter when vertical mixing and energetic sea states prevail, while stratified summer conditions suppress vertical and lateral exchanges.

In contrast, the 2024 regional altimetry-based analysis broadened the investigation to include large-scale circulation and contemporary contamination sources, particularly those related to maritime traffic and fuel combustion. Using SWOT-enhanced altimetry, ERA5 winds, and in-situ weather data, the study characterized the patterns influencing PAH dispersion across the GoN. Lagrangian simulations incorporating both geostrophic currents and windage effects showed that southerly wind regimes play a dominant role in driving onshore advection and coastal accumulation of surface contaminants. Analysis of wind persistence across seasons further highlights that only during winter do southerly and southwesterly winds reach sufficient persistence to drive effective onshore transport. Spring and summer, instead, are dominated by weak and short-lived breezes that favor offshore dispersion. This seasonal contrast reinforces the central role of wind persistence and directionality in modulating pollutant transport to the Lucrino area.

The integration of chemical and metal analyses further indicated that vanadium and nickel — tracers of heavy fuel combustion — co-occurred with PAHs during contamination peaks, highlighting a dual-source scenario involving both legacy sediments (Bagnoli) and ongoing maritime emissions.

Comparison between the two frameworks underscores that PAH contamination in the GoP arises from the interplay between local sediment dynamics and regional surface transport processes. While the 2016 analysis captured nearshore sediment mobilization and short-term contamination events, the 2024 simulations revealed that large-scale atmospheric and oceanic circulation modulate the frequency and extent of pollutant delivery. Thus, the contamination of mussels at Lucrino cannot be attributed to a single mechanism but rather to the superposition of episodic resuspension events and wind-driven advection of fuel-derived PAHs. Overall, these results emphasize the importance of adopting multi-scale and multi-source approaches when investigating contaminant pathways in semi-enclosed coastal systems. The integration of in-situ, modelling, and satellite-based analyses provides a comprehensive understanding of pollutant dynamics, offering a solid foundation for future risk assessment and management strategies aimed at protecting aquaculture in the GoP.

Chapter V

5. Discussion

This thesis integrates two complementary experimental–modelling frameworks — a local, process-based model analysis (2016) and a regional, altimetry-based analysis (2024) — to explain recurrent PAH exceedances recorded in mussels farmed at Lucrino. Together, these two scales of observation provide a comprehensive view of contaminant dynamics in the GoP, highlighting the interplay between meteorological forcing, hydrodynamic variability, and source heterogeneity.

Beyond documenting contamination events, this multi-scale framework advances current understanding by explicitly linking episodic PAH exceedances to the combined action of wind persistence, hydrodynamic confinement, and source-specific activation, rather than to background contamination levels alone.

The local model-based analysis revealed that episodic contamination peaks coincide with periods of enhanced southerly wave energy and northwestward current development linking the Bagnoli brownfield to the Lucrino farm. ADCP data, wind records, and Lagrangian simulations consistently identified the coupling of (i) sediment resuspension driven by high bottom shear stress ($\tau_\beta > \tau c$) and (ii) wind-driven nearshore advection as the primary mechanisms transporting PAH-contaminated particles toward the mussel farm. While sediment resuspension has been widely recognized as a contamination driver in industrialized coastal areas, this study provides direct observational and modelling evidence linking specific wave–current thresholds to downstream bioaccumulation in aquaculture settings.

Conversely, the regional altimetry-based framework 2024 provided a basin-scale perspective using SWOT-enhanced geostrophic velocities, ERA5 reanalysis, in-situ weather data, and Parcels particle tracking. Two winter exceedances (24 January and 14 February 2024) were linked to nautical-fuel residues advected toward the coast under persistent southerly winds. The simulations demonstrated that geostrophic currents alone are insufficient to reproduce onshore transport; however, the inclusion of realistic wind forcing (3 % windage term and local wind correction) produced coastal convergence patterns consistent with contamination observations. Unlike previous altimetry-based studies limited to open-ocean settings, the use of SWOT data demonstrates that satellite-derived geostrophic currents, when coupled with realistic wind forcing, can successfully resolve coastal convergence processes in semi-enclosed basins.

Taken together, these results support a dual-mechanism model for PAH transport at Lucrino: (i) sediment resuspension and nearshore advection of legacy contaminants from Bagnoli, dominant under energetic winter conditions; (ii) wind-driven surface transport of fuel-derived PAHs originating from maritime traffic, modulated by basin-scale circulation. This dual-mechanism conceptual model may explain why contamination hotspots persist in coastal aquaculture sites even in the absence of continuous pollutant inputs, a feature observed in several Mediterranean and industrialized coastal systems.

Significantly, wind persistence analysis revealed that only during winter do southerly and southwesterly winds reach sufficient duration and intensity to sustain effective onshore advection and coastal convergence. In contrast, the spring and summer regimes are characterized by weaker, short-lived winds (mainly sea-breeze cycles), which promote offshore dispersion and limit accumulation near the coast. This explains why PAH exceedances in mussels are consistently restricted to the cold season, when both atmospheric and hydrodynamic conditions favour nearshore transport and retention.

Importantly, the dual mechanisms interact rather than act independently. Sediment resuspension events provide a particulate PAH flux that can be further transported by wind-driven surface currents, while fuel-derived PAHs released at the surface by ships follow combined geostrophic and wind-induced drift pathways. This convergence highlights the synergistic nature of local and basin-scale processes, reinforcing the need for integrated monitoring and management strategies.

5.1 Advantages, Complementarity, and Limitations of this study

The combined methodological approaches employed in this study offer complementary strengths. The 2016 model-based, high-resolution framework provides exceptional local detail, including a validated Eulerian field for event-scale Lagrangian simulations, together with in situ wave diagnostics that reveal a clear temporal association between high-wave-energy events and subsequent contamination peaks. This coupling supports sediment resuspension as a primary PAH transport mechanism, particularly through the reactivation of contaminated coastal deposits. Such a combined local–regional strategy is particularly relevant for semi-enclosed basins where historical contamination coexists with ongoing maritime activities, a condition common to many Mediterranean and temperate coastal systems.

In contrast, the 2024 altimetry-based approach expands the spatial scale, leveraging SWOT-enhanced velocity fields to resolve mesoscale and submesoscale features and explicitly testing maritime traffic as a realistic source, thereby strengthening the attribution of surface-derived PAHs.

This complementarity between a local, process-oriented framework and a regional, circulation-based one allows distinguishing between point-source reactivation (Bagnoli sediments) and distributed-source advection (maritime emissions), providing a more complete mechanistic picture of pollutant transport in the Gulf of Naples.

Despite these advantages, some methodological limitations must be acknowledged. Vertical processes are only partially represented in both frameworks, as GNOME (2016) and Parcels (2024) simulations were primarily surface- or two-dimensional in configuration. Processes such as vertical exchange, particle settling, flocculation, and stratification effects are only implicitly represented, which constrains the quantitative estimation of particle residence times, sediment re-entry, and contaminant bioavailability. Consequently, the simulations should be interpreted as diagnostic rather than predictive, identifying plausible transport pathways rather than exact contamination magnitudes.

Additionally, the in-situ coverage remains relatively sparse: the MEDA A platform delivers high-frequency point measurements but may not fully capture coastal heterogeneity, such as nearshore fronts or small embayments, where microdynamics could play an important role. The combination of sparse in-situ data and model assumptions implies that some localized high-risk events may go undetected without enhanced monitoring coverage.

Finally, both modelling frameworks are subject to uncertainties in external forcing and numerical representation. In the 2016 study, CROM wind forcing was blended with Bacoli weather station observations to better reproduce small-scale variability within the Gulf of Pozzuoli, while in the 2024 experiments, altimetry-derived geostrophic currents describe only the balanced flow component, requiring coupling with wind fields to account for non-geostrophic (Ekman-type) surface drift.

Therefore, model outputs should be interpreted probabilistically, emphasizing transport likelihoods and spatial-temporal windows rather than deterministic predictions.

5.2 Operational Strategies for Mitigation and Monitoring

The combined evidence from local and regional analyses points to several actionable strategies to reduce PAH exposure and support farm management. A real-time early-warning system could integrate local wind measurements, short-range wave forecasts, and rapid Lagrangian nowcasts to generate contamination-risk alerts for farm managers. Such a system leverages the sensitivity of PAH transport to southerly wind episodes.

Complementing this, event-based sampling of mussels and opportunistic water or sediment collections following modelled high-risk windows (typically 4–10 days after resuspension or wind events), would enhance attribution accuracy while reducing unnecessary routine sampling. Long-term mitigation may also include targeted sediment remediation at Bagnoli, focusing on capping, stabilization, or selective removal, in combination with stricter controls on fuel handling and emissions from maritime traffic.

Moreover, wind persistence thresholds identified in this study (e.g., $>\approx 1.5$ hours of continuous S–SW winds) could serve as operational triggers for risk alert systems. Incorporating these meteorological indicators into environmental monitoring protocols would allow early detection of contamination-prone conditions and adaptive management responses.

Finally, expanded monitoring integrating turbidity sensors, near-bottom shear measurements, and biochemical biomarkers in mussels (e.g., oxidative stress endpoints) would link exposure to sub-lethal biological effects and help refine safe exposure thresholds. This multi-tiered approach ensures a connection between physical transport, chemical presence, and biological impact, enhancing evidence-based decision-making.

These operational principles—wind-based triggering, short-term Lagrangian forecasting, and event-driven sampling—are readily transferable to other coastal aquaculture areas exposed to episodic contamination and limited water renewal.

5.3 Research gaps and future prospects

To further advance mechanistic understanding and improve operational application, several research priorities emerge. Developing fully 3-D particle and sediment models, nesting high-resolution coastal models within CROM or similar frameworks, and coupling Lagrangian particles with settling, flocculation, and resuspension processes would reduce uncertainties associated with vertical exchange and sediment dynamics.

Implementing pilot operational forecast validation, where a nowcasting/forecasting chain is tested over a winter season and compared against rapid chemical sampling, would allow quantification of predictive skill and false-alarm rates. Integration of AI and data assimilation techniques to merge heterogeneous datasets—including altimetry, HF-radar, in-situ observations, and model outputs—could further enhance predictive accuracy and operational applicability.

Future research should also aim to couple physical transport simulations with atmospheric emission inventories and biogeochemical degradation modules to represent the full environmental life cycle of PAHs. This integrated framework would allow quantification of atmospheric deposition fluxes, evaluate transformation and degradation rates, and better constrain the relative contributions of atmospheric versus marine sources.

Such coupling has been successfully applied in recent studies addressing semi-volatile organic contaminants in the ocean (Zhang et al., 2025; Mulder et al., 2019; Nizzetto et al., 2016; Gioia et al., 2011), demonstrating its potential for improving source attribution and predictive capacity in coastal pollution models.

5.4 Final synthesis

This thesis demonstrates that combining local process-based analyses with regional satellite-driven Lagrangian modelling provides a robust, multi-scale framework for diagnosing PAH contamination pathways. PAH exceedances at Lucrino result from the superposition of two interacting processes: resuspension and advection of legacy-contaminated sediments from Bagnoli, and wind-driven advection of fuel-derived residues from maritime traffic, recurrently activated under persistent southerly winds and energetic wave regimes.

The seasonal modulation of wind persistence emerges as a key control in determining when and how these processes interact, with winter southerlies acting as the dominant atmospheric trigger for contamination events.

Through the integration of chemical, oceanographic, meteorological, and numerical evidence, this research establishes a comprehensive diagnostic framework for source attribution and coastal contamination management. The methodological paradigm is transferable to other semi-enclosed or industrially impacted basins, providing a scientific foundation for forecast-based monitoring, regulatory planning, and aquaculture risk mitigation.

More broadly, this work highlights how integrating physical oceanography with chemical and biological evidence can shift coastal contamination assessment from descriptive monitoring to process-based risk evaluation.

Chapter VI

6. Conclusions

The findings of this thesis demonstrate that PAH contamination at the Lucrino mussel farm follows a pronounced seasonal pattern, occurring predominantly in late autumn and winter across both the 2016 and 2024 observation periods. This recurrence reflects the interplay between meteorological forcing and coastal hydrodynamics, where persistent southerly winds and high southerly wave energy (Hs $\gtrsim$ 1.2 m, Tp $\gtrsim$ 8 s in 2016) act as recurrent preconditions for both sediment resuspension and efficient onshore transport. These results indicate that PAH exceedances are not random events, but predictable outcomes of recurrent atmospheric–oceanographic configurations.

Two distinct but complementary source–transport pathways have been identified:

- Resuspension of contaminated sediments from the Bagnoli brownfield area, followed by coastal advection toward Lucrino, supported by hydrodynamic simulations, in-situ observations, and compositional fingerprints.
- Surface advection of nautical-fuel residues transported from high-traffic maritime zones under combined influence of southerly winds and surface circulation, demonstrated by 2024 SWOT-altimetry and Parcels-based simulations.

Analysis of wind persistence further confirmed that only winter conditions provide the necessary duration and directionality of S–SW winds to sustain effective onshore advection. Spring and summer, dominated by weaker and short-lived wind events, favor dispersion rather than accumulation, while autumn represents a transitional regime with highly variable transport efficiency.

The integration of high-resolution local modelling and in-situ observations with regional altimetry-based Lagrangian simulations emerges as a particularly powerful approach. Local frameworks elucidate event-scale mechanisms such as bottom shear stress-induced resuspension, while regional analyses resolve basin-scale transport and maritime-source attribution, enhancing predictive capacity and robustness of source identification.

From an operational point of view, forecast-driven risk management is technically feasible: near-real-time wind and wave observations coupled with short-range Lagrangian nowcasts could anticipate high-risk contamination events, allowing event-based sampling, timely mitigation, and reduction of public-health and economic impacts.

Complementary measures, including targeted sediment remediation at Bagnoli and stricter controls on nautical fuel handling and emissions, could further reduce the identified PAH pathways. Beyond the local context, this research establishes a transferable methodological framework that combines high-frequency local observations with regional satellite-driven Lagrangian analyses. Such an integrated approach applies to other semi-enclosed coastal systems affected by both legacy and contemporary pollution sources, providing a basis for oceanography-informed operational policies, food-safety regulation, and aquaculture management.

Future implementation of this framework could enable proactive decision-making in coastal management, reducing both environmental exposure and socio-economic risk.

Scientific publications

PEER-REVIEWED ARTICLES:

- "*The Role of Sea Surface Circulation and Weather Dynamics in the PAH Contamination in Coastal Mussels: A Case Study in the Southern Tyrrhenian Sea*" - Laura Fortunato, Mauro Esposito, Vincenzo Capozzi, Fabio Conversano, Luigi Gifuni, Paola de Ruggiero, Giuseppe Aulicino, Diana Di Luccio, Enrico Zambianchi, Giorgio Budillon, Yuri Cotroneo. Frontiers in Marine Science (2025). DOI: 10.3389/fmars.2025.1565042
- "*Coastal Eddy Detection in the Balearic Sea: SWOT Capabilities*" - Laura Fortunato, Laura Gómez Navarro, Vincent Combes, Yuri Cotroneo, Giuseppe Aulicino, Ananda Pascual. Remote Sensing (2025). DOI: 10.3390/rs17152552
- "*Expendable bathythermograph (XBT) data collected along the Southern Ocean chokepoint between Aotearoa / New Zealand and Antarctica, 1994–2024*"- Giuseppe Aulicino, Antonino Ian Ferola, Laura Fortunato, Giorgio Budillon, Pasquale Castagno, Pierpaolo Falco, Giannetta Fusco, Naomi Krauzig, Giancarlo Spezie,Enrico Zambianchi, Yuri Cotroneo. Earth System Science Data (2025). DOI: 10.5194/essd-17-2625-2025

CONFERENCE PAPER:

- "*Marine circulation and weather conditions during mussel PHAs contamination events in the Pozzuoli Bay (Gulf of Naples) in 2016*"-L. Fortunato, V. Capozzi, G. Aulicino, L. Gifuni, P. de Ruggiero, M. Esposito, F. Conversano, Y. Cotroneo (2024- BEING SEA-EU CONFERENCE)
- "*Analysis of sea surface currents to study correlations between levels and sources of PAHs in the Gulf of Pozzuoli*"-L. Fortunato, Y. Cotroneo, P. De Ruggiero, L. Gifuni, D. Di Luccio, M. Esposito, D. Monaco, R. Montella (2023- AIOL CONVENTION)
- "*Environmental investigation in the Gulf of Pozzuoli (Naples) in relation to PAHs contamination*". M. Esposito, M. Della Rotonda, C. Sbarra, M.

Stefanelli, M. G. Aquila, A. Anastasio, P. Sarnelli, P. Gallo, Y. Cotroneo, L. Fortunato, R. Montella, L. De Maio (2022- 9th International Symposium MONITORING OF MEDITERRANEAN COASTAL AREAS: PROBLEMS AND MEASUREMENT TECHNIQUES).

MANUSCRIPTS UNDER REVIEW:

- "Seasonal Variability of the Surface Circulation in the Tyrrhenian Sea: New Insights from SWOT Altimetry and Tide Gauge Records"- Laura Fortunato, Giuseppe Aulicino, Maxime Ballarotta, Ananda Pascual, Giannetta Fusco, Berardino Buonocore, Yuri Cotroneo. JGR: Oceans. [under review]
- "*New insights on mesoscale activity in the western Mediterranean Sea*"- Laura Gómez Navarro, Maxime Ballarotta, Diego Cortés Morales, Isabelle Pujol, Laura Fortunato, Baptiste Mourre, Ananda Pascual. State Planet Discuss. [preprint]. DOI: 10.5194/sp-2025-17

References

Abdel-Shafy, H. I., & Mansour, M. S. (2016). A review on polycyclic aromatic hydrocarbons: source, environmental impact, effect on human health and remediation. Egyptian journal of petroleum, 25(1), 107-123.

Aiello, G., Giordano, L., & Giordano, F. (2016). High-resolution seismic stratigraphy of the Gulf of Pozzuoli and relationships with submarine volcanic setting. Rendiconti Lincei, 27, 775–801.

Albanese, S., De Vivo, B., Lima, A., Cicchella, D., Civitillo, D., & Cosenza, A.. (2010). Geochemical baselines and risk assessment of the Bagnoli brownfield site coastal sea sediments (Naples, Italy). Journal of Geochemical Exploration, 105(1-2), 19-33.

Amiard, J. C., Journel, R., & Bacheley, H. (2008). Influence of field and experimental exposure of mussels (Mytilus sp.) to nickel and vanadium on metallothionein concentration. Comparative Biochemistry and Physiology Part C: Toxicology & Pharmacology, 147(3), 378-385.

Arienzo, M., Ferrara, L., Toscanesi, M., Giarra, A., Donadio, C., & Trifuoggi, M. (2020). Sediment contamination by heavy metals and ecological risk assessment: The case of Gulf of Pozzuoli, Naples, Italy. *Marine Pollution Bulletin*, *155*, 111149.

Arienzo, M., Donadio, C., Mangoni, O., Bolinesi, F., Stanislao, C., Trifuoggi, M., Toscanesi, M., di Natale, G., & Ferrara, L. (2017). Characterization and source apportionment of polycyclic aromatic hydrocarbons (pahs) in the sediments of gulf of Pozzuoli (Campania, Italy). Marine Pollution Bulletin, 124(1), 480–487.

Armiento, G., Caprioli, R., Cerbone, A., Chiavarini, S., Crovato, C., de Cassan, M., de Rosa, L., Montereali, M. R., Nardi, E., Nardi, L., Pezza, M., Proposito, M., Rimauro, J., Salerno, A., Salluzzo, A., Spaziani, F., & Zaza, F.

(2020). Current status of coastal sediments contamination in the former industrial area of Bagnoli-Coroglio (Naples, Italy). Chemistry and Ecology, 36(6), 579–597.

ARPAL, ICRAM (2005). Progetto Preliminare di Bonifica dell'Area Marina inclusa nella perimetrazione del sito di bonifica di interesse nazionale di Pitelli.

Astraldi, M., & Gasparini, G. P. (1994). The seasonal characteristics of the circulation in the Tyrrhenian Sea. Seasonal and interannual variability of the Western Mediterranean Sea, 46, 115-134.

Astraldi, M., Gasparini, G. P., Sparnocchia, S., Moretti, M., & Sansone, E. (1996). The characteristics of the water masses and the water transport in the Sicily Strait at long time scales. BULLETIN-INSTITUT OCEANOGRAPHIQUE MONACO-NUMERO SPECIAL-, 95-116.

Astraldi, M., Gasparini, G. P., Vetrano, A., & Vignudelli, S. (2002). Hydrographic characteristics and interannual variability of water masses in the central Mediterranean: a sensitivity test for long-term changes in the Mediterranean Sea. Deep Sea Research Part I: Oceanographic Research Papers, 49(4), 661-680.

Aulicino, G., Cotroneo, Y., Lacava, T., Sileo, G., Fusco, G., Carlon, R., ... & Budillon, G. (2016). Results of the first Wave Glider experiment in the southern Tyrrhenian Sea. Advances in Oceanography and Limnology, 7(1).

Ballarotta, M.; Ubelmann, C.; Bellemin-Laponnaz, V.; Le Guillou, F.; Meda, G.; Anadon, C.; Dibarboure, G. (2025). Assimilation of Wide-Swath Altimetry in Level-4 Multi-Mission Satellite Maps. Ocean Sci. 2025, 21, 63–80.

Baumard, P., Budzinski, H., & Garrigues, P. (1997). Analytical procedure for the analysis of PAHs in biological tissues by gas chromatography coupled to mass spectrometry: application to mussels. *Fresenius' journal of analytical chemistry*, *359*, 502-509.

Bayne, B. L. (2004). Phenotypic flexibility and physiological tradeoffs in the feeding and growth of marine bivalve molluscs. *Integrative and Comparative Biology*, *44*(6), 425-432.

Barre, A., Briand, J. F., Vaccher, V., Briant, N., Briand, J. M., Dormoy, B., ... & Bouchoucha, M. (2024). A comparative biomonitoring study of trace metals and organic compounds bioaccumulation in marine biofilms and caged mussels along the French Mediterranean coast. *Environmental Pollution*, *363*, 125239.

Bergamin, I., Romano, E., Gabellini, M., Ausili, A., & Carboni, M. G. (2003). Chemical-physical and ecological characterisation in the environmental project of a polluted coastal area: the Bagnoli case study. *Mediterranean Marine Science*, *4*(2), 5-20.

Beegle-Krause, C.J., 2001. General NOAA Oil Modeling Environment (GNOME): a new spill trajectory model. In: IOSC 2001 Proceedings. Mira Digital Publishing, Inc., Tampa, FL, pp. 865–871.

Boatta, F. (2014). Ocean Acidification studies in the Baia di Levante (Vulcano island, Italy). Advantages and disadvantages of the "in situ" approach.

Bocchetti, R., & Regoli, F. (2006). Seasonal variability of oxidative biomarkers, lysosomal parameters, metallothioneins and peroxisomal enzymes in the Mediterranean mussel Mytilus galloprovincialis from Adriatic Sea. *Chemosphere*, *65*(6), 913-921.

Bonaduce, A., Cipollone, A., Johannessen, J. A., Staneva, J., Raj, R. P., & Aydogdu, A. (2021). Ocean mesoscale variability: a case study on the Mediterranean Sea from a re-analysis perspective. Frontiers in Earth Science, 9, 724879.

Blumberg, A. F., Mellor, G. L. (1987). A description of a three-dimensional coastal ocean circulation model. Three-dimensional coastal ocean models, 4, 1-16.

Bjorseth, A., & Ramdahl, T. (1985). *Handbook of polycyclic aromatic hydrocarbons, Volume 2*. Norsk Hydro Petroleum Research Center, Bergen.

Budillon, G., Gasparini, G. P., & Schroeder, K. (2009). Persistence of an eddy signature in the central Tyrrhenian basin. Deep Sea Research Part II: Topical Studies in Oceanography, 56(11-12), 713-724.

Butcher, J.C. (2016). *Numerical Methods for Ordinary Differential Equations*, 3rd ed.; John Wiley & Sons: Hoboken, NJ, USA.

Carrada, G. C., Hopkins, T. S., Bonaduce, G., Ianora, A., Marino, D., Modigh, M., ... & di Scotto, C. B. (1980). Variability in the hydrographic and biological features of the Gulf of Naples. *Marine Ecology*, *1*(2), 105-120.

Casas, S., & Bacher, C. (2006). Modelling trace metal (Hg and Pb) bioaccumulation in the Mediterranean mussel, Mytilus galloprovincialis, applied to environmental monitoring. *Journal of sea Research*, *56*(2), 168-181.

Castagno, P., de Ruggiero, P., Pierini, S., Zambianchi, E., De Alteris, A., De Stefano, M., & Budillon, G. (2020). Hydrographic and dynamical characterisation of the Bagnoli-Coroglio Bay (Gulf of Naples, Tyrrhenian Sea). *Chemistry and Ecology*, *36*(6), 598-618.

Cesarano, C., Aulicino, G., Cerrano, C., Ponti, M., & Puce, S. (2023). Marine beach litter monitoring strategies along Mediterranean coasts. A methodological review. *Marine Pollution Bulletin*, *186*, 114401.

Cianelli, D., Uttieri, M., Buonocore, B., Falco, P., Zambardino, G., & Zambianchi, E. (2011). Dynamics of a very special Mediterranean coastal area: the Gulf of Naples. *Mediterranean ecosystems: dynamics, management and conservation*, 129-150.

Cranford, P. J., Strain, P. M., Dowd, M., Hargrave, B. T., Grant, J., & Archambault, M. C. (2007). Influence of mussel aquaculture on nitrogen dynamics in a nutrient enriched coastal embayment. Marine Ecology Progress Series, 347, 61-78.

Del Gaudio, C., Aquino, I., Ricciardi, G. P., Ricco, C., & Scandone, R. (2010). Unrest episodes at Campi Flegrei: A reconstruction of vertical ground movements during 1905–2009. Journal of Volcanology and Geothermal Research, 195(1), 48-56.

Delandmeter, P.; van Sebille, E. The Parcels v2.0 Lagrangian framework: New field interpolation schemes. Geosci. Model Dev. 2019, 12, 3571–3584.

De Maio, A., Moretti, M., Sansone, E., Spezie, G., & Vultaggio, M. (1985). Outline of marine currents in the Bay of Naples and some considerations on pollutant transport. *Il Nuovo Cimento C*, *8*, 955-969.

De Maio, A., Moretti, M., Surone, E., Spezia, G., & Voitaggio, M. (1982). Circolazione costiera. *Analisi dinamica e idrologica di una situazione osservata nel Golfo di Napoli. Convegno Risorse Biologiche e Inquinamento Marino del PF Oceanografia e Fondi Marini*, 609-624.

De Maio, L., Capone, S., Celentano, A., Monaco, D., Pignalosa, C., Siciliano, A. (2021). Indagini ambientali sui sedimenti marini svolte da ARPAC in relazione alla reiterata contaminazione da IPA dei mitili nel Golfo di Pozzuoli, località Lucrino.

De Pippo, T., Donadio, C., Pennetta, M., Petrosino, C., Terlizzi, F., & Valente, A. (2008). Coastal hazard assessment and mapping in Northern Campania, Italy. *Geomorphology*, *97*(3-4), 451-466.

de Ruggiero, P., Napolitano, E., Iacono R. and Pierini S. (2016): A high-resolution modelling study of the circulation along the Campania coastal system, with a special focus on the Gulf of Naples., Cont. Shel. Res., 122, 85-101. https://doi.org/10.1016/j.csr.2016.03.026

de Ruggiero, P., Esposito, G., Napolitano, E., Iacono, R., Pierini, S., & Zambianchi, E. (2020). Modelling the marine circulation of the Campania coastal system (Tyrrhenian Sea) for the year 2016: Analysis of the dynamics. *Journal of Marine Systems*, *210*, 103388.

Di Crescenzo, G., Santangelo, N., Santo, A., & Valente, E. (2021). Geomorphological approach to cliff instability in volcanic slopes: a case study from the Gulf of Naples (Southern Italy). Geosciences, 11(7), 289.

Di Martino, G., Innangi, S., Passaro, S., et al. (2020). Mapping of seabed morphology of the Bagnoli brownfield site, Pozzuoli Bay, Italy. Chemistry and Ecology, 36(6), 496–510.

Dohan, K. (2017). Ocean surface currents from satellite data. Journal of Geophysical Research: Oceans, 122(4), 2647-2651.

Durante, S., Oliveri, P., Nair, R., & Sparnocchia, S. (2021). Mixing in the Tyrrhenian interior due to thermohaline staircases. Frontiers in Marine Science, 8, 672437.

Durante, S., Schroeder, K., Mazzei, L., Pierini, S., Borghini, M., & Sparnocchia, S. (2019). Permanent thermohaline staircases in the Tyrrhenian Sea. Geophysical Research Letters, 46(3), 1562-1570.

Esposito, M., Canzanella, S., Lambiase, S., Scaramuzzo, A., La Nucara, R., Bruno, T., ... & Gallo, P. (2020). Organic pollutants (PCBs, PCDD/Fs, PAHs) and toxic metals in farmed mussels from the Gulf of Naples (Italy): Monitoring and human exposure. Regional studies in marine science, 40, 101497.

Esposito, M., Perugini, M., Lambiase, S., Conte, A., Baldi, L., & Amorena, M. (2017). Seasonal trend of PAHs concentrations in farmed mussels from the coastal areas of the Naples, Italy. Bulletin of Environmental Contamination and Toxicology, 99, 333-337.

EUMOFA (2021). The EU Fish Market 2021 Edition.

FAO (2024). *The State of World Fisheries and Aquaculture 2024*.

Farrington, J. W., Goldberg, E. D., Risebrough, R. W., Martin, J. H., & Bowen, V. T. (1983). US" Mussel Watch" 1976-1978: an overview of the trace-metal, DDE, PCB, hydrocarbon and artificial radionuclide data. *Environmental science & technology*, *17*(8), 490-496.

Forget, P., André, G. (2007). Can satellite-derived chlorophyll imagery be used to trace surface dynamics in coastal zone? A case study in the northwestern Mediterranean Sea. Sensors, 7(6), 884-904.

Fortunato, L., Esposito, M., Capozzi, V., Conversano, F., Gifuni, L., De Ruggiero, P., ... & Cotroneo, Y. (2025). The role of sea surface circulation and weather dynamics in the PAH contamination in coastal mussels: a case study in the Southern Tyrrhenian Sea. Frontiers in Marine Science, 12, 1565042.

Fortunato, L., Gómez-Navarro, L., Combes, V., Cotroneo, Y., Aulicino, G., & Pascual, A. (2025). Coastal Eddy Detection in the Balearic Sea: SWOT Capabilities. Remote Sensing, 17(15), 2552.

Fu, L. L., Alsdorf, D., Morrow, R., Rodriguez, E., & Mognard, N. (2012). SWOT: The surface water and ocean topography mission. Wide-swath altimetric elevation on Earth (No. JPL-Publ-12-5).

Fu, L. L., Pavelsky, T., Cretaux, J. F., Morrow, R., Farrar, J. T., Vaze, P., ... & Dibarboure, G. (2024). The surface water and ocean topography mission: A breakthrough in radar remote sensing of the ocean and land surface water. Geophysical Research Letters, 51(4), e2023GL107652.

Fusco, G., Artale, V., Cotroneo, Y., & Sannino, G. (2008). Thermohaline variability of Mediterranean Water in the Gulf of Cadiz, 1948–1999. Deep Sea Research Part I: Oceanographic Research Papers, 55(12), 1624-1638.

Gifuni, L., De Ruggiero, P., Cianelli, D., Drofa, O., Davolio, S., Pierini, S., & Zambianchi, E. (2025). Impact of wind forcing on surface transport in the Gulf of Naples. *Scientific Reports*, *15*(1), 39588.

Gifuni, L., de Ruggiero, P., Cianelli, D., Pierini, S., & Zambianchi, E. (2023). Numerical investigation of the three-dimensional paths of plastic polymers in the Gulf of Naples. *Marine Pollution Bulletin*, *193*, 115259.

Gillio Meina, E., et al. (2020). Investigating the mechanism of vanadium toxicity in freshwater organisms. Aquatic Toxicology, 229, 105648.

Gioia, R., Dachs, J., Nizzetto, L., Berrojalbiz, N., Galbán, C., Del Vento, S., ... & Jones, K. C. (2011). Sources, transport and fate of organic pollutants in the oceanic environment. In Persistent Pollution–Past, Present and Future: School of Environmental Research-Organized by Helmholtz-Zentrum Geesthacht (pp. 111-139). Berlin, Heidelberg: Springer Berlin Heidelberg.

Giunta, G., Mariani, P., Montella, R., Riccio, A. (2007). pPOM: A nested, scalable, parallel and Fortran 90 implementation of the Princeton Ocean Model. Environmental Modelling & Software, 22(1), 117-122.

Guerrini, F., Mari, L., & Casagrandi, R. (2022). A coupled Lagrangian-Eulerian model for microplastics as vectors of contaminants applied to the Mediterranean Sea. *Environmental Research Letters*, *17*(2), 024038.

Hatcher, A. J. G. B., Grant, J., & Schofield, B. (1994). Effects of suspended mussel culture (Mytilus spp.) on sedimentation, benthic respiration and sediment nutrient dynamics in a coastal bay. *Marine Ecology-Progress Series*, *115*, 219-219.

Hersbach, H., Bell, B., Berrisford, P., Biavati, G., Horányi, A., Muñoz Sabater, J., Nicolas, J., Peubey, C., Radu, R., Rozum, I., Schepers, D., Simmons, A., Soci, C., Dee, D., Thépaut, J-N. (2023): ERA5 hourly data on single levels from 1940 to present. Copernicus Climate Change Service (C3S) Climate Data Store (CDS).

Hopkins, T. S. (1988). Recent observations on the intermediate and deep water circulation in the Southern Tyrrhenian Sea.

Iacono, R., Napolitano, E., Palma, M., & Sannino, G. (2021). The tyrrhenian sea circulation: A review of recent work. Sustainability, 13(11), 6371.

Iacono, R., Napolitano, E., Marullo, S., Artale, V., & Vetrano, A. (2013). Seasonal variability of the Tyrrhenian Sea surface geostrophic circulation as assessed by altimeter data. Journal of Physical Oceanography, 43(8), 1710-1732.

ISPRA (2017). Manuali e Linee Guida 170/2017 - Province geochimiche dei metalli e metalloidi nei suoli e nei sedimenti italiani. ISPRA, Istituto Superiore per la Protezione e la Ricerca Ambientale, Roma, 370 pp.

Ko, C. Y., Hsin, Y. C., & Jeng, M. S. (2020). Global distribution and cleanup opportunities for macro ocean litter: a quarter century of accumulation dynamics under windage effects. Environmental Research Letters, 15(10), 104063.

Kokoszka, F., Le Roux, B., Iudicone, D., Conversano, F., & Ribera d'Alcalá, M. (2023). Long-term variability of the coastal ocean stratification in the Gulf of Naples: Two decades of monitoring the marine ecosystem at the LTER–MC site, between land and open Mediterranean Sea. Marine Ecology, 44(3), e12725.

Kong, Y., Jimenez, K., Lee, C. M., Winter, S., Summers-Evans, J., Cao, A., ... & Jay, J. A. (2025). Monitoring Coastal Water Turbidity Using Sentinel2—A Case Study in Los Angeles. Remote Sensing, 17(2), 201.

Krivosheya, V. G., & Ovchinnikov, I. M. (1973). Peculiarities in the geostrophic circulation of the waters of the Tyrrhenian Sea. Oceanology, 13, 822-827.

Le Foche, M., Notargiacomo, T., & Mancini, L. (2005). Rassegna degli indici basati sui macroinvertebrati bentonici come indicatori di qualità degli ecosistemi lacustri. *Annali dell'Istituto superiore di sanità*, *41*(3), 403-413.

Madec, G. (2008). NEMO Ocean Engine. Note du Pole de mod´ elisation. Institut Pierre-Simon Laplace (IPSL), France.

Manoli, E., Samara, C., Konstantinou, I., & Albanis, T. (2000). Polycyclic aromatic hydrocarbons in the bulk precipitation and surface waters of Northern Greece. *Chemosphere*, *41*(12), 1845-1855.

Marani, M., Gamberi, F., & Bonatti, E. (1993). From seafloor spreading to passive margin: Tectonic evolution of the Tyrrhenian Sea. Mem. Soc. Geol. It., 49, 373–385.

Mascorda Cabre, L., Hosegood, P., Attrill, M. J., Bridger, D., & Sheehan, E. V. (2021). Offshore longline mussel farms: a review of oceanographic and ecological interactions to inform future research needs, policy and management. *Reviews in Aquaculture*, *13*(4), 1864-1887.

Mattei, F., Scardi, M. (2022). Mining satellite data for extracting chlorophyll a spatio-temporal patterns in the Mediterranean Sea. Environmental Modelling & Software, 150, 105353.

Meloni, D., Mudadu, A. G., Abete, M. C., Bazzoni, A. M., Griglione, A., Pederiva, S., ... & Squadrone, S. (2022). Occurrence of trace elements in Mediterranean mussels (Mytilus galloprovincialis Lamarck, 1819) from an experimental pilot farm in the Calich Lagoon (Sardinia, Italy). *Italian Journal of Food Safety*, *11*(1), 9970.

Mellor, G. L., & Yamada, T. (1982). Development of a turbulence closure model for geophysical fluid problems. Reviews of Geophysics, 20(4), 851-875. https://doi.org/10.1029/RG020i004p00851

Menna, M., Mercatini, A., Uttieri, M., Buonocore, B., & Zambianchi, E. (2007). Wintertime transport processes in the Gulf of Naples investigated by HF radar measurements of surface currents. *Nuovo Cimento-C*, *30*(6), 605-622.

Mercogliano, R., Santonicola, S., De Felice, A., Anastasio, A., Murru, N., Ferrante, M. C., & Cortesi, M. L. (2016). Occurrence and distribution of polycyclic aromatic hydrocarbons in mussels from the Gulf of Naples, Tyrrhenian Sea, Italy. Marine pollution bulletin, 104(1-2), 386-390.

Millot, C. (1999). Circulation in the western Mediterranean Sea. Journal of Marine Systems, 20(1-4), 423-442.

Millot, C., Candela, J., Fuda, J. L., & Tber, Y. (2006). Large warming and salinification of the Mediterranean outflow due to changes in its composition. *Deep Sea Research Part I: Oceanographic Research Papers*, *53*(4), 656-666.

MIPAAF (2020). *Piano Strategico Nazionale per l'Acquacoltura Sostenibile 2021–2027*.

Moretti, M., Sansone, E., Spezie, G., Vultaggio, M., & De Maio, A. (1976). Alcuni aspetti del movimento delle acque del Golfo di Napoli. Annali Ist Univ Nav XLV-XLVI, 207-217.

Morrow, R., Fu, L.-L., Ardhuin, F., Benkiran, M., Chapron, B., Cosme, E., … Wang, J. (2019). Global observations of fine-scale ocean surface topography with the Surface Water and Ocean Topography (SWOT) mission. Frontiers in Marine Science, 6, 232.

Moschino, V., Delos, A., Marin, M.G., & Da Ros, L. (2012). Assessing metal contamination in surface sediments of the Venice lagoon by means of two distinct benthic invertebrates: Bioaccumulation in soft tissues and shells. Environmental Monitoring and Assessment, 184, 6593–6611.

Mulder, M. D., Dumanoglu, Y., Efstathiou, C., Kukucka, P., Matejovicova, J., Maurer, C., ... & Lammel, G. (2019). Fast formation of nitro-PAHs in the marine atmosphere constrained in a regional-scale Lagrangian field experiment. Environmental Science & Technology, 53(15), 8914-8924.

National Oceanic and Atmospheric Administration (NOAA). (2023). *Mussel Watch Program*. NOAA National Centers for Coastal Ocean Science. Retrieved from https://coastalscience.noaa.gov/science-areas/pollution/mussel-watch/

Newell, R. I. (2004). Ecosystem influences of natural and cultivated populations of suspension-feeding bivalve molluscs: a review. *Journal of Shellfish research*, *23*(1), 51-62.

Nielsen, P. (1992). Coastal Bottom Boundary Layers and Sediment Transport. World Scientific.

Nizzetto, L., Butterfield, D., Futter, M., Lin, Y., Allan, I., & Larssen, T. (2016). Assessment of contaminant fate in catchments using a novel integrated hydrobiogeochemical-multimedia fate model. Science of the Total Environment, 544, 553-563.

OceanParcels project. What is oceanparcels? 2019. Available online: http://oceanparcels.org/ (accessed on 16 October 2019).

Oddo, P., Adani, M., Pinardi, N., Fratianni, C., Tonani, M., Pettenuzzo, D. (2009). A nested Atlantic-Mediterranean Sea general circulation model for operational forecasting. Ocean Sci. https://doi.org/10.5194/os-5-461-2009.

Oliva, A. L., Ronda, A. C., Girones, L., Orazi, M. M., Recabarren-Villalón, T., Marcovecchio, J. E., & Arias, A. H. (2020). Polycyclic Aromatic Hydrocarbons: Sources, Occurrence, Levels, Distribution and Ecotoxicological Fate at Coastal and Deep Ocean. In *Coastal and Deep Ocean Pollution* (pp. 288-316). CRC Press.

Okubo, A. (1971). Oceanic diffusion diagrams. In Deep sea research and oceanographic abstracts, 18 (8), 789-802

Pavlakis, P., Tarchi, D., & Sieber, A. J. (2001). On the monitoring of illicit vessel discharges using spaceborne SAR remote sensing-a reconnaissance study in the Mediterranean sea. *Annals of Telecommunications*, *56*(11-12), 700-718.

Perugini, M., Visciano, P., Giammarino, A., Manera, M., Di Nardo, W., and Amorena, M. (2007b). Polycyclic aromatic hydrocarbons in marine organisms from the Adriatic Sea. Italy. Chemosphere. 66, 1904–1910.

Perugini, M., Visciano, P., Manera, M., Turno, G., Lucisano, A., and Amorena, M. (2007a). Polycyclic aromatic hydrocarbons in marine organisms from the Gulf of Naples, Tyrrhenian Sea. J. Agric. Food Chem. Mar. 55, 2049–2054. doi: 10.1021/jf0630926

Perusini, V., Purini, R., Moretti, M., & De Maio, A. (1992). Modelli di circolazione costiera. Primi risultati per la costa campana. *Annali Ist Univ Nav*, *59*, 65-76.

Phillips, D. J., & Rainbow, P. S. (1994). *Biomonitoring of trace aquatic contaminants* (Vol. 37). Springer Science & Business Media.

Pierini, S., & Simioli, A. (1998). A wind-driven circulation model of the Tyrrhenian Sea area. *Journal of Marine Systems*, *18*(1-3), 161-178.

Poulain, P. M., & Zambianchi, E. (2007). Surface circulation in the central Mediterranean Sea as deduced from Lagrangian drifters in the 1990s. Continental Shelf Research, 27(7), 981-1001. https://doi.org/10.1016/j.csr.2007.01.005

Prins, T. C., Smaal, A. C., & Dame, R. F. (1997). A review of the feedbacks between bivalve grazing and ecosystem processes. *Aquatic Ecology*, *31*, 349-359.

Reijnders, D., Deleersnijder, E., & van Sebille, E. (2022). Simulating Lagrangian subgrid-scale dispersion on neutral surfaces in the ocean. Journal of Advances in Modeling Earth Systems, 14(2), e2021MS002850.

Rinaldi, E., Buongiorno Nardelli, B., Zambianchi, E., Santoleri, R., & Poulain, P. M. (2010). Lagrangian and Eulerian observations of the surface circulation in the Tyrrhenian Sea. Journal of Geophysical Research: Oceans, 115(C4).

Sarà, G., Scilipoti, D., Mazzola, A., & Modica, A. (2004). Effects of fish farming waste to sedimentary and particulate organic matter in a southern Mediterranean area (Gulf of Castellammare, Sicily): a multiple stable isotope study (δ13C and δ15N). *Aquaculture*, *234*(1-4), 199-213.

Serpe FP., Esposito M., Gallo P., Serpe L.(2010). Optimisation and validation of an HPLC method for determination of polycyclic aromatic hydrocarbons (PAHs) in mussels. Food Chem 122:920–925

Srogi, K. (2007). Monitoring of environmental exposure to polycyclic aromatic hydrocarbons: a review. *Environmental Chemistry Letters*, *5*, 169-195.

Sverdrup, L. E., Nielsen, T., & Krogh, P. H. (2002). Soil ecotoxicity of polycyclic aromatic hydrocarbons in relation to soil sorption, lipophilicity, and water solubility. *Environmental science & technology*, *36*(11), 2429-2435.

Sun, R., Sun, Y., Li, Q. X., Zheng, X., Luo, X., & Mai, B. (2018). Polycyclic aromatic hydrocarbons in sediments and marine organisms: Implications of anthropogenic effects on the coastal environment. *Science of the Total Environment*, *640*, 264-272.

Readman, J. W., Mantoura, R. F. C., & Rhead, M. M. (1984). The physico-chemical speciation of polycyclic aromatic hydrocarbons (PAH) in aquatic systems. *Fresenius' journal of analytical chemistry*.

Romano, E., Ausili, A., Zharova, N., Magno, M. C., Pavoni, B., & Gabellini, M. (2004). Marine sediment contamination of an industrial site at Port of Bagnoli, Gulf of Naples, Southern Italy. Marine Pollution Bulletin, 49(5-6), 487-495.

Somma, R., Iuliano, S., Matano, F., Molisso, F., Passaro, S., Sacchi, M., ... & De Natale, G. (2016). High-resolution morpho-bathymetry of Pozzuoli Bay, southern Italy. Journal of Maps, 12(2), 222-230.

Soulsby, R. L. (1997). Dynamics of Marine Sands: A Manual for Practical Applications. Thomas Telford Publishing.

Sparnocchia, S., Gasparini, G. P., Astraldi, M., Borghini, M., & Pistek, P. (1999). Dynamics and mixing of the Eastern Mediterranean outflow in the Tyrrhenian basin. Journal of Marine Systems, 20(1-4), 301-317.

Stolzenbach, K. D., Madsen, O. S., Adams, E. E., Pollack, A. M., & Cooper, C. (1977). A review and evaluation of basic techniques for predicting the behavior of surface oil slicks.

Tornero, V., & d'Alcalà, M. R. (2014). Contamination by hazardous substances in the Gulf of Naples and nearby coastal areas: a review of sources, environmental levels and potential impacts in the MSFD perspective. *Science of the total environment*, *466*, 820-840.

Trinchella, F., Esposito, M. G., Simoniello, P., & Scudiero, R. (2013). Cadmium, lead and metallothionein contents in cultivated mussels (M ytilus galloprovincialis) from the G ulf of N aples (S outhern I taly). *Aquaculture Research*, *44*(7), 1076-1084.

Ubelmann, C.; Dibarboure, G.; Gaultier, L.; Ponte, A.; Ardhuin, F.; Ballarotta, M.; Faugère, Y. (2021). Reconstructing ocean surface current combining altimetry and future spaceborne Doppler data. J. Geophys. Res. Oceans 2021, 126, e2020JC016560.

Ubelmann, C.; Carrere, L.; Durand, C.; Dibarboure, G.; Faugère, Y.; Ballarotta, M.; Briol, F.; Lyard, F. (2022). Simultaneous estimation of ocean mesoscale and coherent internal tide sea surface height signatures from the global altimetry record. Ocean Sci. 2022, 18, 469–481.

Uttieri, M., Cianelli, D., Nardelli, B.B., Buonocore, B., Falco, P., Colella, S., Zambianchi, E. (2011). Multiplatform Observation of the Surface Circulation in the Gulf of Naples (Southern Tyrrhenian Sea). Ocean Dyn. 2011, 61, 779–796.

Van der Oost, R., Beyer, J., & Vermeulen, N. P. (2003). Fish bioaccumulation and biomarkers in environmental risk assessment: a review. *Environmental toxicology and pharmacology*, *13*(2), 57-149.

Van Sebille, E., Griffies, S. M., Abernathey, R., Adams, T. P., Berloff, P., Biastoch, A., ... & Zika, J. D. (2018). Lagrangian ocean analysis: Fundamentals and practices. *Ocean modelling*, *121*, 49-75.

Van Rijn, L.C.; Walstra, D.J.R.; van Ormondt, M., 2007. Unified view of sediment transport by currents and waves. IV: Application of morpho dynamic model. J. Hydraul. Eng., 133, 776–793.

Verger-Miralles, E., Mourre, B., Gómez-Navarro, L., Barceló-Llull, B., Casas, B., Cutolo, E., & Pascual, A. (2025). SWOT enhances small-scale eddy detection in the Mediterranean Sea. *Geophysical Research Letters*, *52*(16), e2025GL116480.

Volpe, G., Buongiorno Nardelli, B., Colella, S., Pisano, A. and Santoleri, R. (2018). An Operational Interpolated Ocean Colour Product in the Mediterranean Sea, in New Frontiers in Operational Oceanography, edited by E. P. Chassignet, A. Pascual, J. Tintorè, and J. Verron, pp. 227–244.

Volpe, G., Colella, S., Brando, V. E., Forneris, V., Padula, F. L., Cicco, A. D., Santoleri, R. (2019). Mediterranean ocean colour Level 3 operational multi-sensor processing. Ocean Science, 15(1), 127-146.

Wang, J. Z., Nie, Y. F., Luo, X. L., & Zeng, E. Y. (2008). Occurrence and phase distribution of polycyclic aromatic hydrocarbons in riverine runoff of the Pearl River Delta, China. *Marine Pollution Bulletin*, *57*(6-12), 767-774.

Wenzl, T., Simon, R., Anklam, E., & Kleiner, J. (2006). Analytical methods for polycyclic aromatic hydrocarbons (PAHs) in food and the environment needed for new food legislation in the European Union. *TrAC Trends in Analytical Chemistry*, *25*(7), 716-725.

Wise, S. A., Sander, L. C., & Schantz, M. M. (2015). Analytical methods for determination of polycyclic aromatic hydrocarbons (PAHs)—a historical perspective on the 16 US EPA priority pollutant PAHs. *Polycyclic Aromatic Compounds*, *35*(2-4), 187-247.

Wortham, H., Nguyen, E. B., Masclet, P., & Mouvier, G. (1993). Study of heterogeneous reactions of polycyclic aromatic hydrocarbons I: weakening of PAH-support bonds under photonic irradiation. *Science of the total environment*, *128*(1), 1-11.

Wu, Z., Chen, X., Wang, Z., Chen, H., Wang, Z., Mu, Q., ... & Jiang, Z. (2024). Modeling of polycyclic aromatic hydrocarbons (PAHs) from global to regional scales: model development (IAP-AACM_PAH v1. 0) and investigation of health risks in 2013 and 2018 in China. *Geoscientific Model Development*, *17*(24), 8885-8907.

Ysebaert, T., Hart, M., & Herman, P. M. (2009). Impacts of bottom and suspended cultures of mussels Mytilus spp. on the surrounding sedimentary environment and macrobenthic biodiversity. *Helgoland Marine Research*, *63*, 59-74.

Zelenke, B., O'Connor, C., Barker, C. J., Beegle-Krause, C. J., Eclipse, L. (2012). General NOAA Operational Modeling Environment (GNOME) Technical Documentation. Dept. of Commerce, NOAA Technical Memorandum NOS OR&R 40.

Zhang, L., Zhong, Y., Fan, Q., Li, S., Zhu, J., Ma, X., ... & Ma, Y. (2025). Coupled Physical-Biogeochemical Dynamics of Polycyclic Aromatic Compounds in the East China Sea. Environmental Science & Technology, 59(9), 4684-4698.

Zhang, Y., & Tao, S. (2009). Global atmospheric emission inventory of polycyclic aromatic hydrocarbons (PAHs) for 2004. Atmospheric environment, 43(4), 812-819.

Zodiatis, G., & Gasparini, G. P. (1996). Thermohaline staircase formations in the Tyrrhenian Sea. Deep Sea Research Part I: Oceanographic Research Papers, 43(5), 655-678.